Loma Linda University Electronic Theses, Dissertations & Projects

12-2016

Anti-tumor Mechanisms of HPV16 E6*

Whitney S. Evans

Follow this and additional works at: https://scholarsrepository.llu.edu/etd

Part of the Medical Pharmacology Commons

Recommended Citation

LOMA LINDA UNIVERSITY
School of Medicine
in conjunction with the
Faculty of Graduate Studies

_____

Anti-tumor Mechanisms of HPV16 E6*

by

Whitney S. Evans

_____

A Dissertation submitted in partial satisfaction of
the requirements for the degree
Doctor of Philosophy in Pharmacology

_____

December 2016

Each person whose signature appears below certifies that this dissertation in his/her opinion is adequate, in scope and quality, as a dissertation for the degree Doctor of Philosophy.

_____, Chairperson
Penelope J. Duerksen-Hughes, Professor of Biochemistry

_____
Eileen Brantley, Assistant Professor of Basic Sciences and Pharmacology

_____
Wonder P. Drake, Associate Professor of Medicine, Pathology, Microbiology, and Immunology

_____
Valery Filippov, Assistant Professor of Basic Sciences and Biochemistry

_____
Mark E. Reeves, Professor of Basic Sciences and Surgery

_____
Lubo Zhang, Professor of Perinatal Biology and Pharmacology

ACKNOWLEDGEMENTS

DEDICATION

I would like to dedicate this dissertation to my parents, Bernard and Beverly

Evans. Thank you for always believing in me, for your prayers, and creating an

atmosphere of freedom to allow me to discover Jesus, myself, and home.

CONTENT

FIGURES

TABLES

ABBREVIATIONS

LR-HPV	Low-risk Human Papillomavirus
HR-HPV	High-risk Human Papillomavirus
ROS	Reactive Oxygen Species
RNS	Reaction Nitrogen Species
Pap test	Papanicolau Cytologic Screening
ORF	Open Reading Frame
VLPs	Virus-like proteins
STI	Sexually Transmitted Infection
VIN	Vulvar Intraepithelial Neoplasia
VIA	Visual Inspection of Cervix using Acetic Acid
VIAM	Magnified Visual Inspection of Cervix using Acetic Acid
VILI	Visual Inspection of Cervix using Lugol's Iodine
CIN	Cervical Intraepithelial Neoplasia
VEGFR-1	Vascular Endothelial Growth Factor Receptor-1
E6AP	E6-associated protein
ILK	Integrin-linked kinase
OXPHOS	Oxidative Phosphorylation
TMT	Tandem Mass Tags
IPA	Ingenuity Pathway Analysis
MMP	Mitochondrial Membrane Permeabilization
GSH	Glutathione
AP	Alkaline Phosphatase
ALPP	Placental Alkaline Phosphatase

ABSTRACT OF THE DISSERTATION

Anti-tumor Mechanisms of HPV16 E6*

by

Whitney S. Evans

Doctor of Philosophy, Graduate Program in Pharmacology
Loma Linda University, December 2016
Dr. Penelope Duerksen-Hughes, Chairperson

High-risk types of the human papillomavirus (HR-HPV) are the causative agents

of nearly all cases of cervical cancer, as well as a significant number of head, neck,

penile, vulvar and anal cancers. Like many other viruses with small genomes, HPV (~8

kb) utilizes numerous mechanisms to increase the capacity of its genome to encode the

proteins necessary for successful completion of its infectious life cycle, including

alternative splicing. Studies over the past few decades have focused intensively on the

activities and roles of E6 proteins from HR-HPVs during the process of cellular

transformation, clearly implicating E6 as a major transforming agent. In contrast, the role

of the smaller splice isoform, E6*, in the carcinogenic process has not yet been

established. Based on previous studies, we proposed that E6* had the potential to reduce

tumor formation in vivo. To test this prediction, we injected HPV16$^+$ SiHa and HPV16$^-$

C33A cervical cancer cells overexpressing E6* into nude mice and monitored tumor

growth over several weeks while comparing them with control tumors lacking E6*

overexpression. E6* was found to reduce growth in both SiHa- and C33A-derived

tumors. These findings were followed up by in vitro experiments showing that E6* binds

to full-length E6 and decreases the growth rate in SiHa cells. Subsequently, we sought to

find the cellular pathways most influenced by E6* in attenuating SiHa and C33A tumor growth. Thus, proteomic analysis was performed on both cell lines, revealing that the β - Integrin pathway in SiHa cells and the mitochondrial dysfunction and oxidative phosphorylation pathway in C33A cells were the most significantly altered. Proteomic data was confirmed using immunoblot, microscopy, and flow cytometry techniques. These findings will assist in our quest for understanding the fundamental driving forces behind HPV-mediated and non-HPV-mediated cervical cancers and introduce novel ideas for small molecule inhibitors. Our studies provide several promising leads for future analyses, specifically in the context of human cancers, and carry with them the exciting possibility of replicating the anti-oncogenic activity of E6* in such a way as to provide therapeutic benefit.

CHAPTER ONE

INTRODUCTION

Cervical cancer was formerly the second most common cause of cancer death in women worldwide. This began to change following widespread adoption of Papanicolau cytologic screening (Pap test) for cervical cancer in the 1950s. As of 2012, high-risk human papillomaviruses (HR-HPVs) caused cervical cancer in more than 527,600 women annually, making it the fourth most common cancer in women worldwide, according to the American Cancer Society (ACS).

Over the past three decades the scientific community has witnessed spectacular advances in the understanding of the underlying pathophysiology of cervical cancer, with the most profound discovery being the identification in 1983 of the HPV within cervical cancer (a discovery that earned Harold Zur-Hausen, M.D the Nobel prize for Medicine and Physiology in 2008). A viral etiology for cervical cancer implied that it might be possible to eradicate cervical cancer through vaccination. This promise was partially fulfilled in 2006 when the United States Food and Drug Administration approved a HPV vaccine for the prevention of HPV-induced cervical dysplasia and/or cancer. In fact, an article published in the Journal of Infectious Disease states that the prevalence of the HR-HPVs 6, 11, 16, and 18 has decreased by 56% in females ages 14-19 between 2003 and 2010 (1). These advances, profound though they are, have yet to eradicate cervical cancer. Although controversial, recent reports have found that HR-HPVs are also present in their invasive forms in approximately 70% of colorectal cancers, the second most common cause of cancer death in the U.S. Similarly, a meta-analysis confirms evidence for an association between colon cancer risk and HPV infection (2). These statistics,

along with the climbing rates of HPV-mediated oropharyngeal cancer, supports the claim for need of continued research on the mechanisms that allow HR-HPVs to interact with their host to cause cellular transformation. In fact, all mucosal sites could be at risk for infection with mucosal virions, a striking commonality that illustrates the resilience of HR-HPVs and substantiates the necessity for HPV-mediated cancer *treatment*. Due to the pervasiveness of HPV infection across all populations and the timeline of disease progression, it will be a few decades before we will be able to determine the impact preventive practices are having on cancer incidence and prevalence. Therefore, those for whom preventative measures are not a solution, including HIV[+] individuals as well as women already infected with HR-HPV, await an answer.

HPV Virology

HPV Genome Structure

The human papillomavirus is a non-enveloped, double-stranded, circular DNA virus that is 8 kilobases long and comprised of 6 early proteins (E1, E2, E4, E5, and E6) and 2 late proteins (L1 and L2). Over 200 viruses have been identified and divided into 5 genera; the papillomaviruses linked to cancer belong to the Alpha genus. HPVs are further divided into types (as opposed to "serotypes" or "strains") based on how similar the virus' L1 gene nucleotide sequence is to other viruses. Fascinatingly, these episomes contain approximately 8 or 9 ORFs, which allows the virus to produce more proteins even with a smaller sized genome. Viral gene expression is augmented by the use of multiple promoters as well as by sophisticated splicing mechanisms that are not fully understood (3).

HPV Infection & Pathogenesis

HPV infection of the cervix begins with a break in the mucosal epithelium deep enough to expose the basal layer of epidermis to virus. Following entry into the cell, HPV occupies the basal cells of the epidermis in its episomal form, producing very little viral DNA. During normal HPV infection, the early expression of E6 and E7 proteins, which is linked to epithelial differentiation, enables the virus to trigger its host cells to re-enter S phase of the cell cycle, leading to viral genome replication and cell proliferation (4). Progeny basal cells containing virus may remain in the basal layer, or they may move up in to more superficial layers of epithelium. In select suprabasal layer cells, the virus may amplify its viral DNA copy number from low to high (5), which is facilitated by the increase in expression of other viral proteins such as E1, E2, E4, and E5 (4). From here, keratinocytes prepare to produce progeny virus particles through the expression of the capsid proteins L1 and L2, as they ascend to the epidermal surface where the virus particles will be released from desquamated cells (6).

In the case of HR-HPV infection, some postulate that the malignant potential of the virus is related to the integration of viral DNA into the host genome, thus favoring the carcinogenic process (7). It has been proposed that when the virus integrates into the cellular genome, the E2 gene, which is a transcriptional regulator of the viral oncoproteins, E6 and E7, is disrupted (8, 9). This event leads to the uncontrolled expression of E6 and E7, causing increased cell survival and division through the weakening of pro-apoptotic processes and cell cycle regulation, respectively. These increased levels of E6 and E7 oncoproteins are thought to mark the transition between viral infection and virus-induced malignancy (10). At this point, affected cells are no

longer committed to a terminal differentiation pathway, but rather, become transformed (11, 12). Though E6 and E7 are both considered indispensable for transformation efficiency, E6 can, in some instances, immortalize cells in the absence of E7 (6, 13, 14). Our lab has focused its resources on E6-dependent mechanisms underlying cervical carcinogenesis.

Splicing Mechanisms of High-Risk HPVs

High-risk, but not low-risk HPVs generate multiple transcripts of full-length E6 mRNA via alternative splicing (AS) (11, 15). AS enables the virus to expand its proteome from a modestly sized genome. This increases the genetic diversity and persistence of the virus in the face of host immunity, and increases its chance of survival (16). The number of E6 splicing patterns available to the virus varies and is dependent on the HR-HPV in question (17). In the case of HPV16, E6 is thought to yield four different species: E6*I, E6*II, E6*III, and E6*IV (18), with E6*I being the most abundant (19). How the virus determines which isoform(s) should be produced at any given time remains unclear. Nevertheless, we know that the splicing process is regulated by various factors, which influence the selection of specific splice sites for the inclusion or exclusion of nucleotide sequences. The full-length E6 isoform will be produced if the introns from the E6/E7 transcript remain unspliced. However, E6*I (E6*) results when the first 5' alternative splice site of the HPV E6/E7 ORF is chosen, leading to the removal of an intron and creating a premature stop codon (11). The E6* mRNA is then translated into a smaller protein consisting of 44 amino acids, approximately one-third the length of E6. Accumulating evidence suggests that E6* can bind and regulate its parental isoform, E6

(17), as well as the activities of cellular proteins like procaspase 8 (20). Indeed, researchers are now realizing that splicing may play an important role in cancer development (21, 22), and that splice variants may act functionally independent of its parent molecule in a biologically significant manner (23, 24). Such factors increase the appeal of exploiting anti-oncogenic properties of E6* for therapeutic interventions (20, 25, 26). Alongside these reports, other studies have shown that alternative-splicing patterns can be tumor-specific, and affect cell proliferation and drug-response. Yet, the mechanisms behind this regulation have not yet been clearly defined (22). Therapies designed to target disease-associated AS incorporate the use of small molecules, antisense oligonucleotides, and bifunctional oligonucleotides to manipulate aberrant splicing events, and are gaining recognition in various disciplines including cancer research (22, 27). These developments demonstrate proof-of-concept in managing splicing mechanisms for cancer treatment. In this proposal, we present data showing that the smaller isoform, E6*, inhibits tumorigenesis caused by full-length E6 in HPV-mediated cervical cancer (19). We find that E6* exhibits several desirable traits of AS therapy in being isoform-specific for and affecting the expression of the targeted protein (E6) (27). Intriguingly, our current studies suggest E6* may also inhibit the growth of tumors derived from cervical cancer cells that lack HPV.

Vaccination, Screening, & Prevention

Prophylactic Vaccination

Presently, the most effective protective factor against the most prevalent and high-risk types of HPV infection is prophylactic vaccination (28). It has been ten years since

the introduction of the first HPV vaccine (29). Since then, three vaccines, Gardasil, Cervarix, and Gardasil 9 have been made available to the public (30). The vaccines induce the production of neutralizing antibodies against HPV L1 capsid virus-like proteins (VLPs), which do not contain virus genetic material. The quadrivalent vaccine, Gardasil, protects against low- and high-risk HPV (LR- and HR-HPV, respectively) types 6, 11, 16, and 18 following full vaccination of all three doses at 0, 1, 2 and 6 months. The bivalent vaccine, Cervarix, prevents infection by HR-HPV types 16 and 18. Both Gardasil and Cervarix possess compelling prophylactic efficacy in preventing cervical, genital, and anal diseases. This protection is expected to persist for 7 years, or at least during the years of high infection risk for most individuals (31-33). Gardasil 9 is our newest prophylactic vaccine and is nonavalent, providing coverage against 9 genital wart-causing and oncogenic HPVs (Types 6, 11, 16, 18, 31, 33, 45, 52, 58). While Gardasil 9 is our most advanced prophylactic solution to HPV-mediated cervical cancer to date, at least a dozen HPVs have been found to cause cancer, and thus vaccination does not preclude the necessity of regular screening.

Although data for Gardasil 9 is lacking regarding cross-protection, we do know HPV infections caused by types other than the four covered by Gardasil and Cervarix (6, 11, 16, 18) are not reliably prevented by vaccination, and re-asserts the importance of continued screening. It is also important to note that Cervarix and Gardasil do exhibit cross-protection for certain high-risk types not included in the vaccine, but not all (*e.g.* HPV 31 is vulnerable to both bivalent and quadrivalent vaccines (34). Also, studies are warranted regarding the vaccine's long-term effects and how they might impact the occurrence of infections by other HPV types. It has already been noted that quadrivalent

and bivalent vaccines may exhibit cross-protection against HPV 31 and other types by 75 to 80 percent (35). However, concerns have emerged relating to HPV type-replacement. Type-replacement is an increased prevalence of other HPV strains that are not included in the vaccines, while vaccine-type HPV prevalence is decreased. It was recently reported that vaccine-type HPV has been reduced in vaccinated and nonvaccinated women, while nonvaccine-type HPV has slightly increased overall (36). Researchers do not expect type-replacement to occur frequently. However, studies are becoming more attentive to changes in the prevalence of various HPV types, which are expected to surface first within the sexually experienced population. Also, the amino acids comprising the L1 capsid protein are hypervariable and have diverged among HPV types due to host immune selection, resulting in poor cross binding (and cross-protection) of antibodies among distantly-related HPV types (3). Such discoveries should encourage the research community to continue seeking multivalent solutions to as many HPV types as possible without eliciting additional harmful results. To date, clinical trials have revealed that the most common adverse response to both vaccines are injection site reactions, which occur more frequently in vaccine groups rather than in participants given placebos (37).

Though most industrialized countries, like Great Britain, have already implemented structured HPV immunization programs, well-functioning programs geared towards adults and young adolescents have yet to be seen in many developing countries. However, there are globally funded systems with strong infrastructure that support the immunization of infants in developing countries (38). This anomaly is due to several challenges, which include the cost of the vaccines, though the biological, economical, and psychological disease burdens of HPV have been considered (37, 38). Therefore, it is no

surprise that less developed countries have not made HPV vaccination programs a

priority while other issues compete for the same limited governmental resources. The

most apparent considerations regarding vaccine distribution in these countries relate to

healthcare infrastructure, which can directly affect a country's ability to establish and

maintain immunization programs that target the vaccine's intended population –

adolescents. Other factors of significant importance comprise how to best promote these

programs in a way that does not aggravate ethnic/cultural sensitivities and attitudes about

vaccination against an STI (39, 40). This would further include easing parental concerns

about what an STI vaccine might imply if perceived as socially acceptable within the

targeted age groups. Perhaps if immunization programs were set up in an educational

setting, a stronger risk-perception might be instilled, which would encourage the

formation of better habits of awareness. In years to come, these types of educational

agendas might also improve adherence to the 3-dose regimen over the six-month

vaccination period and increase compliance with screening routines throughout a

woman's lifetime (41).

One clear limitation of the HPV vaccines is their lack of efficacy for those who

have already been exposed to the virus types included in the vaccines. Of course, this

exposure is directly correlated to increasing age and sexual experience (42, 43). For those

who fall into this group, including older women regardless of vaccination status, it is

important that screenings continue as outlined by the ACS guidelines for Cervical Cancer

Prevention and Early Detection. Therefore, integrated approaches of prevention and

detection are required if efforts against HPV-mediated cervical cancer are to be

maximized. Another important consideration for vaccination is the immune status of

potential vaccine recipients; the immune system must be intact (44). The immune

system's ability to clear antigens depends largely on its strength and competence. Thus,

immunocompromised women are especially in peril of HR-HPV infection progressing to

cancer (45).

The most common scenarios for compromised immunity are seen in HIV positive

individuals and organ transplant beneficiaries. Those infected with HIV have a greater

chance of HPV co-infection and progression to invasive cervical cancer as compared to

those without HIV (46, 47). The disparity observed here is most likely due to the immune

system's inability to effectively clear virus among this subset due to decreased immune

reactivity to HPV antigen (48, 49). It was also found that HPV infection is prevalent

among those receiving organ transplants (50), and that the infection increasingly persisted

throughout immunosuppressive therapy to moderate graft rejection (45). Despite these

challenges, researchers agree that previous prophylactic HPV vaccination is still

beneficial for organ transplant recipients as well as the HPV/HIV co-infected population

who receive HPV vaccination before becoming HIV positive. In these cases, any future

challenges of HPV infection following vaccination would be neutralized by an earlier

developed immunity prior to the individual presenting as HIV positive. This is based on

the premise that the protection conferred against the viral types represented in the vaccine

is expected to last for approximately the same time period as in others who are not

infected with HIV. However, what remains unclear is whether the vaccine will prove

effective for an individual already infected with HIV, or in any immunocompromised

state (49). The current understanding is that humoral immune responses remain relatively

intact following HIV infection. However, in such a state of immune weakness, it is

unknown whether protection against HPV can be sustained. Overall, individuals who have been vaccinated prior to becoming immune compromised are expected to benefit from vaccination by maintaining immune competency, because new HPV infections from these specific types and the risk of lesions reactivating from an ongoing, latent HPV infection would be reduced. Of course, they, like other individuals, will only be protected from types targeted by the vaccine, and it is imperative to note that questions regarding long-term safety in such vulnerable groups remain unanswered (42, 43, 45, 51, 52).

To this end, it is important that innovative therapeutic approaches to improve immunological surveillance and clearance of HPV continue to develop. It is well documented that cellular immune components contribute directly to natural clearance of the virus in most people. For instance, CD4+ and CD8+ cytotoxic T cells (CTLs) are thought to target HPV 16 early and late proteins, and active HPV-specific CTLs have been identified in patients with existing infections (53). Furthermore, researchers have found that in response to a vaccine containing E6 and E7 oncoproteins, CD4+ and CD8+ CTLs were stimulated, thus inducing the regression of HPV-mediated vulvar intraepithelial neoplasia (VIN) in 50 percent of subjects (54). Thus, a variety of other immunotherapy investigations are underway.

Screening

The ultimate goal of cervical cancer screening, as outlined by the ACS guidelines for the prevention and early detection of cervical cancer, is to prevent morbidity and mortality by determining appropriate treatment plans. In detecting the presence of HPV in the cervix, screening methods should serve to distinguish transient from persistent

infections, and to effectively diagnose disease while minimizing or avoiding unnecessary complications induced by these techniques. Because 50 percent of women diagnosed with cervical cancer in the U.S. have never been screened, the importance of diligent watchfulness cannot be over-stated. Moreover, when HIV positive women comply with regular detection methods and schedules, their otherwise 10-fold higher risk of progression to invasive cervical carcinoma is diminished (42, 43, 55). Earlier detection corresponds to better prognosis (56). Thus, it is ideal for precancerous women who are at significantly higher risk for invasive cervical carcinoma to be promptly identified and to undergo intervention. Though cervical monitoring is an integral component of preventing invasive disease at all stages (57), the U.S. Preventive Task Force (USPSTF) recommends that cervical cancer screening by pap smear start no earlier than age 21 for both non-vaccinated and vaccinated women and continue until age 65. The USPSTF also advises against routine HPV testing until age 30 unless indicated by abnormal cytology, as it is believed that younger women clear HPV infections more easily. Because cervical cancer detection programs are the most expensive preventive measure in developed countries, enhancements to existing screening techniques, or the development of completely innovative and economical methods would be beneficial.

The most utilized and successful of screening methods in lowering cervical cancer incidence rates (by 70 percent) is exfoliative cervicovaginal cytology, or the Pap test. The Pap test satisfies the aforementioned objectives for reducing the occurrence of squamous cervical carcinoma through appropriate screening (57). Pap tests are recommended for all sexually active women and/or women ages 21 and above. Now, a modified liquid-based version of the Pap smear is available. In a liquid-based Pap test such as Cytoscreen or

Thinprep, the cells are first filtered and fixed in preservative. Then the specimen is smeared on a glass slide, which is slightly in contrast to the conventional method of directly smearing a sample onto a microscope slide. Other tests such as visual inspection with acetic acid (58) (58) are useful in resource-limited settings. Further modifications of VIA include magnified visual inspection with acetic acid (VIAM) and visual inspection with Lugol's iodine solution (VILI) (59). Colposcopy, though considered more diagnostic, also allows a magnified visualization of abnormal cervical cells (56). Other cervical cancer screening tests may also be applied: pelvic examination – involving internal palpation of the reproductive organs; automated cervical screening techniques – supplemental imaging that reduces false positives from the cytological tests; computer imaging; polar probe – measuring the differences in electrical stimulation between normal and abnormal cervical tissue; laser-induced fluorescence – measuring spectroscopic differences in florescence between normal and diseased cervix; speculoscopy – cervical inspection using acetic acid with chemiluminescent light; and cervicography – photo development while using acetic acid (56).

Complementing the Pap test is the detection of HPV DNA. The direct testing for HPV DNA is becoming standard in many cervical cancer screening regimens, as its combined use with liquid-based cytology has generated results with even better sensitivity (up to 100 percent) for predicting high-grade cervical dysplasia (60). HPV DNA is usually obtained from cervical scrapes and/or biopsy specimens, and recent clinical studies continue to assert the unique value of HPV-DNA testing over cytology (61-63). Nevertheless, only time will tell the extent to which the Pap test will be replaced by the more economically appealing HPV-DNA test. To date, the FDA has approved

several HPV-DNA tests: the Hybrid Capture 2 HPV DNA test, the Cervista HPV HR test, the Cervista HPV16/18 test, the Cobas 4800 HPV test, and the Aptima HPV assay. Other commonly used assays not approved by the FDA include PCR and Southern Blot hybridization, the latter being the laboratory gold standard. Some other recent innovative HPV detection methods are complete HPV genotyping, HPV mRNA detection, HPV load quantitation, identifying HPV integration, p16 ELISA, methylation profiles, and the E6 Strip test (64, 65). Nevertheless, cervical cancer incidence and mortality seem to be on a downward swing in the U.S., primarily due to cytological gynecologic screening through the Pap test. Nevertheless, the global burden of HPV infection remains.

Prevention

The use of condoms can reduce the rate of HPV infection. One study showed that when condoms are used during all vaginal intercourse encounters, HPV transmission/infection is reduced by 70 percent. Even if a condom is used greater than half of the time, the risk of infection is still reduced by 50 percent (58). Another study similarly reports that condoms benefit users by promoting viral clearance and possible regression of CIN (66). The use of barrier protectors such as microbicidal and spermicidal gels can also reduce the risk of HPV infection (67, 68). The recent utilization of pseudoviruses has proven helpful in better understanding HPV invasion into keratinocytes through cell surface proteins. In these pseudovirus studies, carrageenan exhibited a microbicidal function by blocking virus particle attachment to heparin sulphate proteoglycans on cell basement membranes. Beyond its function on the tissue surfaces, carrageenan also exhibited post-attachment inhibitory actions. Carrageenan has

been used as a thickening agent in sex lubricants and Pap smear gels, and has shown

microbicidal function against a host of STI-causing microbes including HPV (68, 69).

Originally derived from red algae, it is structurally similar to heparin but several times

more potent. Therefore, it is able to bind virus more effectively than host cells and

thereby acts as a decoy receptor (67, 68).

During the decades that frequently occur between HPV infection and cancer

development, there exists a window of opportunity to intercept the process. Any

interventions that increase viral clearance, for example, would fit into this category.

Another possible approach would be to target the process by which viral DNA integrates

into the host chromosome, a relatively rare event that greatly increases the incidence of

cancer. One study, for example, has postulated that chronic inflammation and the

subsequent generation of reactive oxygen/nitrogen species (ROS/RNS) are harbingers of

DNA damage, causing high HPV integration rates. Furthermore, smoking, cervical

trauma induced by high parity, co-infection with other STDs, and long-term use of oral

contraceptives have all been linked to cellular oxidative stress (70). Thus, breaks in the

DNA induced by this oxidative stress increase the probability of viral integration (8). In

support of this model, HR-HPV types integrate more frequently than do LR-HPV. The

difference in integration occurrence suggests a distinction in the molecular variation

and/or susceptibility between high- and low-grade lesions. Therefore, progression to

cervical, and some anogenital, cancers is dependent on the presence of HR-HPV

integration into the host genome. Furthermore, scientists are finding certain patterns in

HPV integration events. In particular, the E2 ORF region of the viral genome is strongly

preferred over other sites of integration, and integration at this site, with its

accompanying loss of functional E2 protein, is linked to an increase in E6 and E7 oncogene expression (71, 72). Consequentially, integration leads to uncontrolled expression of the oncogenes and ultimately to cellular transformation.

The role of chronic inflammation and its link to radical species production in cancer pathogenesis is widely recognized. If increased levels of oxidative stress and ROS do indeed increase the frequency of integration and cancer, one would predict that antioxidant mechanisms that counteract the generation of radical species could therefore exert chemopreventative and chemotherapeutic effects; such mechanisms have indeed been described (73, 74). In contrast, other groups are studying ways to therapeutically harness the power of oxidative stress for actions against cancer cells. For example, the antimalarial drug, artemisin, was found to induce apoptosis in cervical cancer cells. The mechanism of action involves artemisin interacting with reduced iron to generate oxidative stress through ROS, as well as the destabilization of mitochondrial oxidative mechanisms (67, 75). These discoveries merit further research that continues to seek ways of preventing HPV-mediated oncogenesis.

Novel Therapeutic Initiatives to Treat HPV-mediated Cancers

The development of polyvalent HPV vaccines like Gardasil and Gardasil 9, in addition to Cervarix, were essential considering that at least a dozen additional HR-HPV types, which are also capable of causing HPV-mediated cervical cancer, were not covered by the first two vaccines (Cervarix and Gardisil) (20). In addition to these preventive strategies, it is also essential to invest in therapeutic strategies for the continuous management of microbe-related problems. Such a well-rounded approach to preventing

and curing HPV-mediated cervical cancer will increase treatment options for cervical cancer patients, the immunocompromised, and others with no or limited access to preventive programs.

The development of polyvalent HPV vaccines like Gardasil and Gardasil 9, in addition to Cervarix, were essential considering that at least a dozen additional HR-HPV types, which are also capable of causing HPV-mediated cervical cancer, were not covered by the first two vaccines (Cervarix and Gardisil) (20). In addition to these preventive strategies, it is also essential to invest in therapeutic strategies for the continuous management of microbe-related problems. Such a well-rounded approach to preventing and curing HPV-mediated cervical cancer will increase treatment options for cervical cancer patients, the immunocompromised, and others with no or limited access to preventive programs.

Current Clinical Treatments

Despite prevention initiatives to stay the tide of carcinogenesis caused by HR-HPV, thousands worldwide still require treatment. Currently, the most effective course of managing cervical carcinoma involves surgery and/or radiation. Surgery provides the management team with better insight into the extent of the disease because it allows the assessment of lymph node involvement (76, 77). The surgical options available range from total removal of the cervix (radical hysterectomy) to less extreme options that preserve the fertility of the patient (radical trachelectomy), and are somewhat contingent upon disease progression. Other procedures such as chemotherapy, radiotherapy, or a combination thereof are routinely used, and their utilization depends on cancer stage as well. Factors further impacting the course of management include pregnancy; disease

recurrence; fertility preservation; cervical location of the lesion; cancer type; age and general physical health. In any case, the most important treatment determinant for cervical cancer is stage of disease.

The staging of cervical cancer is based on the physical examination and is established by the International Federation of Gynecology and Obstetrics (FIGO). The World Health Organization reaffirms the FIGO organization of cervical carcinoma progression into four stages (I-IV):

- *Stage I:* cancer found only in the cervix

- *Stage II:* cancer found beyond the cervix in the vagina, excluding the lower third of the vagina, but has not spread to the pelvic wall.

- *Stage III:* cancer has spread to the lower third of the vagina and/or pelvic sidewall, and includes cases with kidney involvement

- *Stage IV:* cancer has grown beyond the pelvis and involves tissue of the rectum, bladder, and/or distal sites of metastasis.

The four main stages are then organized into sub-categories that further describe the extent of growth, adjacent tissue involvement, local organ participation, and metastasis to distal sites through the lymphatic system (78).

Surgery is the advised treatment for cervical carcinoma at stages I and II. The preferred procedure, radical hysterectomy (66), has a 75 to 80 percent cure rate according to the NCI and is the gold standard of treatment. Radical hysterectomy is the complete removal of the uterus, cervix, and upper portion of the vagina, and involves measuring metastasis to the parametrial and pelvic lymph nodes (79, 80). Surgery is immensely valuable for determining lymph node status, which is strongly correlated to survival (81).

The risk of lymph node metastasis is increased by 10 percent if tumor invasion reaches between 3 and 5 mm beyond the primary lesion. However, limitations of surgery include pelvic sepsis and thrombosis as well as vesicovaginal fistulas. There is no doubt that surgery is vital in the prospective treatment planning of the patient following operation because it allows the delineation of tumor metastasis. Yet, surgical options are contingent upon early detection, and thus time will always be one of the most important factors in predicting a prognosis (77).

Post-surgery radiotherapy (RT) is indicated if the tissue collected during surgery has a positive margin, which alludes to residual cancer and commonly occurs in late stage I (77). More advanced cervical cancer (stage IIb and higher) is treated with radiotherapy (RT), chemotherapy, or a combination of the two. However, surgery and RT both aim to completely eradicate malignancy and have equally positive results in attenuating disease in the initial phases. RT is generally substituted for surgery when circumstances render an operation less than optimal as in the case of elderly patients, obese patients, or patients with several co-morbidities (81, 82). Usually younger patients elect for surgery in order to preserve sexual function and to avoid side effects such as vaginal dryness and narrowing caused by scar tissue (as described by the ACS). There are two main types of radiation therapy: external beam radiation, and internal (implant) radiation usually referred to as intracavitary brachytherapy (83). External beam radiation therapy is aimed wholly at the pelvis, much like a regular x-ray, and is often accompanied by cisplatin chemotherapy.

Chemotherapy is the principal treatment option for recurrent and metastatic cervical cancer, and it is recommended by the ACS for the management of late stage I of

cervical cancer or higher. Chemotherapy can be curative or palliative. In early cervical disease, chemotherapy can be curative, but may also be given in more advanced stages (stage IV and recurrence) to alleviate the ravaging effects of the cancer itself and its related symptoms. Chemotherapy may also be given in the later stages to postpone the toxicities associated with it until absolutely necessary. Thus, designing optimal regimens suited for each case is essential to attaining both patient comfort and treatment success. Chemotherapy can also be given adjunctively to strengthen the effects of primary treatment, or provided post-operatively (84). In fact, the ways in which chemotherapy can be administered are numerous, ranging from single, doublet, triplet, or quartlet-agent regimens to combined chemoradiation routines. However, a few agents such as cisplatin, paclitaxel, and ifosfamide are distinguished for being somewhat autonomously potent (85). However, the success of single-agent chemotherapy generally depends on histology. Cisplatin, a platinum-based agent, is the accepted standard of chemotherapy for cervical cancer, and it improves survival in chemoradiation recipients as compared to the use of other chemotherapeutic drugs (86-90).

Multidisciplinary treatment might be indicated throughout any of the stages of cervical carcinoma, mainly depending on its aggressiveness. In fact, it is quite common for treatment schedules to include chemotherapy, radiation therapy, and surgery (82). The concurrent use of chemotherapy and radiation therapy is reported by the NCI to reduce cervical cancer mortality by 30 to 50 percent, particularly in late stage II. Alternatively, neoadjuvant therapy, defined as a specific sequence for delivering any treatment before a definitive therapy such as surgery or radiotherapy, may be employed. Neoadjuvant therapy is intended to prime the target tissue, thus making it more susceptible to primary

treatment (89, 91). The chemotherapeutic drugs most commonly used with radiation are

cisplatin, 5-FU, mitomycin C, and hydroxyurea, though cisplatin produces the largest

increase in survival by reducing mortality and recurrence (89, 90). Many times, the

sensitizing effects of drugs are needed to accentuate the value of other treatment methods

(82).

Molecular Therapeutic Strategies Underdevelopment

Along with clinical treatment of cervical cancer, molecular therapies that target

cervical cancer processes are also anticipated to contribute to the elimination of the

disease. The currently available treatment options described above for HPV-associated

malignancies are limited, however. According to the ACS, the 5-year survival rate drops

to 35% when a woman is diagnosed with Stage III cervical cancer, and the survival rate is

further halved if the cancer is stage IV. Research focusing on the development of the

prophylactic vaccine has forever changed the course of HPV-mediated cervical disease.

Nevertheless, it is clear that there is still an immense need for therapeutic options,

especially in developing countries where the positive, yet costly measures of preventative

initiatives remain to be implemented.

In contrast to prophylactic vaccines that target the L1 and L2 proteins and are

protective against HPV infections, therapeutic vaccines would ideally target molecules

such as E6 and/or E7 post-infection, which are directly linked to HPV-mediated

carcinogenesis (92). HPV early proteins will continue to provide insights regarding the

viral mechanisms used to take control over cellular processes. Of these viral components,

the E6 and E7 oncoproteins have long been recognized as the main mediators of HPV-

associated malignancies. Therefore, the idea that approaches targeting these two

oncoproteins are likely to act in an anti-oncogenic manner is reasonable. Such discoveries have the potential to exert a broad impact in the field of virology, as they will enable researchers to more fully understand virus-host interactions and how to better equip the body to respond to or even prevent infection. A few of the many strategies being developed to make HPV more immunogenic are discussed below.

One of the many challenges of HPV research that has left scientists puzzled is how it escapes detection by the immune system, since the time interval between infection and diagnosis can be several years. Therefore, many resources have been allocated to improve the virus' visibility to protective host mechanisms. Live, vector-based vaccines, bacterial and viral, can generate very robust cell-mediated and adaptive immune responses, and because of this they are preferred over peptide/protein vaccines. Specifically, bacterial vectors function well when they are packaged with antigen (genes or proteins), thereby alerting antigen-presenting cells (APCs) to initiate an immune response (93-96). With regards to viral vectors, a few viruses, such as the vaccinia virus, adenovirus, vesicular stomatitis virus, and alphavirus, show great potential. However, safety factors remain a high priority when viral vectors are considered, and these vectors must be properly reconstructed for use in both immunocompetent and immunocompromised individuals (92).

Though bacterial and viral show promise in their ability to deliver HPV antigens to elicit an immune response, they are not ideal therapeutic vaccine candidates for reasons relating to cost effectiveness and safety. However, in peptide-based vaccines, antigens from HPV are directly administered to induce a response from dendritic cells (DCs) via toll-like receptor (TLR) activation (97). The peptide vaccine platform would be

optimal for mass production, but the breadth of its efficacy is limited by the expression of only one major histocompatibility complex I (MHC I) phenotype; protein-based vaccines are not encumbered in the same way. If, however, specific immunogenic epitopes on peptides could be identified it would greatly remedy this difficulty. Similarly, protein-based therapeutic vaccines, like peptide-based vaccines, are advantageous for safety and tolerability. Protein-based vaccines are not restricted by MHC compatibility, but they cannot directly stimulate cytotoxic T lymphocytes (CTL). Yet, protein vaccine adjuvants are being considered to compensate for this weakness. Therefore, in general, any strategy that increases HPV antigen uptake by APCs, antigen presentation, or the CTL response is expected to improve the immunogenicity of viral proteins such as E6 or E7.

In the previously mentioned methods, HPV antigens would need to be presented to the host via a carrier (bacterial or viral) or produced outside of the system (protein or peptide) and then introduced to the host in this way. In contrast, one advantage of DNA-based vaccination is its capacity to increase immunological memory through constant antigen production. Because the immune response itself is not anti-vector, multiple "vaccinations" originating from a single DNA molecule are possible. Moreover, the antigens produced by DNA vaccines can be delivered in a variety of ways, resulting in the stimulation of both APCs and T lymphocyte immune defenses (98, 99). However, DNA vaccines also present the challenge of overcoming low immunogenicity due to limited APC specificity. Therefore, future developments must focus on antigen modifications so as to elicit a stronger dendritic cell adaptive immune response. RNA replicon-based vaccines have some advantages over DNA vaccines: 1) they are less likely to integrate into the host genome, thus decreasing the risk of cell transformation and 2)

they can potentially generate more protein than can DNA methods. One significant

limitation of using replicons is that RNA is inherently unstable (92, 100, 101).

Because tumor cell-based vaccines have shown promise in malignancies like

melanoma, colon and prostate cancers, many subscribe to this paradigm as the key to

solving the cervical carcinoma dilemma. The idea of manipulating cervical cancer tumor

cells into becoming more discernible by the immune system is based on the principle of

inducing their expression of immunomodulatory cytokines like IL-2 and IL-12 (102).

However, at present, it is unclear which cytokines might work best for HPV-mediated

cervical cancers. Furthermore, such an individualized treatment is costly and may border

on the impractical as compared to other recent advances in the field of cervical cancer

vaccination.

The use of monoclonal antibodies in cancer treatment is an appealing concept due

to the selectivity and specificity with which an antibody can bind to the molecule of

interest. Molecules participating in tumor progression can be targeted by antibodies

through three general mechanisms: 1) Recognition of specific tumor-associated receptors,

such as EGFR; 2) Binding to immune effector cells, and 3) Binding to tumor-promoting

molecules such as VEGF (which is of major importance since we found that HPV16 E6*

overexpression reduces VEGFR-1 expression in our SiHa tumor model). Though no

monoclonal antibodies have been approved for the treatment of cervical cancer,

researchers are accruing more convincing evidence of their value (103).

Though no small molecule inhibitor of HPV has yet been approved, a significant

amount of antiviral agent research has focused on five major potential targets for

intervention: 1) Inhibition of E1/E2 interactions, 2) E6 and E7 oncoprotein blockade, 3)

Direct interference with E6AP-mediated p53 degradation, 4) Interference with interactions between HPV and other apoptotic factors (i.e. Bax and FADD), and 5) Stalling the ubiquitin proteasome system to reduce the degradation of anti-tumor proteins.

E1 is the only enzymatic product of the viral genome, coding for an ATPase, and is thus an appealing target for molecular intervention. Indeed, if E1's binding and helicase properties could be blocked, DNA replication would be halted. Inevitably, impeding this process would also thwart the hijacking of cellular replication machinery for viral genome multiplication. Because the virus uses cellular replication factors derived from the host, current antiviral agents that block viral proteases and polymerases are ineffective in opposing HPV. Small molecular inhibitors called indandiones are recognized as the first class of molecules to block HPV DNA replication by interrupting E1-E2 binding. The presence of indandiones induces conformational changes in E2, forming a deep binding pocket through which the small molecule modifies protein activity (104). Repaglinides operate similarly to indandiones in disrupting E1-E2 binding, though their effect is reversible, and they are reported to occupy a larger area of the binding pocket than do their indandione counterparts. An important factor that must be considered is the fact that viral integration into the host genome frequently leads to loss of E1/E2 gene expression, meaning that established cancers are likely to have lost the molecules targeted by inhibitors of E1 and/or E2, thereby severely limiting their usefulness (105, 106).

E6 and E7 are frequently over-expressed in established cancers, making these two proteins potentially quite attractive as targets. E6 and E7 are zinc finger-containing proteins primarily responsible for the malignant alterations and de-differentiation of

keratinocytes observed during cell transformation. These changes occur following

integration of the HPV genome into host DNA (107, 108). During this process, the

regulators of viral replication, E1 and E2, are frequently disrupted, allowing over-

expression of E6 and E7. HR-HPV types induce cell immortalization and transformation

primarily through the over-expression of E6 and/or E7, which are best known for their

ability to accelerate the degradation of the p53 and retinoblastoma proteins (pRB),

respectively. The E6-mediated loss of p53 function leads to an insensitivity to apoptotic

signals as well as to a loss of cell cycle regulation at the G1/S checkpoint in response to

DNA damage. E7 contributes to the hyperplasia crisis by accelerating the degradation of

pRB and thereby stimulating cells in Interphase to re-enter the cell cycle at S phase (109-

111). Together, over-expression of the E6 and E7 oncoproteins decrease apoptosis and

increase cell division, setting the stage for cancer (112). Antiviral agents that could

partially, if not fully, inhibit E6 and/or E7 functions clearly have the potential to

negatively impact the carcinogenic process. One target of E6 is the p53 tumor suppressor,

which is degraded following association of E6 with the ubiquitin protein ligase, E6AP.

The E6/E6AP complex binds to p53 and initiates its ubiquitination and consequent

proteolytic destruction (113). This means that the downstream targets of p53, which

mediate cell cycle arrest and apoptosis, are not activated. Therefore, interference with the

E6/E6AP-mediated proteasomal degradation of p53 has been seen as another possible

strategy for treatment.

  While p53 and the proteins to which it is connected are clearly targets worth

exploring, other pro-apoptotic targets could prove just as important in halting the

progression of HPV-mediated disease. HPV16 E6 binds to several additional signaling

molecules in the intrinsic and extrinsic apoptotic pathways, including Bax, FADD, and procaspase-8, thus blocking their ability to interact with their normal partners and leading to their premature disposal by the proteasome (114, 115). It has also been reported that HPV16 E6 binds to both FADD and caspase 8 via DED residues, and a peptide corresponding to the binding site of FADD blocked both of these interactions. Expression of this peptide in HPV$^+$ cells was able to re-sensitize those cells to apoptosis triggered through the extrinsic pathway (20, 116). A search for small molecules capable of interfering with these interactions was conducted and several candidates were identified, primarily among the flavones and flavonols. Of these compounds, myricetin generated the lowest IC50 (850 nM) in assays designed to detect the inhibition of E6-procaspase 8 binding. (117) Unfortunately, myricetin lacks desired specificity in that it is known to inhibit several cellular proteins including kinases. Further library screening of small molecules to inhibit the interaction between E6 and its cellular partners such as caspase 8 and E6AP lead to the identification of an additional candidate, spinacine, an imidazole amino-acid derivative of histidine (117, 118). Of the molecules tested, spinacine demonstrated the greatest capacity to specifically inhibit E6 interactions with E6AP as well as caspase 8, and exhibited the lowest EC50 for E6/caspase and E6/E6AP binding (118). Interestingly, HR-HPVs seem to have their own natural inhibitor of the full-length E6 oncoprotein, suggesting that this property could be exploited for the purpose of designing small molecule inhibitors to mimic the activities of E6's natural inhibitor (19).

Purpose of Study

The scientific community has witnessed tremendous progress in the recent years towards the goal of eradicating HPV-mediated cervical carcinoma. Of these endeavors, routine Pap testing and the three prophylactic vaccines are particularly noteworthy for their documented and anticipated progress in decreasing disease burden. While progress in prevention must continue, complementary approaches providing better treatment options to populations not directly benefiting from vaccine therapies must also be developed. These groups include women who are already infected with HPV; immunocompromised individuals such as individuals co-infected with HPV/HIV; and organ transplant patients.

Over the past years, developments have made the eradication of cervical cancer a more achievable goal than in the past, and progress is occurring at each level of clinical management ranging from detection to the development of small molecule antiviral leads. Research targeting the HPV early proteins will continue to provide valuable insights regarding the viral mechanisms used to hijack cellular processes. Of the viral components, the E6 and E7 oncoproteins have long been recognized as the main mediators of HPV-associated malignancies. Therefore, approaches targeting these oncoproteins are quite reasonable. Such discoveries have the potential to exert a broad impact in the field of virology, as they will enable researchers to more fully understand virus-host interactions and how to better equip the body to respond to or even prevent infection.

Much is already known about the HPV life cycle, HPV-mediated cell transformation, and the mechanisms manipulated by the viral proteins, E6 and E7, to advance the virus' oncogenic agenda. However, there are many viral processes we know

much less about, such as the intricacies of splicing and the significance of its varying products in HR-HPVs. Thus, in exploring these phenomena we posed the following questions: 1) Which the of splicing products of HPV16 E6 are the most abundant and, in turn, what affect would its/their overexpression have on the growth of HPV$^+$ and HPV$^-$ cervical cancer cells *in vivo*? 2) What are the distinguishing molecular and histological features of tumors overexpressing E6* compared to control tumors in a xenograft model? 3) If the overexpression of HPV16 E6* in HPV$^+$ and HPV$^-$ cervical cancer cells causes a reduction in tumor growth, what cellular mechanisms are targeted by E6* to induce this change in tumor volume? Together, the result of these studies will allow researchers to pinpoint the mechanisms most important in regulating HPV-mediated cervical cancer, and will provide deeper insight into how best to neutralize or arrest the oncogenic influence of HR-HPVs.

CHAPTER TWO

THE SMALL SPLICE VARIANT OF HPV16 E6, E6*, REDUCES TUMOR

FORMATION IN CERVICAL CARCINOMA XENOGRAFTS

Maria Filippova, Whitney Evans, Robert Aragon, Valery Filippov, Vonetta M. Williams,

Linda Hong, Mark E. Reeves, and Penelope Duerksen-Hughes

Abstract

High-risk types of human papillomavirus (HPV) cause nearly all cases of cervical cancer. The E6 oncoprotein is produced as a full-length variant (E6) as well as several shorter isoforms (E6*). E6* inhibits certain oncogenic activities of E6, suggesting that it might play an anti-oncogenic role *in vivo*. To test this, we created E6*-expressing SiHa (HPV$^+$) and C33A (HPV$^-$) cells, then examined the ability of both the parental and E6*-expressing cells to form tumors in nude mice. We found that over-expression of E6* indeed decreased the growth of tumors derived from both SiHa and C33A cells, with the reduction greatest in tumors derived from E6*-expressing SiHa cells. These findings point to multiple anti-oncogenic characteristics of E6*, some of which likely involve down-regulation of the full-length isoform, and others that are independent of HPV. These data represent the first demonstration of biologically relevant E6* activities distinct from those of the full-length isoform *in vivo*.

Introduction

High-risk types of the human papillomavirus (HPV) are the causative agents of nearly all cases of cervical cancer, as well as a significant number of head, neck, penile, vulvar and anal cancers. Like many other viruses with small genomes, HPV (~8 kb) utilizes numerous mechanisms to increase the capacity of its genome to encode the proteins necessary for successful completion of its infectious life cycle. Alternative splicing of viral mRNA is one common mechanism used by many viruses, including HPV, to produce multiple proteins from a limited genetic sequence. The early HPV genes (E1, E2, E4, E5, E6 and E7), and in particular, E1, E2, E6 and E7, have been studied intensively over the last 2 decades (119-125). Their activities and roles in the virus life cycle and during cellular transformation have been well established, with the E6 and E7 oncogenes from high-risk types implicated as the major transforming agents. However, the functions of their alternatively spliced products have not yet been closely examined, even though increasing evidence suggests that these proteins may play important roles in the viral life cycle as well as contribute to carcinogenesis. For example, the splicing product E1^E4 has been linked to the productive life cycle. This function is associated with keratin networks, although the exact mechanism has not yet been elucidated (126). Additionally, overexpression of HPV-11 and HPV-16 E1^E4 has been shown to induce G2 arrest (127). Another example of an HPV splice product with a biologically important role is the spliced E8^E2C fusion protein, which functions as a negative regulator of viral transcription and replication for HPV 31 (128, 129).

The E6 and E7 oncogenes of high-risk HPVs are predominantly transcribed as an early transcript from the early promoter that produces bicistronic E6/E7 pre-mRNA. If

the introns within this E6/E7 transcript remain unspliced, the resulting mRNA expresses oncogenic full length E6. If, however, these introns are spliced out, several splice variants are possible. High-risk HPVs possess one 5′ donor splice site within the E6 coding region as well as multiple acceptor splice sites localized within E6 as well as in other genes (130). The E6*I and E6*II splice variants are produced when the acceptor sites are localized within the E6 sequence, and their protein products are quite similar as they differ only in the last 7 aa (Figure 1A). The ability to produce splice variants of E6 appears to be a characteristic of high-risk types of HPVs, as HPV 16, HPV 18, HPV 31, HPV 33 and HPV 45 do produce these variants (131), while low-risk types such as HPV 6b and HPV 11 do not (17, 18). This difference in the presence of E6 splice variants between low- and high-risk HPV types may suggest that E6 splicing plays a role in viral oncogenesis (132). An alternative suggestion is that this alternate splicing is somehow required for successful completion of the high-risk (but not the low-risk) life cycle.

One initial explanation for these splice variants was that such splicing, particularly splicing of intron 1 resulting in the E6*I transcript, benefited E7 expression (133). Investigators showed that when protein translation occurs on E6E7 mRNA, the space between termination of E6 translation and the initiation of E7 is not sufficient for effective translation of E7 (134). However, there is enough space on the spliced E6*I-E7 mRNA for termination of E6*I translation and re-initiation of E7 translation (134), leading to the suggestion that the purpose of E6 splicing was simply to promote E7 expression. Interestingly, although the presence of transcripts coding for E6 splice variants has been acknowledged for several years the activity and existence of the E6* protein has remained under question. The recent availability of antibodies with improved

45

sensitivity and specificity for E6 and E6* has now allowed us to demonstrate the presence of E6* at the protein level in cervical cancer cell lines, and also to observe differences in the expression levels of both E6 and E6* between the CaSki and SiHa cervical carcinoma cell lines (135). We found not only that E6* is indeed produced at detectable levels, but also that it is biologically active. For example, we demonstrated that the over-expression of E6* in SiHa cells sensitized these cells to apoptosis induced through the TNF and Fas pathways (135), indicating a possible pro-apoptotic role for this protein. Additional functions of E6* from HPV18 have been demonstrated by the Banks group (25), which showed that HPV 18 E6* can suppress the growth of transformed cells, and decrease the ability of the full-length isoform to degrade p53.

This type of data, suggesting that E6* possesses anti-oncogenic activities, led to the intriguing suggestion that the truncated isoform might play a distinct role in carcinogenesis, possibly by opposing activities of the full-length isoform. Each of the studies noted above was carried out in the context of cell lines, so to test the prospect that E6* might act as an anti-oncogene in vivo, we examined the influence of E6* on tumor formation in a cervical cancer xenograft model. To discriminate between activities that require the presence of the full-length isoform and activities that are independent of E6, we asked whether E6* could affect the formation of tumors from both HPV16^{+} SiHa cells and HPV16^{-} C33A cells. We were able to demonstrate that indeed, over-expression of E6* in both HPV16^{+} SiHa cells and HPV16^{-} C33A cells led to the inhibition of tumor growth in nude mice, with the inhibition of tumor growth greatest in tumors derived from HPV^{+} cells. These findings suggest the involvement of both E6-specific and E6-independent activities.

Materials & Methods

Reagents

MG132 (Sigma-Aldrich)) was dissolved in DMSO to yield a 10 mM stock, then stored at -20 o C until use. Doxycycline (Dox) (BD Biosciences) was dissolved in PBS to a 1 mg/ml stock. α-Flag agarose, α-Flag-HRP conjugated antibodies and α-β-actin were obtained from Sigma-Aldrich. α-VEGFR-1 antibodies were purchased from Epitomics, α-E6 N-terminus antibodies were obtained from Euromedex (France), α-E-cadherin was purchased from Cell Signalling Technology, α-caspase 8 antibodies were purchased from BD Biosciences, α-HA was obtained from Roche Applied Science, and secondary ImmunoPure Antibody HRP conjugated antibodies were obtained from Fisher Scientific. α-p53 p122 antibodies were purified from conditioned media obtained during hybridoma growth.

Cell Culture

U2OS cells, derived from a human osteosarcoma, as well as SiHa, C33A, and CaSki cells, derived from cervical carcinomas, were obtained from the ATCC. U2OS cells and their derivatives were cultured in McCoy's 5A medium (Invitrogen), and SiHa, C33A, and CaSki cells were maintained in MEM medum (Mediatech, Inc). Media was supplemented to contain 10% fetal bovine serum (Invitrogen), penicillin (100 u/ml) and streptomycin (100 µg/ml) (Sigma-Aldrich). Media for U2OS cells expressing E6 under the control of the tet-responsive element (UtetE6wt and UtetE6) was supplemented with Tet-FBS (BD Biosciences). The description and production of stably transfected U2OS cell lines capable of expressing variable amounts of HA-E6 wt, regulated by different

concentrations of Dox present in media, has been described previously (136, 137).

Plasmids, Transfection, & Production of Stable Cell Lines

The plasmid pTre-E6 (BD Clontech), which expresses HA-tagged HPV 16 E6 wild type (E6 wt) has been cloned and described previously (137, 138). The plasmids pFlag-E6 wt (pE6wt), pFlag-E6*(pE6*), and pFlag-E6 large (pE6) were obtained by cloning E6 wt, E6*I, or E6 large, respectively, in frame with the N-terminal Flag-tag and the C-terminal C-myc-tag into the pFlag-myc CMV-22 vector (Sigma-Aldrich). To produce stable cell lines expressing E6, pE6*, or the vector control, the appropriate plasmids were transfected into SiHa or C33A cells using the TransIt-LT1 Transfection Reagent (MirusBio), as directed by the manufacturer. Forty-eight h post-transfection, G418 (500 μg/ml) was applied to cells and antibiotic selection applied for 3 weeks. Expression of the desired protein was assessed by immunoblot.

Cell Viability & Growth Assays

To measure cell survival following TNF-α treatment, SiHa-derived cells were seeded at a density of 104 cells per well on a 96-well plate and allowed to adhere overnight. TNF-α (50 ng/ml) was applied in the presence or absence of 10 μg/ml of cycloheximide (Cx), and cells were incubated for 16 h prior to measuring cell viability by CellTiter-Glo Luminescent Cell Viability Assay (Promega).

To estimate cell growth, 5×10^3 cells were seeded into four 96-well plates and allowed to adhere overnight. The next day (day 0) and for the 3 days following, cells were fixed in 10% formaldehyde. Staining of cells was performed using crystal violet

solution (Sigma-Aldrich). Absorbance at 570 nm was measured after dissolving crystal violet in 100 μl of 10% acetic acid (Fisher Scientific).

Immunoblotting & Co-immunoprecipitation

For immunoblot analysis, cells (10^6) were lysed in 100 μl of Laemmli lysis buffer, then lysates were sonicated and loaded onto a SDS-PAGE gel. After protein transfer to Immobilon P membranes (Millipore Corporation) and blocking the membrane with 1% BSA, primary antibodies were applied in TBST containing 1% BSA. After incubation with primary antibodies overnight at 4°C, membranes were washed with TBST. Secondary ImmunoPure Antibodies (α-mouse or α-rabbit) conjugated with horseradish peroxidase (Fisher Scientific) were applied to the membrane for 1 h, and the detection of signals was performed using the chemiluminescent SuperSignal West Dura or Pico Maximum Sensitivity substrate (Fisher Scientific).

For immunoprecipitation and co-immunoprecipitations, cells were treated with 5 or 10 μM MG132 for 16 h prior to preparation of lysates. For co-immunoprecipitation 107 U2OS cells were co-transfected with pFlag or pFlag-E6* together with pHA-E6 for 48 h, Flag-tagged proteins were precipitated using Flag-agarose, and bound proteins were subjected to SDS-PAGE, then transferred to a PVDF membrane and detected by immunoblot. For the SiHa- and C33A-related experiments, 5×10^6 pooled cells were lysed, then the Flag-E6* proteins were precipitated using Flag-agarose. Detection of Flag-E6* was performed using α-Flag-HRP antibodies.

PCR

Total RNA from cells was isolated using TrizolR, then tissues were homogenized in TrizolR using a Tissue Miser homogenizer (Fisher Scientific). cDNA was synthesized using SuperScript II reverse transcriptase (Invitrogen) according to the manufacturer's protocols. Semi-quantitative RT-PCR was performed using:

5'-GCACCAAAAGAGAACTGCAATGT-3' and

5'-TGGGTTTCTCTACGTGTTCTTGAT-3' primers

to detect both E6 isoforms (E6 primers), or

Flag-F 5'-CCAAAATCAACGGGACTTTC-3' and

Flag-R 5'-CACAGGGATGCCACCCGGG-3'

to detect FlagE6* transcripts.

Quantitative real-time PCR was performed to measure the concentration of E6 isoforms using primers designed by Hafner et al. (106), using the iTaq Universal SYBR Green Supermix kit according to the manufacturer's protocol (Bio-Rad). Concentrations of cDNAs were normalized using GAPDH or β-actin expression.

Implantation of Tumor Xenografts in Mice

Five–week old female Crl:CD-1-Foxn1nu nude mice were obtained from Charles Rivers (Cambridge, MA), maintained in pathogen-free conditions and fed a standard irradiated chow diet while housed within the Animal Research Facility of the Loma Linda VA Medical Center (Loma Linda, CA). Mice were kept at 25o C, with a 12 h light-dark schedule and free access to food and water. All experiments were done under protocols approved by the Institutional Animal Care and Use Committee.

Six mice were injected subcutaneously with 31 Ga. needles in the flanks bilaterally. On the left side, 7.5 x10^6 SiHa pFlag cells or 5x10^6 C33A pFlag cells were injected; and on the right side, 7.5 x10^6 SiHa E6* cells or 5x10^6 C33A pE6* cells were injected, forming two tumors per mouse. Tumor formation and size were evaluated at 4-7day time intervals for approximately 13 weeks for SiHa-derived tumors and for 8 weeks for C33A-derived tumors. Tumors were measured using calipers for two perpendicular measurements, and tumor volume was calculated according to the formula: Width2 x Length/2. In one mouse injected with SiHa-derived cells, and in one mouse injected with C33A-derived cells, both tumors gradually decreased until they disappeared. These mice were excluded from the reported averages.

All mice were killed by CO2 inhalation followed by thoracotomy. Tumors were explanted and dissected to obtain 2 samples from each xenograft: formalin-fixed for paraffin-embedding for morphological and immunohistochemical assays, and snap frozen in liquid nitrogen for RNA isolation.

Histochemistry & Immunohistochemistry

Tumor pieces fixed in formalin were embedded in paraffin, and sections were cut from tumors. For histochemical analysis, sections were stained with haematoxylin-eosin and analyzed under a light microscope. Localization of VEGFR-1 was performed using immunohistochemistry. Rabbit monoclonal antibodies (Epitomics) specific to VEGFR-1 (N-term) were applied to tissue sections at 1:100 dilutions. Visualization of VEGFR-1 was performed using Vestastain Elite ABC kit (Vector Laboratories). Slides were counter-stained by haematoxylin and analyzed under a light microscope.

p53 ELISA

The procedure for performing the p53 ELISA has been previously described (139). The protein concentration in the cell lysates was measured using the Bio-Rad DC protein assay (Bio-Rad).

Results

E6*I is Expressed at a Higher Level than is E6*II in Both CaSki & SiHa Cells

When expressed in mammalian cells, the high-risk E6 oncoprotein is expressed as both full-length and smaller isoforms, with the smaller isoform comprising approximately one-third of the full-length sequence from the N-terminus of E6 (Figure 1A, highlighted residues). Because the two smaller isoforms expressed from the E6 gene differ only in the last 7 aa of their C-terminus (Figure 1A), the difference in size between them is too small to be distinguished by immunoblot (Figure 1B). At the RNA level, however, 3 transcripts of ~0.5 kb, ~0.3 kb and ~0.2 kb can be detected, which can be respectively translated into 3 proteins: the full length isoform of 158 aa and two smaller isoforms of 50 aa (E6*I) and 55 aa, (E6*II) (Figure 1A). To determine which transcript corresponds to the smaller protein band (Figure 1B), we estimated the relative levels of E6*I and E6*II expression using qRT-PCR. qRT-PCR of E6*I and E6*II transcripts was performed using mRNA isolated from the cervical cancer cell lines, CaSki and SiHa (Figure 1C), as well as from U2OStetE6 cells (18, 135) (Figure 1D). In these U2OStetE6 cells, E6*I and E6*II are expressed from a stably-transfected plasmid expressing the wild-type sequence for E6 (pE6 wt). Expression of E6 wt is under control of the tet response element, and high and low levels of HA-E6 expression are regulated by the concentration of doxycycline in the

culture medium (Figure 1D bottom panel). As shown in Figure 1C and D, the E6*I transcript is several times more abundant than the E6*II transcript in CaSki, SiHa and U2OS cells, and the ratio of the levels of the E6*I transcript to the E6* II transcript does not depend on the level of E6 expression in U2OStetE6 cells. This data, therefore, suggests that the smaller E6 band detected by immunoblot (Figure 1B) is translated primarily from the E6*I transcript. The prevalence of E6*I over E6*II expression allowed us to focus on E6*I in the following experiments, and this gene and its corresponding protein are henceforth referred to as E6*.

E6 Expression Increases Levels of Caspase 8, p53 & E-cadherin*
& Sensitizes SiHa Cells to TNF

To assess the properties of E6* during tumor formation, we first created and characterized cervical cancer-derived cell lines expressing E6* in the context of both an HPV$^+$ and an HPV$^-$ background. SiHa cells stably transfected with the empty vector pFlag are HPV$^+$ cells with a low level of E6* expression (control), while SiHa cells stably transfected with pE6* are HPV$^+$ cells with a high level of E6*. A similar pair of cell lines originating from the HPV$^-$ C33A cervical cancer cell line was also created by stably transfecting these cells with either pFlag (C33A pFlag, control) or pE6* (C33A E6*). After selection in G418, pE6*-expressing SiHa-derived lines were analyzed for their level of E6* expression by immunoblot. Eighteen clonal lines were expanded and screened, and of these, six were selected on the basis of high levels of E6* expression (data not shown). An equal number of cells from each of these six lines were combined, and the resulting pooled cells (SiHa pE6*) were used for further study.

A


```
             *        20          *        40          *        60          *        80
E6large :  MHQKRTAMFQDPQERPRKLPHLCTELQTTIHDIILECVYCKQQLLRREVYDFAFRDLCIVYRDGNPYAVCDKCLKFYSKI :  80
E6*II   :  MHQKRTAMFQDPQERPRKLPHLCTELQTTIHDIILECVYCKQQLLRREIIKNTYA------------------------- :  55
E6*I    :  MHQKRTAMFQDPQERPRKLPHLCTELQTTIHDIILECVYCKQQLLRREVY------------------------------- :  50

             *        100         *        120         *        140         *
E6large :  SEYRYYCYSVYGTTLEQQYNKPLCDLLIRCINCQKPLCPEEKQRHLDKKQRFHNIRGRWTGRCMSCCRSSRTRRETQL :  158
E6*II   :  ----------------------------------------------------------------------------- :   -
E6*I    :  ----------------------------------------------------------------------------- :   -
```

B

Figure 1. Alignment and expression of E6, E6*I and E6*II. A) Alignment of the protein sequences for E6, E6*I, and E6*II. The common amino acids for these three proteins are highlighted. B) Expression of Flag-E6 wt, Flag-E6, and Flag-E6*I at the protein level. U2OS cells were transiently transfected with Flag-E6 wt, Flag-E6, or Flag-E6*I. Forty-eight h post-transfection, expression was analysed by immunoprecipitation using α-Flag agarose, followed by detection using antibodies directed against Flag-HRP. C and D)
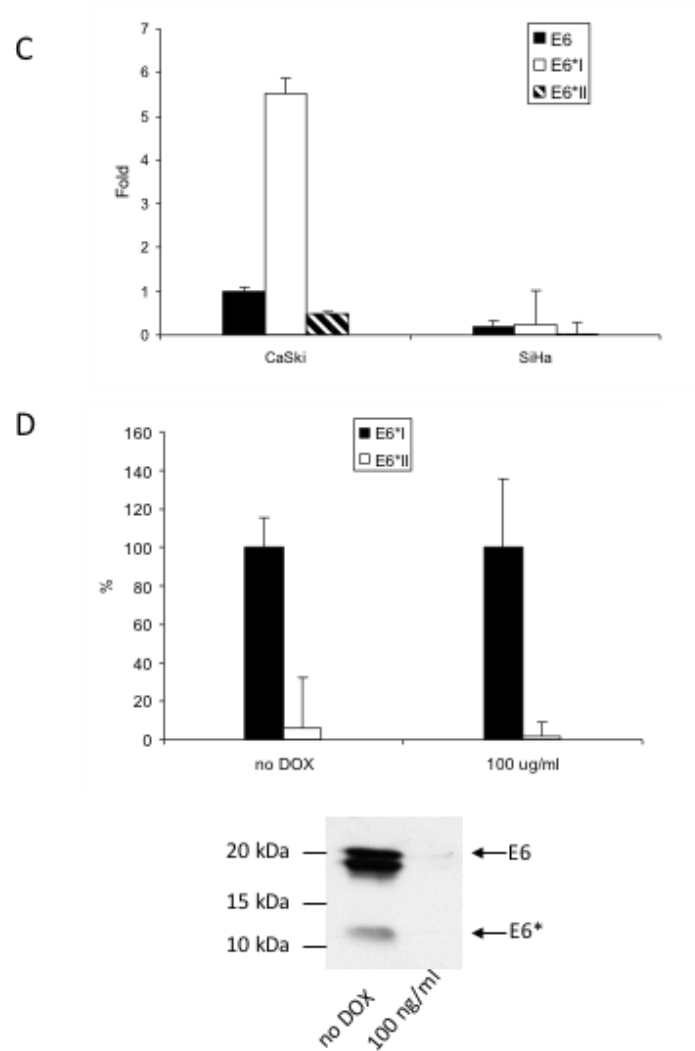
Figure 1. C and D) Expression of E6*I is higher than expression of E6*II in cervical cancer cell lines (C) and in U2OS cells stably transfected with pHA-E6 wt under the control of the tet promoter (UtetE6wt) (D). qRT-PCR was performed using primers designed specifically for E6*I and E6*II. 5' primers for E6*I and E6*II were homologous to exon-exon splicing regions, while the 5' primer for E6 was designed for intron I of E6. The 3' primer used for each of the three isoforms was homologous to the C-terminus of E6. Primers for GAPDH were used to normalize input of cDNA. C) The ratio between the levels of mRNA expression of E6, E6*I, and E6*II in CaSki and SiHa cells is presented as a fold-change relative to E6 expression in CaSki cells. D) UtetE6wt cells were grown in media without Doxycycline (Dox) (high level of E6 expression), or in media containing 100 ng/ml of Dox (low level of E6 expression). The level of E6*I expression in UtetE6wt cells at low and high levels of Dox was set at 100%, and the level of mRNA expression of E6*II was expressed as a percentage of E6*I expression. The lower panel of (D) shows the expression of E6 and E6* in UtetE6wt cells in the presence and absence of 100 ng/ml Dox, as determined by immunoblot using antibodies directed against the N-terminus of E6.

55

The use of pooled cells was employed in order to minimize the possible impact of site-specific integration events. Figure 2A shows expression of E6* in the pooled SiHa pE6* cells as compared to those in the pooled SiHa pFlag cells, demonstrating increased expression levels of E6* in cells harboring the pE6* plasmid. The relative levels of E6 and E6* expression at the mRNA level are shown in Figure 2B, and demonstrate that the level of the full-length E6 transcripts does not change significantly following over-expression of E6*. Expression of E6* in the analogous pooled C33A-derived lines is shown in Figure 2C. To create these cells, 24 stable cell lines were isolated, characterized, and equal numbers of the six C33A-derived lines with the highest expression of E6* were pooled.

We have previously demonstrated that E6 protects U2OS cells from TNF-induced apoptosis by decreasing the level of procaspase 8. In contrast to E6, E6* stabilizes procaspase 8, sensitizing these cells to TNF-induced apoptosis (18, 135), and we found this to be true in SiHa cells as well. Figures 2D and 2E demonstrate that increasing the level of E6* expression in SiHa cells (SiHa pE6*) leads to higher levels of procaspase 8 as well as p53, and Figure 2F shows that this increase in E6* sensitizes cells to TNF. With regards to cells derived from C33A, it is known that mutant p53 is expressed in these cells at high levels (140); thus, over-expression of E6* was unable to change the levels of p53 in these cells (data not shown). We also found that E6* expression causes an increase in E-cadherin levels in SiHa cells, though not to the level observed in CaSki cells (Figure 2G). E-cadherin is a marker of epithelial cell-cell adhesion and its function is lost in many epithelial cancers (141). C33A cells expressed no detectable E-cadherin,

initially, and expression of E6* did not increase expression of the adhesion protein in these cells (data not shown).

Expression of E6 in HPV16$^+$ SiHa Cells Dramatically Reduces Tumor Formation in a Xenograft Mouse Model*

To determine whether expression of E6* affects tumor formation in vivo, 7.5 x 10^6 cells of SiHa pFlag and of SiHa pE6* were injected subcutaneously into each of five nude mice. SiHa pFlag cells were injected on the left side, while SiHa pE6* cells were injected on right side of the same mouse. Tumor formation was assessed by measuring the tumor size approximately every four or five days with calipers. On the 88th day, mice were sacrificed, and the tumor was isolated and divided into two pieces. One piece was paraffin embedded, sectioned, and stained using haematoxylin-eosin, or used for immunohistochemical detection of VEGFR-1; the other part was used for RNA isolation. Figure 3A shows a representative mouse with developed tumors. On the left side of each mouse, a large tumor derived from SiHa pFlag cells developed, while on the right side of the same mouse, a tumor derived from SiHa pE6* cells was in most cases barely noticeable. The relative size of the two tumors following dissection is shown in the bottom panel. Figure 3B shows the relative tumor growth for SiHa pFlag and SiHa pE6* tumors, calculated as a percent of the tumor size on day 4 when measurements began. During the first 19 days following injection, the size of all tumors decreased and remained fairly constant until day 34. SiHa pFlag and SiHa pE6* tumors experienced a similar pattern of reduction in size, probably due to a gradual decrease in the inflammation that accompanied the initial injection of the cells.
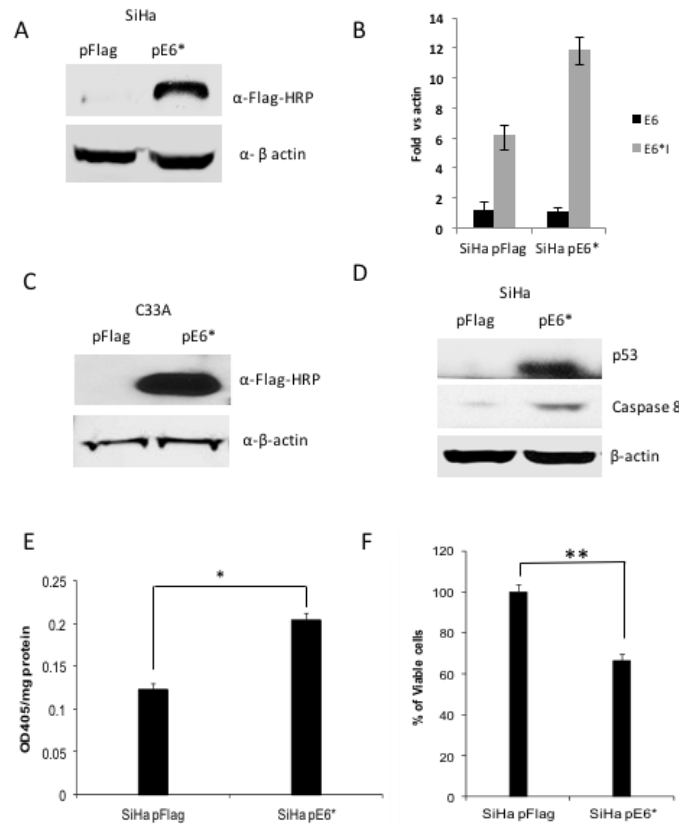
Figure 2. Expression and activity of E6* in SiHa and C33A cells. A and C) Pooled SiHa pE6*(A) and C33A pE6* (C) cells express Flag-E6*. PVDF membranes carrying the SDS-separated proteins were probed with α-Flag-HRP antibodies, and α-β-actin antibodies were used to normalize for protein load or immunoprecipitation input, respectively (A and C) (bottom panels). B) The ratio between the levels of mRNA expression of E6 and E6* in SiHa pFlag and SiHa pE6* cells is presented as a fold-change relative to β-actin expression as determined by qRT-PCR. D, E, F and G) Expression of E6* in SiHa cells affects the level of expression of procaspase 8 and p53 as detected by immunoblot (D) and by p53-ELISA (E), as well as TNF-α-induced apoptosis (F) and expression of E-cadherin (G). D) Cell lysates prepared from SiHa pFlag and SiHa pE6* cells were treated with 10 uM MG 132 for 16 h prior to lysis. Detection of p53 and caspase 8 was performed by immunoblot, β-actin was used for normalization. E) 10^6 SiHa pFlag or SiHa pE6* cells were treated with either mitomycin C or DMSO (control) for 16 h prior to lysis. p53 ELISA was performed as described in Material and Methods. Data is presented as the optical density at 405 nm per mg protein in cells treated with mitomycin C, minus that same measurement in cells not treated with mitomycin C. Measurements were made in triplicate, and the error bars represent the standard deviation. * indicates a 0.98 level of confidence. F) 10^4 cells per well were seeded onto a 96-well plate. Cells were treated with 10 ug/ml of cycloheximide in the presence or absence of 50 ng/ml of TNF-α for 16 h. Cell viability was monitored using the CellTiter-Glo Luminescent Cell Viability Assay (Promega). ** indicates a 0.99 level of confidence.
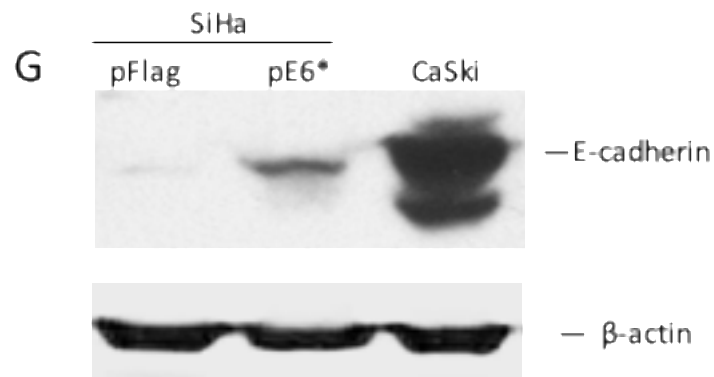
Figure 2. G) The E-cadherin level was detected by immunoblot in lysates prepared from SiHa pFlag, SiHa pE6* and CaSki cells, normalized by β-actin.

Following day 34, tumors derived from the SiHa pFlag cells began a rapid period of

growth, reaching an average volume of more than 320 mm^3, (650% of the day 4 value) by

the 88th day. In contrast, tumors derived from the SiHa pE6* cells did not grow until day

74. Following this, a slow growth of SiHa pE6* tumors was observed, reaching an

average volume of 67 mm3 (less than 200% of the day 4 value) by day 88 (Figure 3B).

Overexpression of E6* in the tumors derived from the SiHa E6* cells was

demonstrated by RT-PCR (Figure 3C). Sections from corresponding tumors were pooled

and used for RNA isolation. When the Flag F and Flag R primers were used,

corresponding to sequences in the cloning vector, the product detected in the SiHa pFlag

tumors was less than 0.1 kb in size, while in the SiHa pE6* tumors, the PCR product was

greater than 0.3 kb (left and middle panels). When primers designed for the E6 gene were

used, both the full-sized E6 and the E6* isoform were detected in both types of tumors

(right panel). However, E6* was detected at a much higher level in tumors derived from

the SiHa pE6* cells than in tumors derived from the control cells, demonstrating that this

over-expression had not been lost during *in vivo* passage.

Analysis of cross-sectioned tumors stained with haematoxylin-eosin revealed that

tumors derived from SiHa pFlag and SiHa pE6* cells differ in their morphological

characteristics (Figure 4). The large tumors derived from SiHa pFlag cells were

consistently heterogeneous with sheets and nests of squamous cell carcinoma combined

with extensive leukocytic cell infiltration and large areas of unstructured necrotic masses

with imbedded damaged cells (Figure 4A and 4B, left-side panels).

In contrast, the tumors derived from SiHa pE6* cells were significantly smaller

than the SiHa pFlag tumors. These smaller tumors were more consistently well

circumscribed and encapsulated, and the structure was more homogenous, with the majority of the tumor being composed of squamous cells (Figure 4A and 4B, right-side panels). One dramatic difference between the SiHa pFlag and SiHa pE6*-derived tumors was in the size of necrotic areas; only a small focal amount of this necrosis was observed in 3 of the 5 SiHa pE6*-derived tumors.

In addition, we employed immunohistochemistry to assess VEGFR-1 expression in these tumor sections because the distribution and level of expression of this molecule has frequently served as a marker of tumor angiogenesis (142). In tumors derived from the SiHa pFlag cells, high levels of VEGFR-1 expression were observed in large areas of the tumor, where cells presumably had a low oxygen supply, while areas with healthy squamous cells exhibited low levels of VEGFR-1 (Figure 4C, middle panel). However, in tumors derived from the SiHa pE6* cells, where tumors consisted primarily of healthy cells, expression of VEGFR-1 was nearly undetectable (Figure 4C, right panel). Only a slight staining was observed in areas where necrotic cells were also found.

Expression of E6* Also Reduces Tumor Formation
When Expressed in HPV⁻ C33A Cells

To determine whether expression of E6* would be able to reduce tumor formation in the absence of HPV proteins, we repeated the in vivo experiment using the HPV-negative C33A pFlag and C33A pE6* cell lines (Figure 2C). In this experiment, 5×10^6 cells of C33A pFlag and C33A pE6* cells each were injected subcutaneously into five nude mice. C33A pFlag cells were injected on the left side, and C33A pE6* cells were
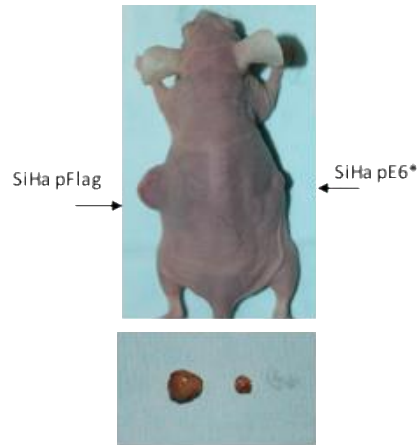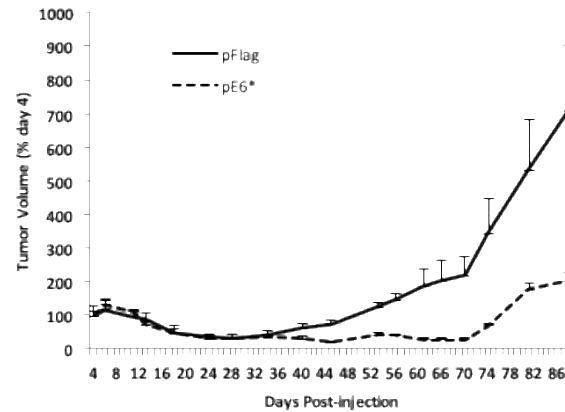
Figure 3. Overexpression of E6* in SiHa cells reduces tumor growth in a tumor xenograft model. A) A representative mouse bearing a tumor derived from SiHa pFlag cells on the left side and a tumor derived from SiHa E6* cells on the right side (upper panel). The bottom panel shows representative tumors following isolation the 88th day post-injection. B) The relative average tumor volume observed for the SiHa pFlag and SiHa pE6* tumors. The volume of the tumor at day 4 was set at 100%, and error bars represent the standard error of the mean. ** indicates that the mean tumor volumes at day 88 were significantly different between the two groups (P>0.99).
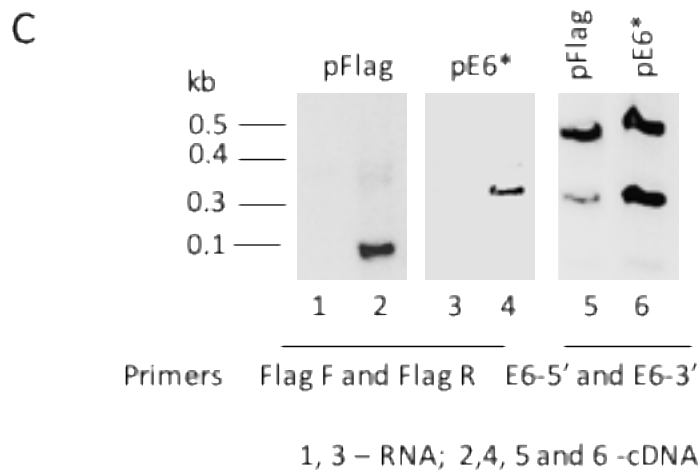
Figure 3. C) Expression of E6 and E6* at the mRNA level in dissected tumors derived from SiHa pFlag and SiHa pE6*. Expression of Flag-E6* and Flag-E6 transcripts in tumors was detected by RT-PCR using primers specific for Flag-E6* (Flag F and Flag R primers) (left and medium panels) and for E6 (E6-5' and E6-3') (right panel). 1, 3 – RNA; 2, 4, 5 and 6 – cDNA.

injected on right side of the same mouse. Tumors produced by C33A cells were observed to grow more rapidly than the tumors derived from SiHa cells. Two mice were sacrificed at day 48 due to the rapid growth and resulting size (>1500 mm^3) of the tumor, and the other three mice were sacrificed when tumor size reached 1500 mm^3. Figure 5A shows a representative mouse with tumors. On the left side of each mouse a large tumor derived from C33A pFlag cells developed, while on the right side of the same mouse a smaller tumor derived from C33A pE6* cells was formed. The relative size of the two tumors following dissection is shown in the bottom panel of Figure 5A.

Figure 5B shows the relative tumor growth for C33A pFlag and C33A pE6* tumors, which is calculated as a percent of the tumor size on day 7 when measurements began. In contrast to the growth of tumors induced by SiHa-derived cells, the tumors derived from C33A cells did not show a reduction in size at the beginning. Tumors started to grow a week after cell injection and gradually enlarged, with more rapid tumor growth observed following day 45 post-injection. At day 53, the average size of tumors derived from C33A pFlag reached >900 mm^3, corresponding to more than 1200% of their size at day 7. However, tumors derived from the C33A pE6* cells reached a size of only 273 mm^3, slightly exceeding a 400% increase (Figure 5B).

Cross-sectioned tumors derived from C33A pFlag and C33A E6* cells and stained with haematoxylin-eosin were characterized by consistently heterogeneous sheets and nests of squamous cell carcinoma combined with large areas of unstructured necrotic masses with imbedded damaged cells and patches of connective tissues.
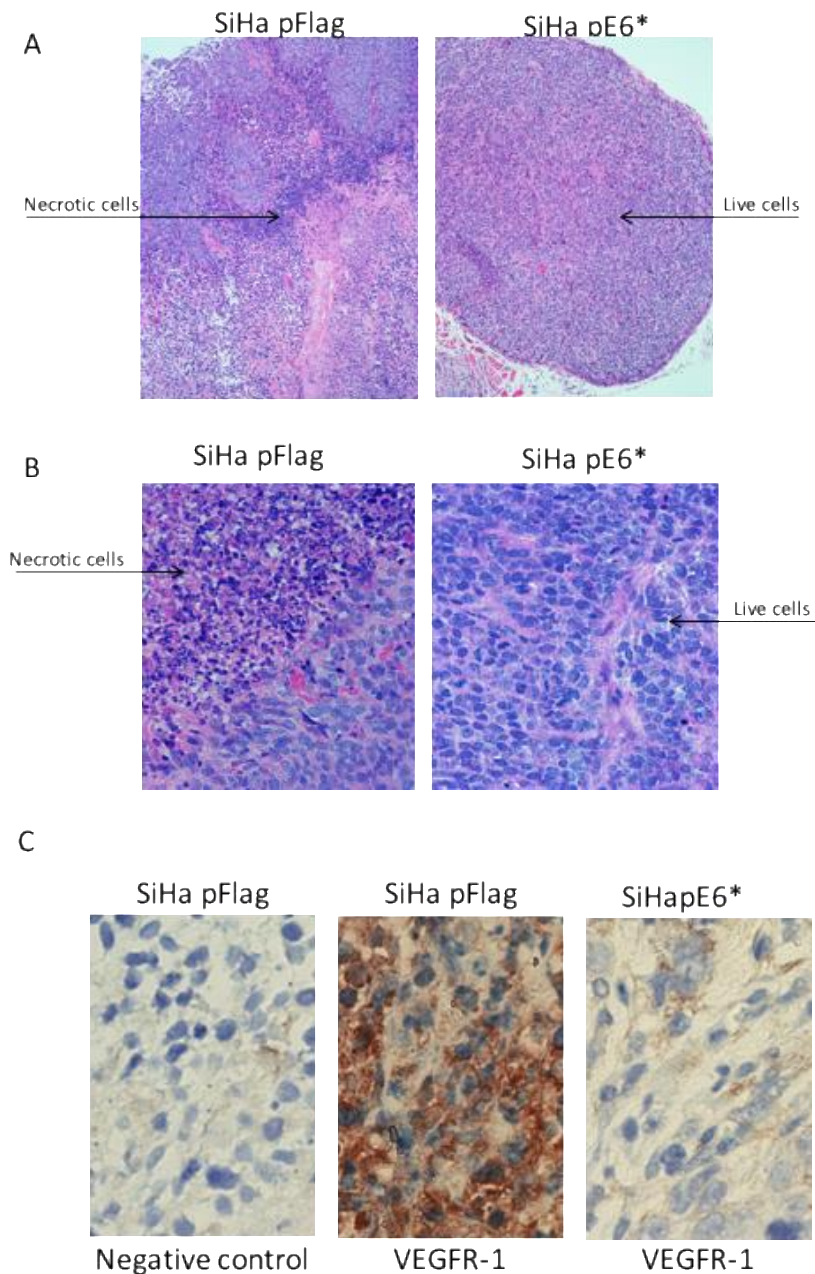
Figure 4. Sectioned SiHa tumor xenografts were stained with haematoxylin-eosin (A and B), and VEGFR-1 was detected by immunohistochemistry (C). A) Objective x10; B and C) Objective x40. Arrows indicate live cells, necrotic cells, and connective tissues. C) α-VEGFR-1 antibodies were applied to the indicated sections, while no primary antibodies were applied to negative controls. Sections were then counter-stained with haematoxylin.

Differences between C33A pFlag and C33A E6* included larger areas of necrotic masses and connective tissues and smaller areas of squamous cells in C33A pFlag tumors (Figure 6A and B). However, no significant difference in the expression of VEGFR-1 between C33A pFlag and C33A pE6* tumors was detected by immunohistochemistry (Figure 6C, middle and right panels).

Reduction of Tumor Growth by E6 in Tumors Derived from HPV$^+$ SiHa Cells is Greater than in Tumors Derived from HPV$^-$ C33A Cells*

A comparison of the growth curves (Figures 3B and 5B) revealed that the development of tumors from the SiHa and C33A cells followed different dynamics. To determine how expression of E6* impacted these dynamics in both the HPV$^+$ SiHa and the HPV$^-$ C33A cells, the average relative sizes of E6*-expressing tumors as a percentage of the control pFlag tumors (in the same mouse) in SiHa and C33A cells were compared. For this comparison, we selected the time period beginning when tumors were first detectable and ending just prior to sacrifice (days 40 – 88 post-injection for SiHa cells, Figure 3B; and days 17 – 48 post-injection for C33A cells, Figure 5B), during which exponential tumor growth occurred. Figure 7A shows the relative sizes of the E6*-expressing tumor as compared to the corresponding control tumor during this period. Interestingly, the trends differed between the two cell lines. While the relative sizes of the E6*-expressing SiHa tumors were relatively low throughout this period of exponential growth with the ratio changing less than two-fold, the relative sizes of the E6*-expressing C33A tumors were higher throughout the experiment, and decreased more than two-fold over this time period.
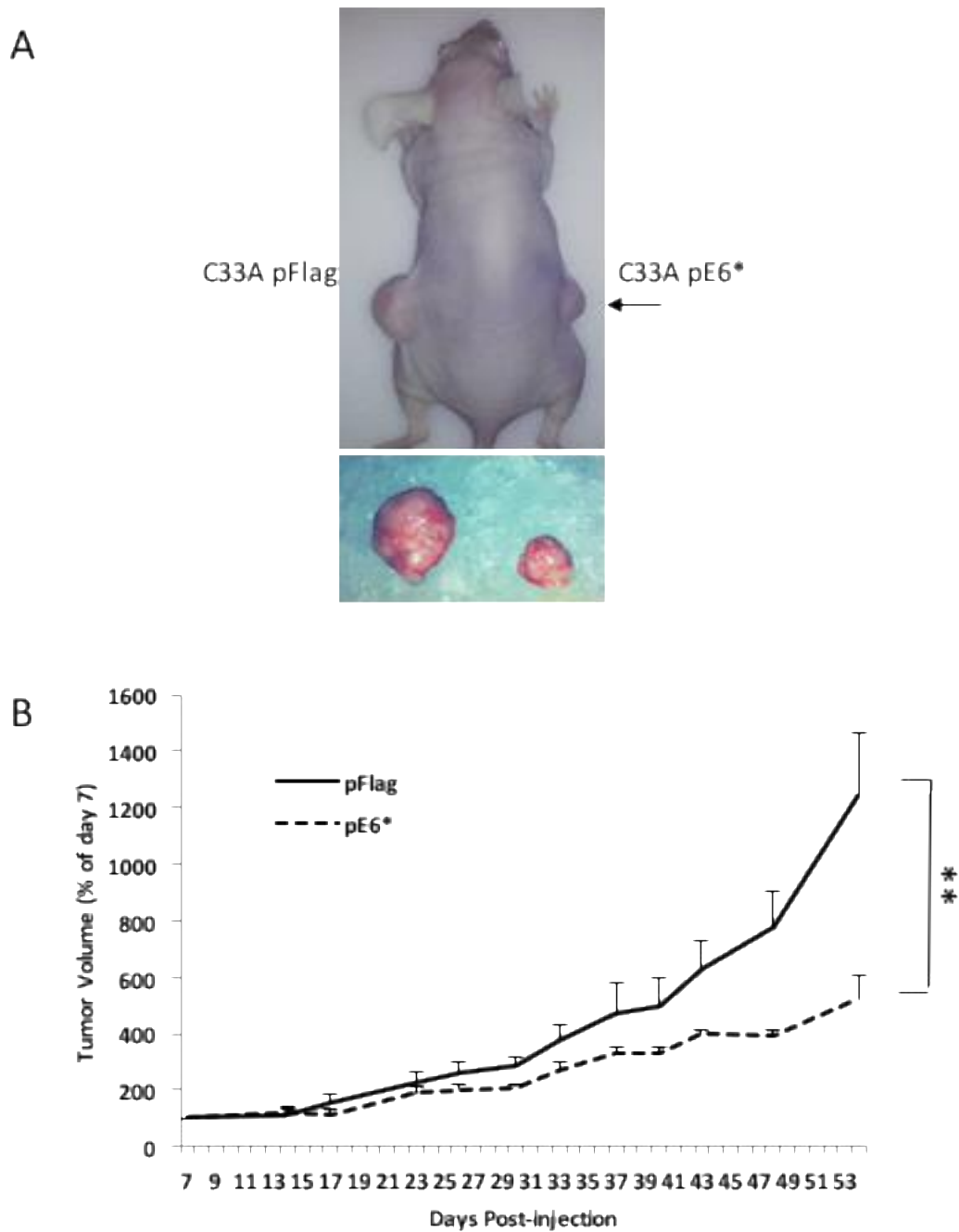
Figure 5. Over-expression of E6* in C33A cells reduces tumor growth in a tumor xenograft model. A) A representative mouse bearing a tumor derived from C33A pFlag cells on the left side and a tumor derived from C33A E6* cells on the right side (upper panel). The bottom panel shows representative tumors following isolation on day 53 post-injection. B) The relative average tumor volume observed for the C33A pFlag and C33A pE6* tumors. The volume of tumor at day 7 was set at 100%. Error bars represent the standard error of the mean. ** indicates that the mean tumor volumes at day 53 were significantly different between the two groups.

Figure 6. Sectioned C33A tumor xenografts were stained with haematoxylin-eosin (A and B), and VEGFR-1 was detected by immunohistochemistry (C). A) Objective x10; B and C) Objective x40. Arrows indicate live cells, necrotic cells, and connective tissues. C) α-VEGFR-1 antibodies were applied to the indicated sections, while no primary antibodies were applied to negative controls. Sections were then counter-stained with haematoxylin.
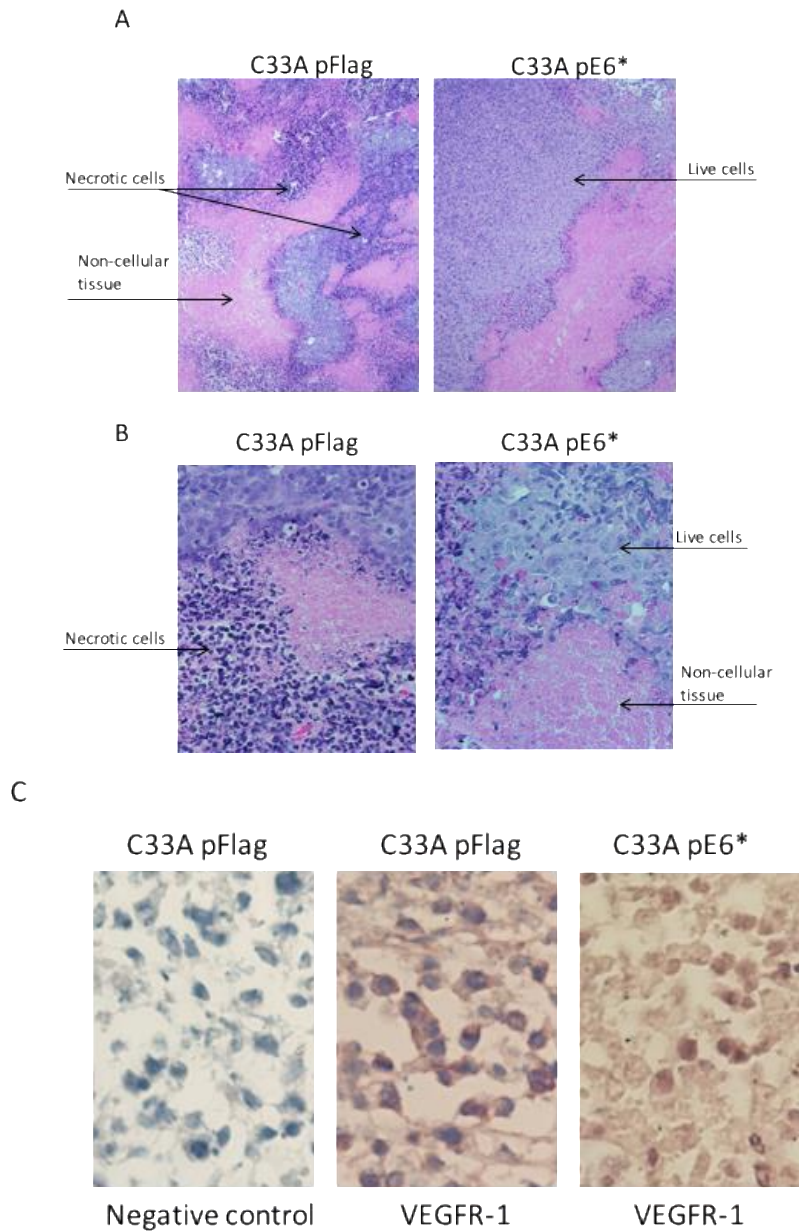
One conclusion from this comparison is that the control SiHa tumors grew

significantly faster than did the corresponding SiHa E6* tumors, with the relative

difference remaining somewhat constant over time. In contrast, the difference between

the size of control C33A-derived tumors and those derived from the corresponding E6*-

expressing cells was smaller and increased over time, implying increasing effectiveness

of the viral protein. In particular, the E6*-mediated reduction in size in the context of

SiHa cells ranged from 67% to 92% on day 88, (average of 79%), while the

corresponding values for the C33A cells ranged from 44% to 72% at day 53 (average of

56%), a difference of more than 20% (Figure 7B). The significance of the difference in

these curves was estimated by one-way ANOVA (P-value = 2.51×10^{-7}). These results

suggest that E6* may act through a different set of pathways in the two cell lines. In

summary, E6* appears to be more effective in suppressing tumor growth in the presence

of E6 (SiHa cells) than in its absence (C33A cells).

E6 Binds to & Inactivates the Full-length Isoform*

One possible explanation for the greater reduction of tumor size caused by E6* in

SiHa as compared to C33A cells is that the shorter isoform inhibits the oncogenic

activities of the full-length isoform. It is known, for example, that E6* proteins from

both HPV16 (135) and 18 (26) can bind to E6 and modify its activities. Figure 7C

demonstrates this binding. In this co-immunoprecipitation experiment, U2OS cells were

co-transfected with either pFlag or pFlag-E6* together with HA-E6. Flag-tagged proteins

were precipitated using Flag-agarose, and the co-immunoprecipitated HA-E6 was

detected by immunoblot. The results show that HA-E6 was precipitated by Flag

antibodies from cell lysates where Flag-E6* was expressed, confirming the binding interaction between the proteins.

Inactivation of E6 activity by E6* has the potential to affect cell viability and growth. To determine if this was likely to account for the difference in tumor growth, the growth rates of both SiHa and C33A control cells and cells expressing E6* were compared. Cells from each line were plated and allowed to grow for 3 days, and the number of viable cells measured every 24 h using crystal violet. These results (Figure 7D) demonstrate a difference in growth rate between SiHa pE6* as compared to SiHa pFlag cells, as well as a lack of variance in the growth rate between C33A pFlag and C33A pE6* cells. Because the SiHa pE6* cells grow slower than SiHa pFlag cells, an E6*-mediated reduction in growth rate could contribute to the observed difference in SiHa-derived tumor formation from SiHa cells, though this is unlikely to be the case for C33A-derived tumors. Colony-forming assays also suggest that the over-expression of E6* in SiHa cells impedes the formation of colonies, though this trend is not apparent in C33A cells (data not shown).

Overall, these data show that E6* can bind to the larger protein, and that its expression reduces the growth rate of HPV$^+$, but not of HPV$^-$ cells. Clearly, this mechanism has the potential to contribute to the reduction of tumor size in our HPV$^+$ SiHa xenograft model. However, the C33A data (Figure 5) indicates that additional mechanisms, which are independent of the interaction(s) of E6* with other HPV proteins, participate as well.

A

B
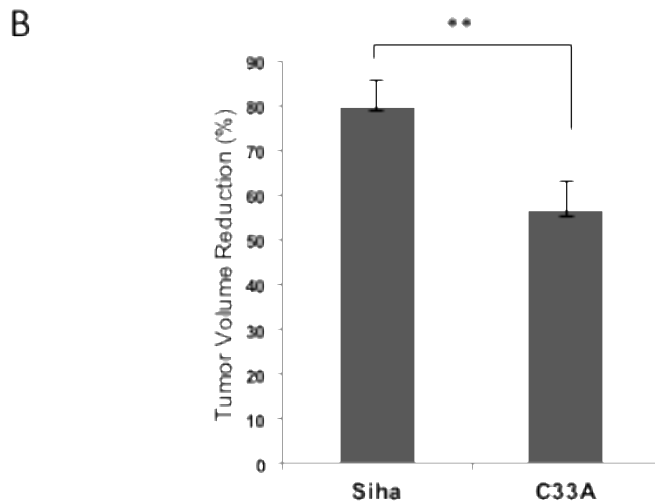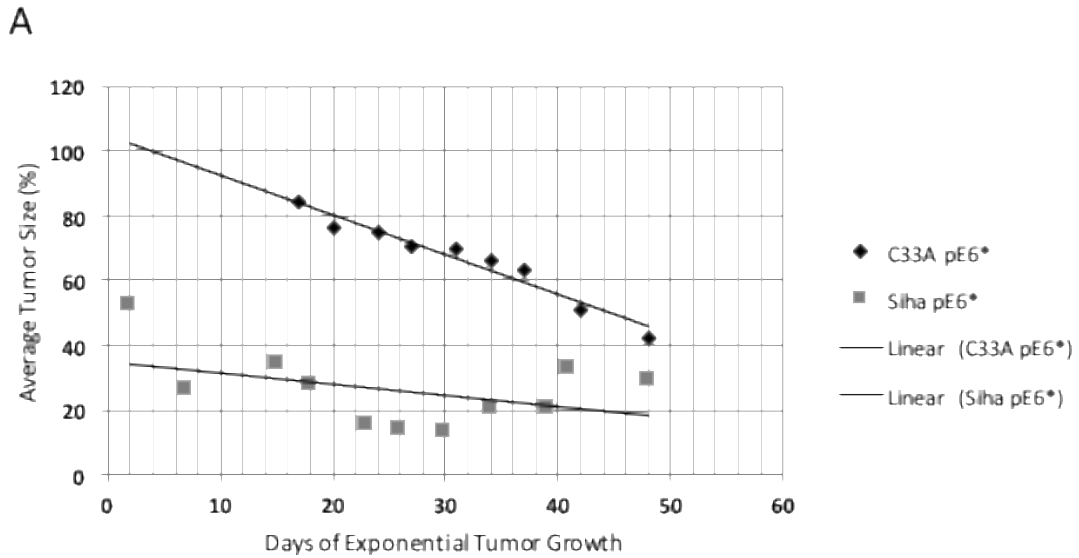
Figure 7. Expression of E6* resulted in a greater reduction of tumor volume in tumors derived from SiHa cells than in tumors derived from C33A cells. A) The relative volume of pE6* tumors in each cell line was calculated as a percentage of the volume of the pFlag tumor in the same mouse during exponential tumor growth, and the average relative size of the E6* tumors was plotted along with the linear trend. B) The average reduction in tumor volume was calculated as the difference between the volume of the pE6*-derived tumor and the volume of the pFlag-derived tumor from the same mouse at the date of harvest, expressed as a percentage of the volume of the corresponding pFlag tumor. The significance of A) and B) was determined by one-way ANOVA. ** indicates that the means of tumor volume reduction at day 53 were significantly different between the two groups.
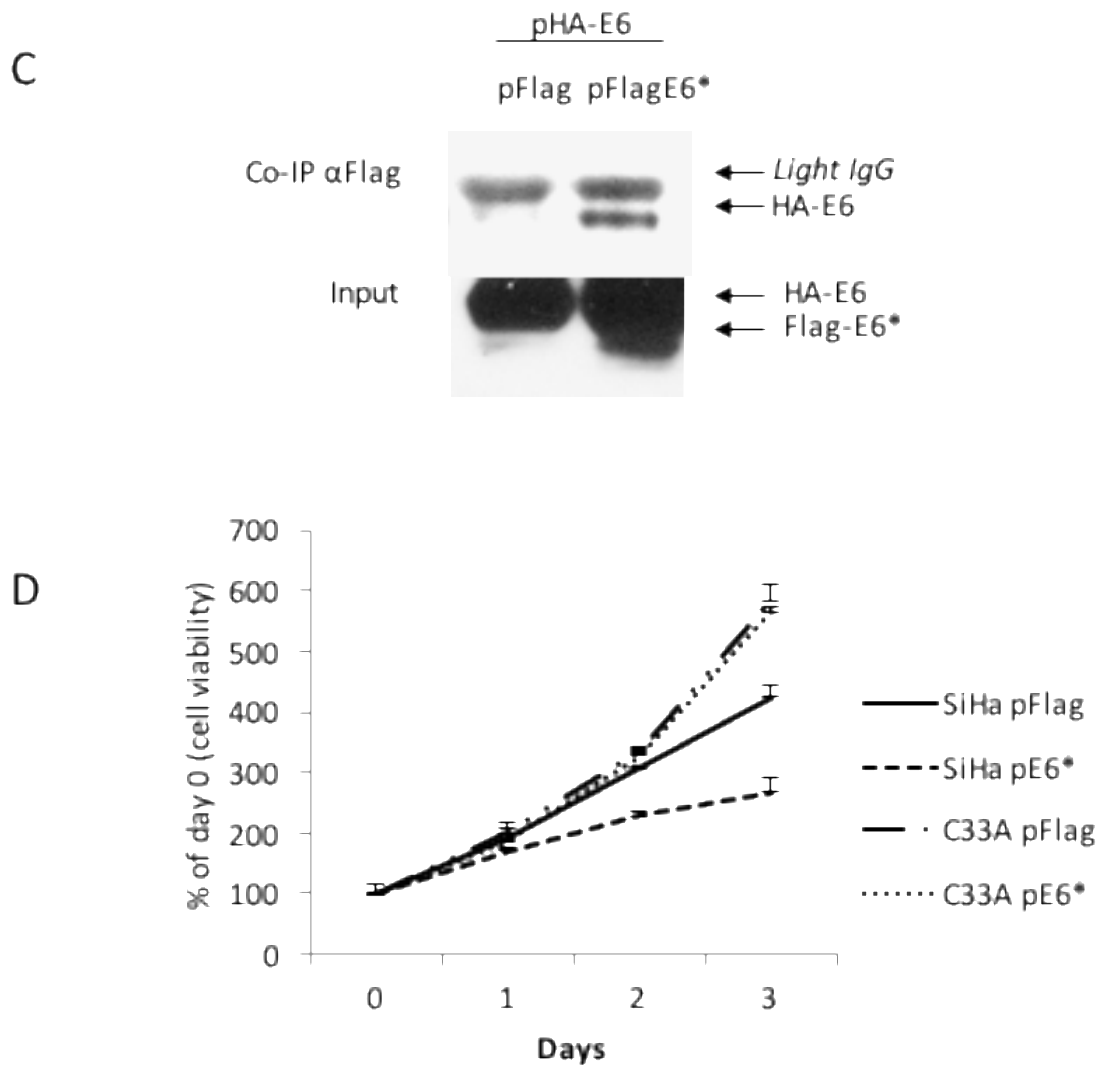
Figure 7. C) E6* binds to E6. 10^7 U2OS cells were co-transfected with pFlag or pFlag-E6* together with pHA-E6 for 48 h, and cells were treated with 10 μM MG132 for 16 h prior to preparation of lysates. Flag-tagged proteins were precipitated by Flag-agarose, and HA-E6 was detected using HRP-coupled antibodies directed against HA (upper panel). Input levels of E6 and E6* in the lysates (lower panel) were determined by immunoblot using antibodies directed against the N-terminus of E6. D) E6* inhibits cell growth in SiHa but not C33A cells. 5 x 10^3 cells per well were seeded into four 96-well plates. Twenty-four h later (day 0) and on the following three days, cells were fixed in 10% formaldehyde. Staining of live cells was performed using crystal violet. Absorbance at 570 nm was measured after dissolving the crystal violet in 100 μl of 10% acetic acid. Measurements were made in triplicate, and error bars represent the standard deviation.

Discussion

Studies over the past few decades have focused intensively on the activities and roles of E6 proteins from high-risk types of HPV during the process of cellular transformation, clearly implicating E6 as a major transforming agent. However, the role of the smaller splice isoform, E6*, in the carcinogenic process (if any) has not yet been established. In the present study, we provide insight into the behavior of the E6* protein during tumor growth in an in vivo nude mouse xenograft model demonstrating that E6* displays both E6-dependent and E6-independent anti-tumor activity. The difference in tumor size observed in the presence and absence of E6*, when expressed in both HPV$^+$ (SiHa) and HPV$^-$ (C33A) cells (Figures 3 and 5), is dramatic and consistent, strongly indicating an anti-oncogenic role for E6* in this context.

Opposing functions of alternatively spliced variants have previously been demonstrated for a large number of cellular and viral genes, including many that are associated with cancer (21, 143). Alternative splicing of viral transcripts is a well-known phenomenon, as it provides a way to increase the encoding capacity of viral genomes, and thus to enhance viral versatility and adaptability. Although alternatively spliced HPV transcripts for the E6 isoforms have been known for over two decades (reviewed in (Zheng, 2006 #190)), an appreciation of the opposing biological functions of the full-length and truncated isoforms is relatively recent (25, 135, 144). One reason for this delayed appreciation has been the historical difficulty of demonstrating significant expression of E6* at the protein level. Indeed, it was only after the availability of appropriate antibodies (Euromedex, France) that our laboratory was able to document, for

the first time, endogenous expression of E6* as a protein in cervical cancer cells at levels comparable to that seen for expression of the full-length isoform (135).

Cellular models have previously been used to demonstrate opposing functions of E6 and E6* on components of cellular apoptotic pathways. In particular, we have reported that E6 expression protects cells from apoptosis induced by members of the TNF superfamily (such as TNFα, FasL and TRAIL) by accelerating the degradation of procaspase 8. In contrast, the binding of E6* to procaspase 8 leads to its stabilization and increased cellular levels of the protein (18, 116). Consistent with these differential effects, we found that E6 and E6* actually bind to different sites on procaspase 8 (20). Extending and supporting these findings, we demonstrate here that plasmid-expressed Flag-E6* is able to re-sensitize SiHa cells to TNFα–induced apoptosis (Figure 2F) through an increase in the level of endogenous procaspase 8 (Figure 2D). Radio-sensitization by HPV 16 E6*I has previously been reported in cells derived from oropharyngeal squamous cell carcinoma (145), again indicating that E6* can enhance apoptosis. In addition, the negative influence of E6* on cell growth in lines transformed both by HPV and by other mechanisms has been demonstrated for HPV18 E6* (25), in good agreement with the data from our SiHa model (Figure 7D). Interestingly, E6* expression can affect functions in addition to apoptosis and cell growth. During the transformation process, epithelial cells frequently lose their epithelial cell-cell contacts (146). One of the epithelial adhesion proteins involved is E-cadherin, which is responsible for Ca^{2+}-dependent cell-cell adhesion (147). We found that expression of E6* was partially able to restore the level of E-cadherin in SiHa cells (Figure 2G), although not in C33A cells.

Interestingly, E6* can sometimes mimic E6 activity in the absence of E6. Banks and coworkers found that E6* from HPV 18 can accelerate the degradation of some PDZ-containing proteins, including Akt, Dlg, and MAGI-1 (17, 25, 26, 144). In the absence of the full-length isoform, it may be that E6*, corresponding to the N-terminal half of E6, can mimic E6 through self-oligomerization and in this way down-regulate the expression levels of certain PDZ-proteins. Together, these data indicate that E6* is not simply a smaller version of E6, capable of carrying out only a subset of the biological activities executed by E6, but that E6* can act independently of full-length E6.

The *in vivo* studies described here deepen and expand our understanding of E6*, and build on previous cellular data by showing that E6* activity can indeed reduce tumor growth in a xenograft nude mouse model (Figures 3 and 5). Interestingly, we found that tumor growth inhibition by E6* is greater in tumors derived from SiHa cells, which are HPV16-positive, than in tumors produced by C33A, which are HPV-negative (Figure 3B, 5B 7A and 7B). This difference implies that E6* acts by interfering with the oncogenic activity of the full-length protein as well as through one or more HPV-independent mechanisms. Consistent with this idea, we found that E6* does indeed bind to the full-sized isoform (Figure 7C) and inhibits its ability to accelerate degradation of p53 (Figures 2D and 2E). Together, the biological activities of E6* reduce the growth rate of SiHa pE6* cells (Figure 7D), contributing to a reduced growth rate of E6*-expressing tumors. These findings are consistent with earlier studies showing inhibition of tumor growth in a xenograft model following expression of shRNA directed against E6 (148). In another study, the inhibition of both E6 and E7 expression led to reduced cell growth and invasive ability for SiHa cells both *in vitro* and *in vivo* (149).

E6* also displays HPV-independent anti-tumor activity, as it was able to reduce the size of tumors derived from HPV- C33A cells (Figure 5). Interestingly, this anti-tumor activity is likely not p53-related because C33A cells express mutant p53 (140). In addition, we found that the over-expression of E6* in C33A cells does not affect cellular growth, at least *in vitro* (Figure 7D). In this case, therefore, it is likely that E6* engages one or more other mechanisms to reduce tumor growth. For example, activation of AMPK, a cellular metabolic sensor that modulates normal and cancer cell metabolism, inhibits cervical cancer cell growth through a decrease in FOXM1 levels. FOXM1 is a transcription factor reported to be abnormally upregulated in human cervical squamous cell carcinomas, and is involved in down-regulating p27 and p21 (150). Since the phenomenon of growth inhibition through decreased levels of FOXM1 by AMPK activation was observed in four different cervical carcinoma cell lines, including C33A (150), we speculate that perhaps oncogenic factors such as FOXM1 could play an important role in the mechanisms through which E6* inhibits growth of C33A-derived tumors in our *in vivo* system as well. In addition to this possibility, we note that the deregulation of Wnt/B-catenin signaling is prevalent in many cancers of epithelial origin, including cervical cancer (151, 152), and it may be that expression of E6* leads to Wnt/B-catenin dysregulation. Our future studies will focus on elucidating the mechanisms through which E6* mediates inhibition of tumor growth in both C33A and SiHa cells by identifying pathways affected by E6* expression.

Epidemiological studies of actual cases of cervical cancer have shown differential splicing in the E6/E7 region for both HPV 16 and HPV 18 (153, 154), and demonstrated that patterns of HPV18 E6/E7 splicing associated with E6 variants can be related to

differences in cancer aggressiveness and prognosis for treatment. For example, cells isolated from tumors expressing the African variant of E6, which express relatively high levels of E6*, formed tumors in nude mice more slowly than did cells possessing the Asian-Amerindian variant of E6, which express relatively low levels of E6* along with high levels of E6 (154). In addition, the data reported by De la Cruz-Hernandez and coworkers linked E6* expression in patient samples to higher levels of p53, which is also consistent with our data.

The role of E6* in the virus life cycle has not yet been established. It is known, however, that splicing of the E6/E7 transcript enhances E7 expression (134), suggesting that the potential for alternative splicing is of functional significance. Furthermore, HPV16 E6 alternative splicing in the epithelia depends on the level and presence of EGF, indicating that the splicing of E6 is not a random process (11). E6* may work by regulating the activity of E6 (and/or other HPV proteins such as E2), as well as cellular proteins through protein-protein interactions within the differentiating epithelium. Such questions await further research. In summary, we report here for the first time that the smaller isoform of E6, E6*, possesses anti-oncogenic activities that can be demonstrated in vivo. Importantly, these biological activities are distinguishable from those of E6. Future work will focus on the significance of these findings in the context of human cancers, where we will explore the possibility of mimicking or replicating the anti-oncogenic activity of E6* in such a way as to provide therapeutic benefit. Another direction for future research will be to determine what role E6* plays in the viral life cycle.

CHAPTER THREE

OVEREXPRESSION OF HPV16 E6* ALTERS

BETA-INTEGRIN & MITOCHONDRIAL DYSFUNCTION PATHWAYS

IN CERVICAL CANCER CELLS

Whitney Evans, Maria Filipppova, Valery Filippov, Svetlana Bashkirova,

Guangyu Zhang, Mark E. Reeves, and Penelope Duerksen-Hughes

Abstract

High-risk human papillomaviruses (HPV) cause nearly all cases of cervical cancer, as well as many types of oral and anogenital cancer. Alternative splicing increases the capacity of the HPV genome to encode the proteins necessary for successful completion of its infectious life cycle. However, the roles of these splice variants, including E6*, the smaller splice isoform of the E6 oncogene, in carcinogenesis are not clear. SiHa (HPV16$^+$) and C33A (HPV$^-$) cells were transfected with the E6* plasmid, and tandem mass taglabeled protein levels were quantified by mass spectrometry. Proteomic analyses identified pathways affected by E6* in both HPV$^+$ and HPV$^-$ cells, and pathways were validated using in vitro methods. A total of 4,300 proteins were identified and quantified in lysates of SiHa and C33A cells with and without HPV16 E6* expression. SiHa and C33A cells expressing E6* underwent changes in protein expression affecting integrin signaling and mitochondrial dysfunction pathways, respectively. Subsequent experiments were performed to validate selected E6*-mediated alterations in protein levels. E6* modifies the expression of proteins involved in mitochondrial dysfunction and oxidative phosphorylation in C33A cells, and β-Integrin signaling in SiHa cells.

Introduction

High-risk human papillomaviruses (HR-HPVs) cause cervical cancer in approximately 500,000 women annually, making it the third most common cancer in women worldwide (155, 156). Nearly half of these women will not survive. In addition to cervical cancer, HR-HPVs are the cause of malignancy in 60% of oropharyngeal cancer cases; 90% of anal cancer; 40% of vaginal, vulvar, and penile cancer; and cancer of other regions of the body such as the skin, colon, and rectum (157, 158). Numerous studies agree that the transformative properties of E6 and E7 are central to HPV-induced carcinogenesis, and the oncogenic roles of E6 and E7 have been well-characterized.

Increased cellular oxidative stress has been proposed to increase the likelihood that the virus will integrate into the host genome (8). This event often leads to up-regulation of E6 and E7 expression via disruption of the E2 gene, causing increased cell survival and division through the weakening of pro-apoptotic processes and cell-cycle regulation, respectively. Although E6 and E7 are both considered indispensable for transformation efficiency, E6 can, in some instances, immortalize cells in the absence of E7, indicating that E6-dependent mechanisms underlying cervical carcinogenesis are of vital importance (13, 14, 159).

Interestingly, high- but not low-risk HPVs generate multiple transcripts of full-length E6 mRNA via alternative splicing (11, 15). In mammalian cells, the HR-HPV E6 oncoprotein is expressed as both full-length and spliced isoforms, with the smaller isoforms (generally referred to as E6*) corresponding approximately to the N-terminal third of the full-length protein. Relatively little is known about the smaller variants as compared to the full-length isoform, and E6 splicing patterns vary between HR-HPV

types (17, 18, 160). Alternative splicing enables the virus to expand its proteome from a modestly-sized genome, thereby increasing the genetic diversity and persistence of the virus against host immunity and raising its chance of survival (16).

Previously, our group demonstrated that the overexpression of E6* reduced tumor growth by both HPV$^+$ SiHa and HPV$^-$ C33A cervical carcinoma cells in a nude mouse xenograft model (160), raising the question of what changes in cellular pathway activation might contribute to the E6*-mediated decrease in tumor size. In the present study, proteomic analyses of HPV$^+$ (SiHa) and HPV$^-$ (C33A) cervical carcinoma cells were used to demonstrate how E6* influences protein expression, and to examine the impact such modifications have on the activation of cellular pathways in vitro. Additionally, we sought insight into how E6* may affect tumor growth through its effects on these pathways.

Materials & Methods

Reagents

Monoclonal antibodies against Kindlin-1 and polyclonal β-1 Integrin were obtained from Millipore Chemicon (Temecula, CA, USA), while those to RAS homolog gene family, member A (RHOA) and glyceraldehyde 3-phosphate dehydrogenase (GAPDH) were acquired from Cell Signal Technology (Beverly, MA, USA). α-Flag agarose, α-Flag-HRP antibodies, MG132, a reversible proteasome inhibitor, and α-β-actin were purchased from Sigma-Aldrich (St. Louis, MO, USA). Secondary fluorescent antibodies were obtained from LI-COR Biosciences (Lincoln, NE, USA).

Cell Culture

SiHa and C33A cells, derived from human cervical carcinomas, were obtained from the American Type Culture Collection (Manassas, VA, USA). All cells were cultured in modified Eagle's medium (MEM) (Thermo Fisher Scientific, Hanover Park, IL, USA) and supplemented with 10% fetal bovine serum (Invitrogen, Carlsbad, CA, USA), penicillin (100 µg/ml), and streptomycin (100 µg/ml) (Sigma-Aldrich, St. Louis, MO, USA).

Plasmids, Transfection, & the Creation of Stable Cell Lines

The pFlag-E6* (pE6*) plasmid was constructed by cloning E6*I in frame with the N-terminal Flag-tag and the C-terminal C-myc-tag into the pFlag-Myc CMV-22 vector (Sigma-Aldrich). Stable cell lines expressing pE6* or vector control (e.g. pFlag) were produced using the Mirus Bio transfection kit, TransIt-LT1 Transfection reagent (Thermo Fisher Scientific), to transfect the appropriate plasmids into SiHa and C33A cells, as directed by the manufacturer. G418 (neomycin, which is an aminoglycoside antibiotic) (500-800 µg/ml) was added to cells 48 h post-transfection and antibiotic selection was carried out for 3 weeks. Subsequently, expression of E6* was evaluated by immunoblot analysis.

Immunoblot Analysis

Approximately 10^6 cells were lysed in ~100 µl lysis buffer, and lysates were sonicated and separated by sodium dodecyl sulfate polyacrylamide gel electrophoresis followed by protein transfer onto polyvinylidene difluoride membranes (Thermo Fisher Scientific). Membranes were blocked with 1% bovine serum albumin, and primary

antibodies (α-mouse or α-rabbit) in Trisbuffered saline and Tween 20 (TBST) were

applied overnight at 4˚C. Membranes were washed with TBST the following day.

Secondary Immunopure Antibodies (α-mouse or α-rabbit) conjugated to horseradish

peroxidase (Thermo Fisher Scientific) were incubated with the membrane for 1 h.

Chemiluminescent SuperSignal West Dura and Pico Maximum Sensitivity substrates

were used to detect signals. In the case of fluorescent secondary antibodies (LI-COR,

Lincoln, NE, USA), signals were detected using the Odyssey imaging system and relative

densities were quantified against standard controls using ImageJ software analysis

[v1.48; see reference (161)].

Microscopy

Morphological analysis of SiHa and C33A cells was conducted using an Olympus

IX70 inverted microscope (Olympus America, Center Valley, PA, USA). Cells were

seeded at a density of 103 per 100×20 mm tissue culture-treated dish 3-7 days prior to

imaging. Live images, using Hoffman Modulation contrast, were captured with a digital

SPOT RT3™ camera and SPOT Insight software (SPOT Imaging, Sterling Heights, MI,

USA). All images were acquired with uniform settings and magnification (×20).

Mitochondrial Membrane Depolarization

The Mito-ID membrane potential detection kit (Enzo Life Sciences, Farmingdale,

NY, USA) was used as directed by the manufacturer. Mitochondrial membrane

depolarization was estimated using the dual-emission mitochondrial membrane potential

(MMP)-sensitive dye, cationic carbocyanine. Following treatment, cells were collected in

1X phosphate buffered saline and analyzed on a Becton-Dickinson FACSCalibur FLOW

cytometer (Becton-Dickinson, San Francisco, CA, USA). The FL-1 channel detected

depolarized mitochondria, indicated by green fluorescence, while the FL-2 channel

gathered orange fluorescence from energized mitochondria. The data were collected and

analyzed using Flow-Jo software (Ashland, OR, USA).

Secreted Embryonic Alkaline Phosphatase Analysis

Alkaline phosphatase activity was measured using the Great EscAPe SEAP

Detection Kit provided by BD Biosciences (Clontech, Mountain View, CA, USA) as

directed by the manufacturer. Lysates of SiHa and C33A cells were collected and a

luminometer was used to detect signals produced by the phosphatase/substrate reaction.

This measured activity was normalized against total protein concentration, which was

acquired by a spectrophotometer plate reader.

Proteomic Analysis

Protein lysates were collected from ~5×10^6 cells from each of the cell lines (SiHa

pFlag, SiHa E6*, C33A pFlag, and C33A E6*). Samples were sonicated, denatured,

reduced, and alkylated as recommended by the directions provided with the TMT Mass

Tagging Kit (Thermo Fisher Scientific,). Cell lysates were prepared, run on an LTQ-

Orbitrap Velos mass spectrometer (Thermo Fisher Scientific) and analyzed as previously

described (162). Protein identification from each mass spectrometry raw data file was

performed against the human library using Proteome Discoverer 1.2 software (Thermo

Fisher) with a signal to noise threshold of 1.5. A false-discovery rate of less than 1% was

applied and detection included that of unique peptides only. A fold change cut-off value of 1.5, comparing one group of cells (e.g. E6* overexpressing cells) to a control group of cells, (e.g. pFlag vector-containing cells) was applied during Ingenuity Pathway Analyses.

Comet Assay

To measure nuclear DNA damage in SiHa and C33A cells, the Comet assay kit was obtained from Trevigen (Trevigen, Gaithersburg, MD, USA) and used according to the manufacturer's instructions as previously described (163). Briefly, cells were lysed and gel electrophoresis was carried out under alkaline conditions. SYBR gold from Invitrogen was used to stain cells. One hundred DNA tails were photographed and analyzed on a BIOREVO fluorescence microscope (BZ-9000) (Keyence Corporation, Itasca, IL, USA) with Comet IV software (Perceptive Instruments Ltd., St Frances House, Bury St Edmunds, UK) using uniform magnification ($\times 10$ for counting; $\times 20$ for photographs) and settings.

Glutathione (GSH) Assay

The GSH-Glo assay from Promega (Madison, Wisconsin) was used to quantify glutathione levels in SiHa and C33A cells. Cell lysates were placed in 96-well plates and GSH levels were detected by luminescence following a coupled reaction between firefly luciferase and GSH-S-transferase. Background luminescence was subtracted from that for GSH for each sample and the values were converted to molar GSH concentrations based on a standard curve. Total protein concentration was measured using a spectrophotometer

plate reader. The average GSH concentration from each sample well was divided by the same well's corresponding total protein concentration to yield the reported ratio (μM/mg).

Statistics

All experiments were repeated at least three times with results reported as mean±standard deviation. Student's t-test was used to analyze differences, and a p-value of less than 0.05 was considered significant.

Results

E6 Expression Alters Pathway Activation in Both HPV⁺ & HPV⁻ Contexts*

Our first task in determining how E6* affects the cellular proteome was to overexpress E6* in both HPV⁺ and HPV⁻ systems. Therefore, HPV⁺ SiHa and HPV⁻ C33A cervical cancer cells were stably transfected with either the empty vector pFlag, or with pE6* to create clones with either very low/lack of (SiHa pFlag and C33A pFlag, respectively) or high (SiHa pE6* and C33A pE6*, respectively) E6* expression. Following selection of the E6* cells using G418, equal numbers of cells from the three clones with the highest levels of E6* expression were combined (SiHa pE6*; C33A pE6*) (Figure 1A and B, respectively).

To determine the effect of HPV16 E6* on the levels of cellular proteins, and to thereby gain insight into how this small viral protein orchestrates cellular activities in the presence and absence of full-length E6, protein expression in SiHa pFlag, SiHa pE6*, C33A pFlag and C33A pE6* cells was evaluated using mass spectrometry followed by

pathway analysis as indicated by the scheme shown in Figure 2. Data were analyzed

through the use of QIAGEN's Ingenuity Pathway Analysis (164), (Redwood City,

www.qiagen.com/ingenuity).

Mass spectroscopy identified a total of 4,300 proteins. Based on a 1.5-fold change

as the cut-off value, 253 proteins for SiHa cells and 328 proteins for C33A cells were

selected for further IPA investigation. Together, the analyses for SiHa and C33A cells

revealed a total of 75 pathways whose proteins exhibited statistically significant changes

in expression (using a fold change cut-off value of 1.30=negative log of 0.05 as the p-

value) in the presence of E6*. The top 10 cellular pathways affected by E6* for SiHa and

C33A cells are presented in Tables I and II, respectively. IPA revealed that integrin-

linked kinase signaling was the pathway most altered by E6* overexpression in SiHa

cells, while oxidative phosphorylation (OXPHOS) and mitochondrial dysfunction

pathways were influenced the most in C33A pE6* cells.

E6 Expression in SiHa Cells*
Affects the β-Integrin Pathway & Cell Morphology

IPA analysis suggested involvement of β-Integrin signaling, via ILK, in response

to E6* overexpression in SiHa cells (Figure 3A). ILK is known to bind the cytoplasmic

domain of β1-Integrin (165). To verify the biological effect of E6* on β-Integrin

pathways in SiHa cells, immunoblot and phase-contrast microscopy analyses were

conducted. Immunoblot data suggest that overexpression of E6* in SiHa cells increased

cellular levels of β1-Integrin (Figure 3B), a finding consistent with the proteomic data.

To confirm activation of β1-Integrin, we probed for the expression of kindlin-1, a co-

stimulatory molecule of β1-Integrin. We found that kindlin-1 expression in SiHa pE6*

cells was significantly ($p<0.05$) increased (Figure 3C), reinforcing the notion that E6*

stimulates the β-Integrin signal cascade in SiHa cells, but not in C33A cells, consistent

with the mass spectroscopic analysis.

Notably, Kindlin-1 regulates cytoskeleton components by targeting Rho family

GTPases (166). Therefore, E6*-expressing SiHa and C33A cells were evaluated for

RhoA GTPase (RhoA) expression to further investigate the possible downstream effects

of β-Integrin signaling. Figure 3D shows that SiHa E6* cells express reduced levels of

RhoA as compared to SiHa pFlag cells ($p<0.05$). C33A pE6* cells also exhibited a slight

decrease in RhoA levels compared to C33A pFlag cells, although statistical significance

was not achieved. Interestingly, RhoA is implicated in cell motility (167) and cytoskeletal

reorganization (168), suggesting that E6* might operate through kindlin-mediated RhoA

expression to regulate cell shape (169) in SiHa cells.

To test whether E6* causes changes in morphology of cervical cancer cells with

active β-Integrin signaling, we analyzed SiHa and C33A cells by microscopic imaging

using Hoffman Modulation contrast, which showed conspicuous morphological changes

resembling cell spreading and outward membrane protrusion of SiHa E6* cells as

compared to SiHa pFlag cells (Figure 4A), although these changes were not seen in C33A

cells (Figure 4B). Collectively, the data presented here suggest that E6* may directly or

indirectly affect key components of the integrin signaling pathway in SiHa, but not C33A
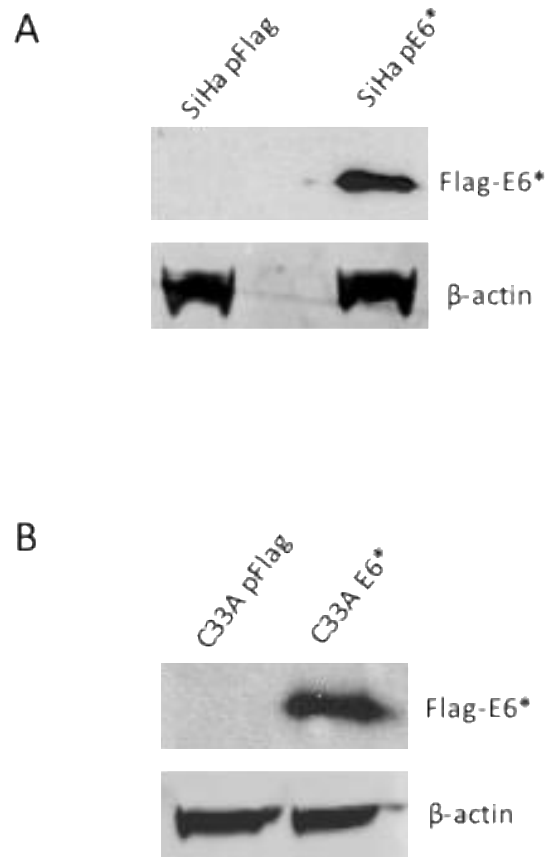
cells.

Figure 1. Expression of E6*I (E6*) in HPV$^+$ SiHa (A) and HPV$^-$ C33A (B) cells. Cells were stably transfected with Flag-E6*I or empty pFlag vector, and E6*-expressing clones were selected by resistance to G418. E6* expression of cells in pooled clones was analyzed by immunoprecipitation with α-Flag agarose, followed by detection using antibodies directed against Flag-Horseradish peroxidase. α-β-Actin antibodies were used to normalize for immunoprecipitation input.

Table I – Top 10 Canonical Pathways Affected by E6* in SiHa Cells

Ingenuity Canonical Pathways - SiHa E6*/SiHa pFlag	p value
ILK Signaling	9.77×10^{-7}
Role of BRCA1 in DNA Damage Response	8.51×10^{-6}
Virus Entry via Endocytic Pathways	2.29×10^{-5}
Caveolar-mediated Endocytosis Signaling	4.46×10^{-5}
Agranulocyte Adhesion and Diapedesis	1.07×10^{-4}
Clathrin-mediated Endocytosis Signaling	1.70×10^{-4}
Hereditary Breast Cancer Signaling	2.75×10^{-4}
Purine Nucleotides De Novo Biosynthesis II	3.55×10^{-4}
5-aminoimidazole Ribonucleotide Biosynthesis I	5.25×10^{-4}
AMPK Signaling	7.41×10^{-4}

Table I. Top 10 canonical pathways affected by E6* overexpression in SiHa cells. Ingenuity Pathway Analysis revealed that E6* expression in SiHa cells significantly influences multiple pathways including the Integrin-linked kinase (53) pathway.

Table II – Top 10 Canonical Pathways Affected by E6* in C33A Cells

Ingenuity Canonical Pathways - C33A E6*/C33A pFlag	p value
Oxidative Phosphorylation	1.26×10^{-19}
Mitochondrial Dysfunction	3.16×10^{-19}
TCA Cycle II (Eukaryotic)	6.61×10^{-8}
Proline Biosynthesis I	7.59×10^{-8}
2-ketoglutarate Dehydrogenase Complex	1.82×10^{-5}
Proline Biosynthesis II (from Arginine)	8.91×10^{-5}
Arginine Degradation VI (Arginase 2 Pathway)	8.91×10^{-5}
Granzyme A Signaling	1.51×10^{-4}
Valine Degradation I	1.95×10^{-4}

Table II. Top 10 canonical pathways affected by E6* expression in C33A cells. Overexpression of E6* in C33A resulted in significant changes to several pathways, including the oxidative phosphorylation (OXPHOS) and mitochondrial dysfunction pathways.
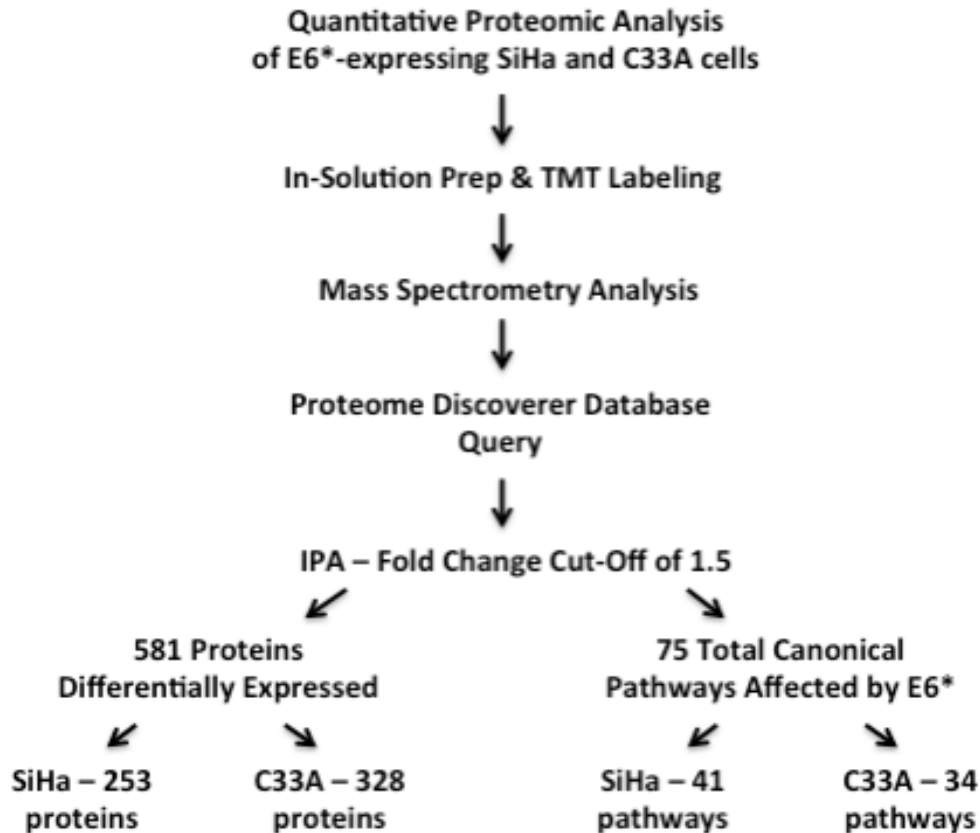
Figure 2. Workflow for the relative quantitative analysis of SiHa and C33A cell lysates by mass spectrometry and Ingenuity Pathway Analysis. Proteins from cell lysates were reduced and alkylated for subsequent trypsinization, and the resulting peptides were labeled using multi-plex tandem mass tags (TMT) for quantitation of proteins from each sample. Labeled peptides were combined and fractionated using strong cation exchange in increasing concentrations of KCl solution. Sample enrichment was performed using Pierce C18 tips. Identical proteins from the different samples were separated and quantified according to isobaric tag labeling. Proteins identified by mass spectrometry were compared against the Proteome Discoverer human library. Raw Data files were uploaded to IPA and a fold-change of 1.5 was applied to filter insignificant changes in protein levels between cells expressing E6* and those not expressing E6*. Core analysis revealed that the levels of 581 proteins from SiHa and C33A cells were affected by E6* expression and that 75 pathways were involved in these cellular proteomic changes.
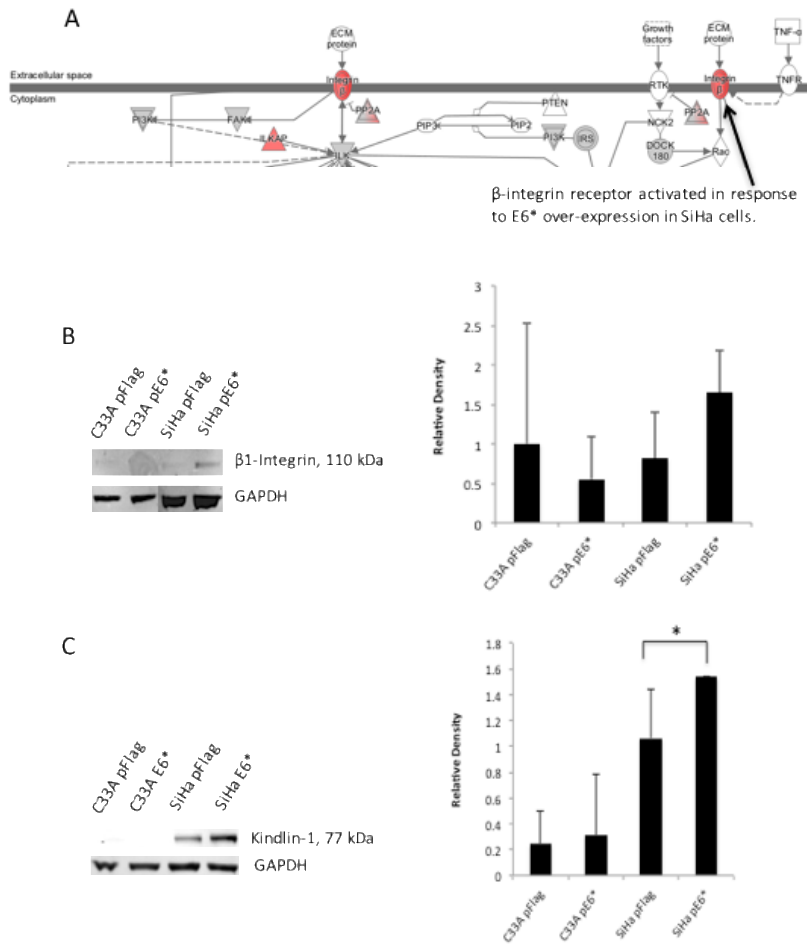
Figure 3. Activation of β-Integrin signaling by overexpression of E6* in SiHa cells. A: Increased expression of several members of the β-Integrin signaling pathway in SiHa cells overexpressing E6* (pE6*) compared to SiHa pFlag cells; red color tones suggest an up-regulation of molecules compared to control cells. B: Immunoblot of SiHa cells showed increased expression of β1-Integrin in cells overexpressing E6* compared to controls. C33A cells expressing and not expressing E6* displayed no discernible difference in β1-Integrin levels. C: Increased expression of an upstream regulator of β-Integrin signaling, Kindlin-1, was detected in SiHa pE6* cells compared to SiHa pFlag cells. C33A cells exhibited no measurable difference in Kindlin-1 expression.
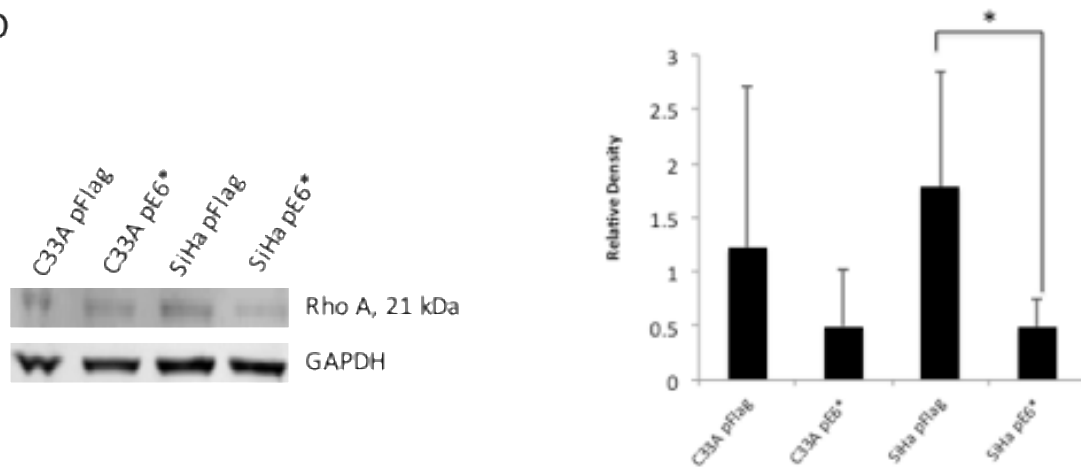
Figure 3. D: A decrease in Ras homolog gene family, member A (RhoA) expression, which is downstream of β1-Integrin and Kindlin-1 regulation, was also detected in SiHa pE6* cells, with the same trend observed in C33A pE6* cells. The relative density of three repeats is presented in the graphs, and error bars represent the standard deviations. *Significantly different at $p < 0.05$.

Alkaline Phosphatase Activity is Significantly Reduced in SiHa,

but not in C33A Cells Following E6* Overexpression

In addition to the β-Integrin pathway analysis, several individual SiHa cellular proteins affected by the overexpression of E6* were noted; placental ALPP was one of these proteins. ALPP was of particular interest because this was one of the proteins with the highest fold-change; moreover, high ALPP is correlated with pluripotency and undifferentiated cell phenotypes, while low ALPP implies differentiation (170). Furthermore, the tumors of patients with decreased ALPP levels tend to progress more slowly than those with higher ALPP levels (171, 172). The secreted embryonic AP assay was utilized to investigate the effect of E6* on ALPP activity in SiHa cells, since embryonic AP is a truncated form of ALPP. Our data demonstrate that E6* reduces the activity of ALPP in HPV$^+$ SiHa cervical cancer cells ($p<0.05$; Figure 5), which is consistent with a predicted association between lower serum ALPP levels and better clinical outcomes in certain cancers (173). However, ALPP activity was not greatly affected in HPV$^-$ C33A cervical cancer cells expressing E6*.

E6* Impairs Mitochondrial Function in SiHa pE6* Cells

& Affects the Mitochondrial Dysfunction Pathway in C33A Cells

Proteomic analysis revealed that expression of E6* in C33A cells interferes with the overlapping mitochondrial dysfunction and OXPHOS pathways.

A
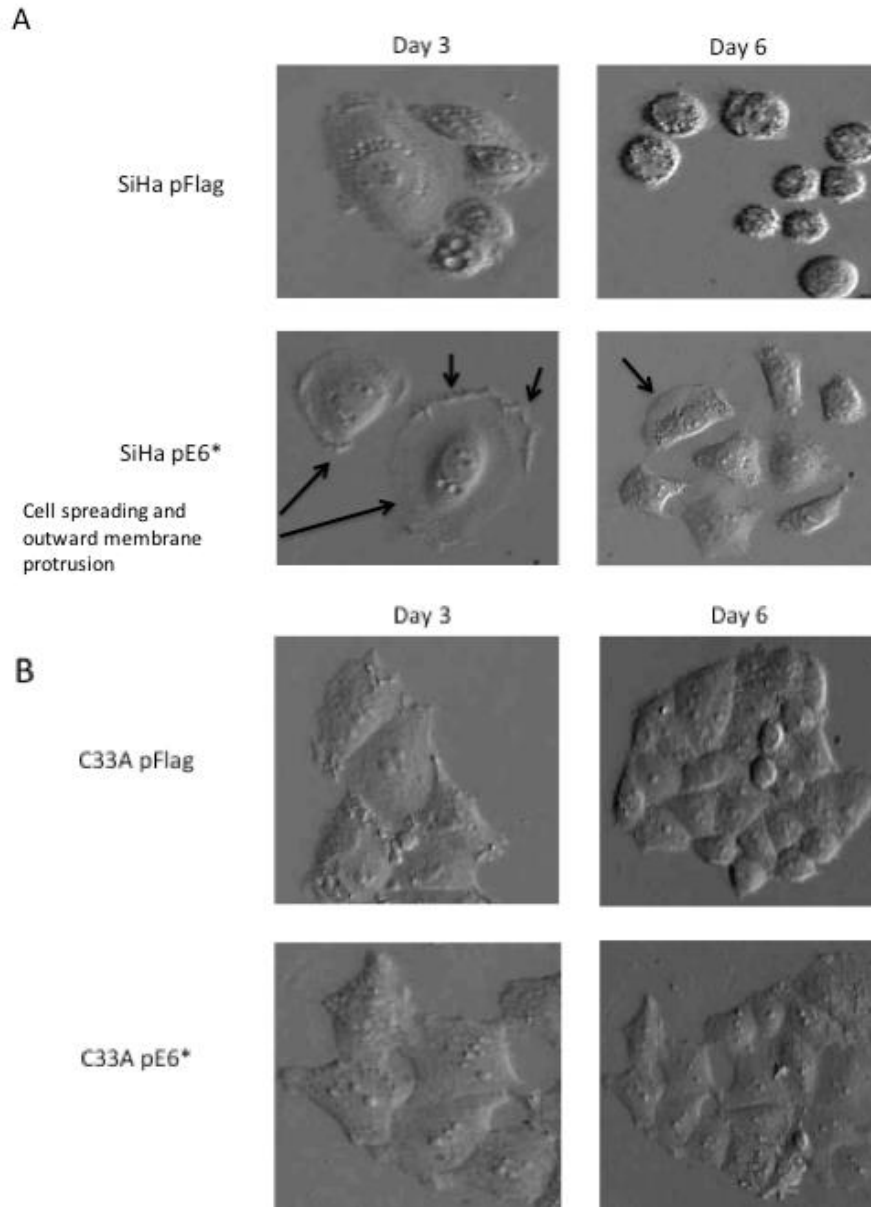
Figure 4. Morphological analysis of SiHa pFlag and SiHa pE6* cells by microscopy. A: Images of SiHa cells captured using Hoffman modulation contrast (×20) show differences in cell appearance between cells overexpressing E6* and those transfected with the empty vector. Top panels show SiHa pFlag cells approximately 3-6 days following seeding at a cell density of 10^3 while the bottom panels show images of SiHa pE6* cells acquired at the same time. SiHa pE6* cells can be described as exhibiting more cell spreading and membrane protrusion (black arrows) as compared to the more closely positioned SiHa pFlag cells. B: Images of C33A pFlag and C33A pE6* cell obtained under the same conditions (Hoffman modulation contrast at 3-7 days; (×20) as SiHa cells did not demonstrate cell spreading behavior.

Figures 6A and B illustrate that the proteins most perturbed due to E6* expression in C33A cells are involved in the electron transport chain (174), located in the inner mitochondrial membrane, and that these proteins play roles in both the mitochondrial dysfunction and OXPHOS pathways. Since mitochondrial function is linked to the maintenance of mitochondrial membrane depolarization (175), we measured MMP in SiHa and C33A cells by the Mito ID assay and flow cytometry.

Mito ID analysis demonstrated a modest increase in mitochondrial membrane depolarization in C33A pE6* cells compared to C33A control cells. Mitochondrial membrane depolarization was detected by the FL-1 channel and is indicated by the migration of carbocyanine dye out of the organelle (Figure 7A, left bars and histogram). Additionally, our data suggest an increase in energized mitochondria in C33A pE6* cells compared to controls, as shown by the FL-2 channel (Figure 7A, right bars and histogram). The FL-2 channel detects orange fluorescence caused by dye aggregation in mitochondria with an intact membrane potential, therefore implying an increase in energized mitochondria. Surprisingly, although proteomic analysis did not detect changes in the expression of proteins involved in mitochondrial dysfunction in SiHa pE6* cells as compared to SiHa controls, Mito ID analysis of the MMP in SiHa cells demonstrated that mitochondrial membrane depolarization was modestly more pronounced in SiHa pE6* cells compared to SiHa pFlag cells (Figures 7B, left bars and histogram). This finding is indicated by an increase in membrane permeability and a reduction in dye aggregation in the organelle (FL-1 channel). Furthermore, SiHa pE6* cells exhibited decreased orange fluorescence (FL-2 channel, right bars and histogram), implying a less energized population of mitochondria compared to SiHa pFlag cells.
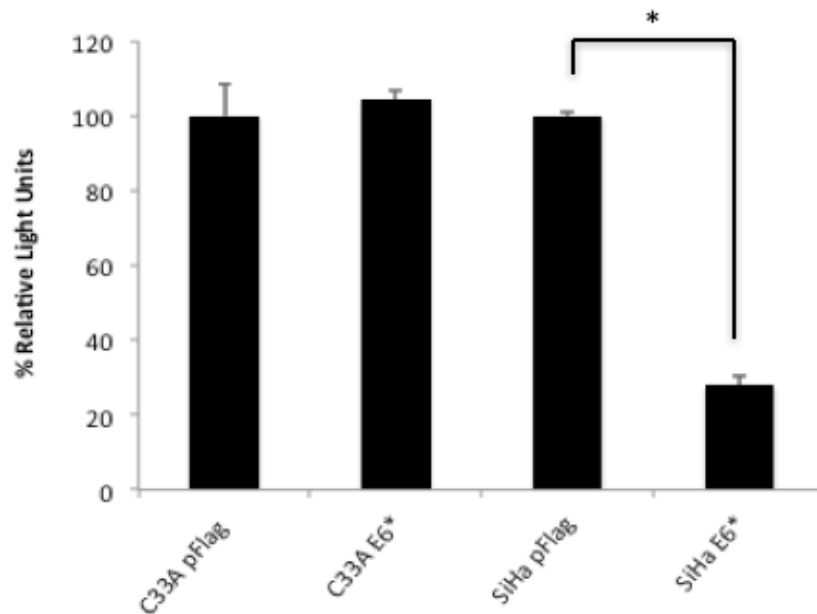
Figure 5. E6* overexpression reduces alkaline phosphatase (AP) levels in SiHa but not C33A cells. Cell lysates were collected to measure AP levels in triplicate, and the Great EscAPe SEAP Detection Kit by BD Biosciences was used to detect E6*-mediated changes in AP expression in cells. When AP was normalized against protein concentration, we found that AP levels in SiHa pE6* cells were greatly reduced compared to SiHa pFlag cells. No decrease in AP was detected in C33A cells. The relative light units of triplicate measurements are presented in the graphs, and error bars represent the standard deviations. *Significantly different at $p < 0.05$.

Figure 6. Expression of E6* in C33A cells affects mitochondria. A: Pathway analysis comparing over-/under-expression of proteins in C33A pE6* cells compared to C33A pFlag cells indicates considerable involvement of the mitochondrial dysfunction pathway in E6*-expressing C33A cells. Molecules affected by E6* in C33A pE6* cells include those associated with the protein complexes of the electron transport chain within mitochondria, with the red color tones denoting increased expression in C33A pE6* cells.

B

Figure 6. B: The oxidative phosphorylation canonical pathway, which is closely related to the mitochondrial dysfunction pathway, also experienced changes in protein expression due to E6* expression in C33A cells. Consistent with mitochondrial dysfunction pathway analysis, the oxidative phosphorylation pathway demonstrated increased levels of molecules involved in the electron transport chain of mitochondria.
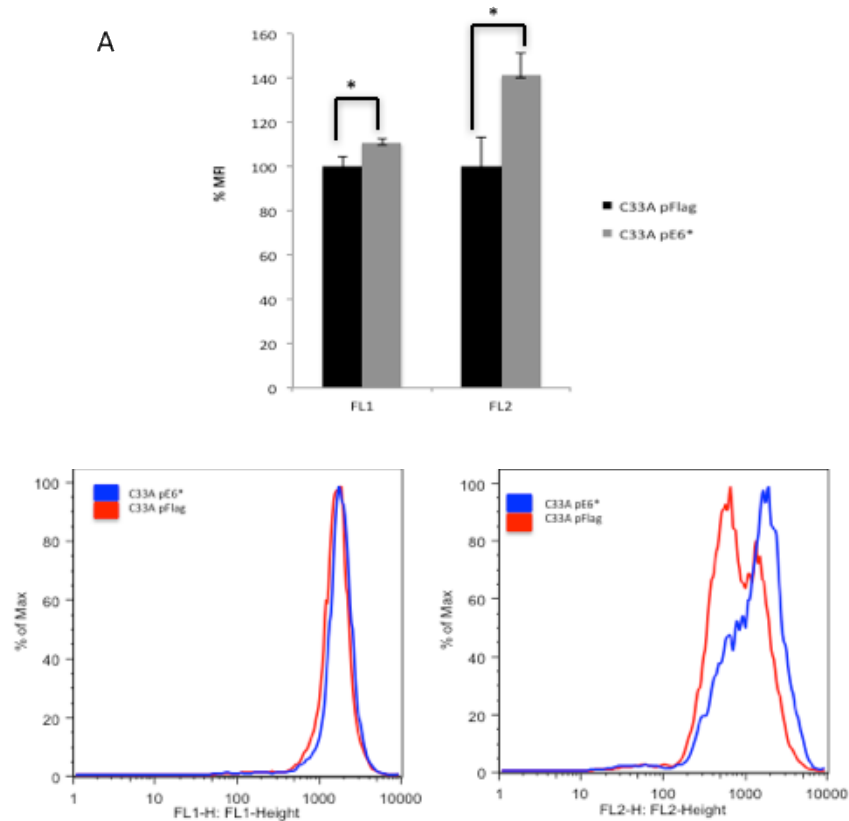
Figure 7. Mitochondrial changes following E6* expression. Analysis of mitochondrial dysfunction by Mito ID assay and flow cytometry. Mito ID detects changes in mitochondrial activity. A: E6* caused greater depolarization of mitochondria in C33A pE6* cells compared to those in C33A pFlag cells. The FL2 channel, on the other hand, detected a substantial shift in orange fluorescence, inferring increased dye aggregation and suggesting that a large population of mitochondria in C33A pE6* cells were energized. Mean Fluorescence Intensity .
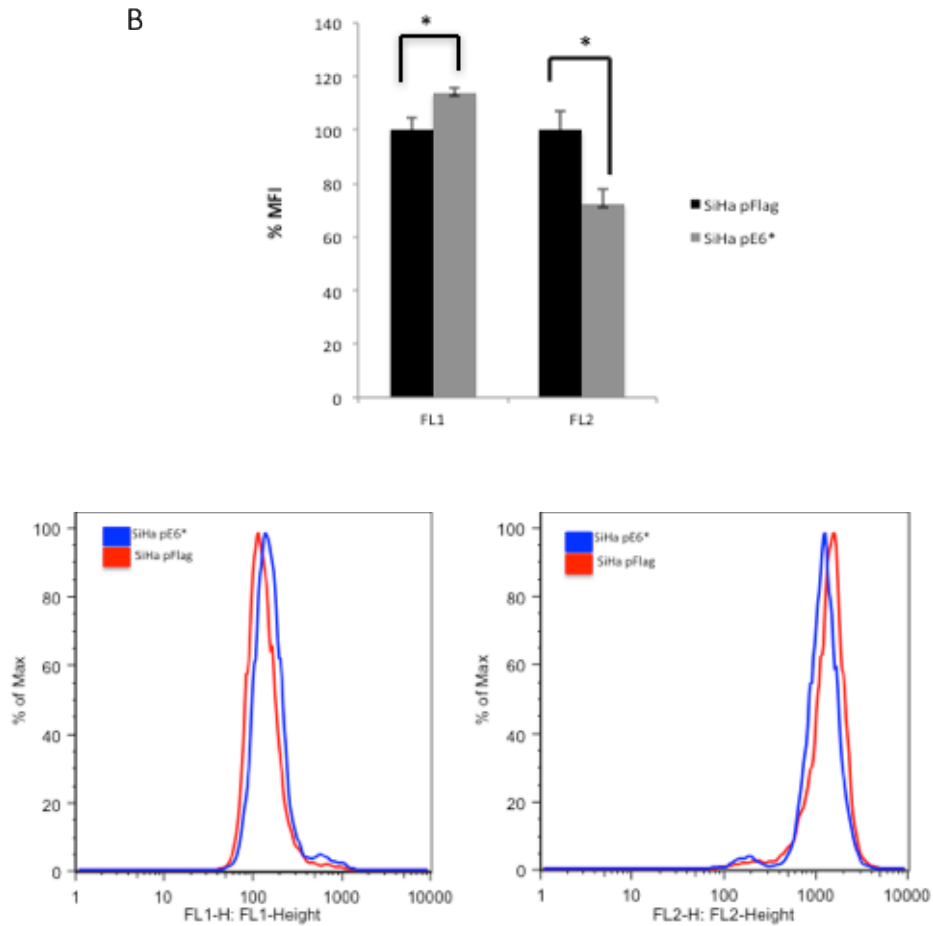
Figure 7. Mitochondrial changes following E6* expression. Analysis of mitochondrial dysfunction by Mito ID assay and flow cytometry. Mito ID detects changes in mitochondrial activity. B: Mitochondrial membrane depolarization in SiHa pE6* cells was augmented compared to SiHa pFlag cells, which is demonstrated by the detection of increased green fluorescence in the FL1 channel. The increased mitochondrial membrane depolarization in SiHa pE6* cells was accompanied by a decrease in energized mitochondria, as indicated by a decrease in the orange fluorescence signal detected by the FL2 channel. Triplicate measurements of the mean fluorescence intensity of carbocyanine were performed to generate the bar graph. The mean fluorescence intensity of C33A pFlag and SiHa pFlag cells was set at 100%. Error bars represent the standard deviations. *Significantly different at $p < 0.05$. MFI: Mean fluorescence intensity.

Increased DNA Damage in C33A E6* and SiHa E6* Cells

Accompanies a Reduction in GSH Levels

Increased reactive oxygen species (ROS) due to mitochondrial dysfunction causes cellular oxidative stress and DNA damage (163, 176). Therefore, markers of oxidative stress, such as a decrease in expression of antioxidant enzymes, or the presence of DNA damage, can be harbingers of a cell population's inability to manage oxidative stress that surpasses the tolerance threshold. We, therefore, employed the comet assay to measure DNA damage and assessed GSH levels to estimate antioxidant defense in E6*-expressing SiHa and C33A cells.

Figure 8A shows representative images from the comet assays performed on SiHa and C33A cells transfected with pFlag or pE6*. We found that SiHa and C33A pFlag cells had approximately the same amount of DNA damage and an equivalent distribution of cells with minimal to medium migration patterns (scores of 50-100 or 100-150, respectively) (Figure 8B). However, when the E6*-expressing cells were compared with each other and to their pFlag controls, different trends emerge. SiHa pE6* cells displayed the most severe DNA damage among the four lines tested, with greater than ~60% of the cell population displaying medium DNA damage (score of 100-150), and the remaining 40% divided between undamaged and minimal damage (scores of 0-50 or 50-100, respectively). In contrast, the DNA damage observed in SiHa pFlag cells was divided evenly into thirds between the varying levels of comet tail lengths. Surprisingly, C33A pE6* cells displayed slightly less medium DNA damage than did the C33A control cells, although C33A pE6* cells overall suffered more minimal to medium DNA injury than did the C33A pFlag cells.
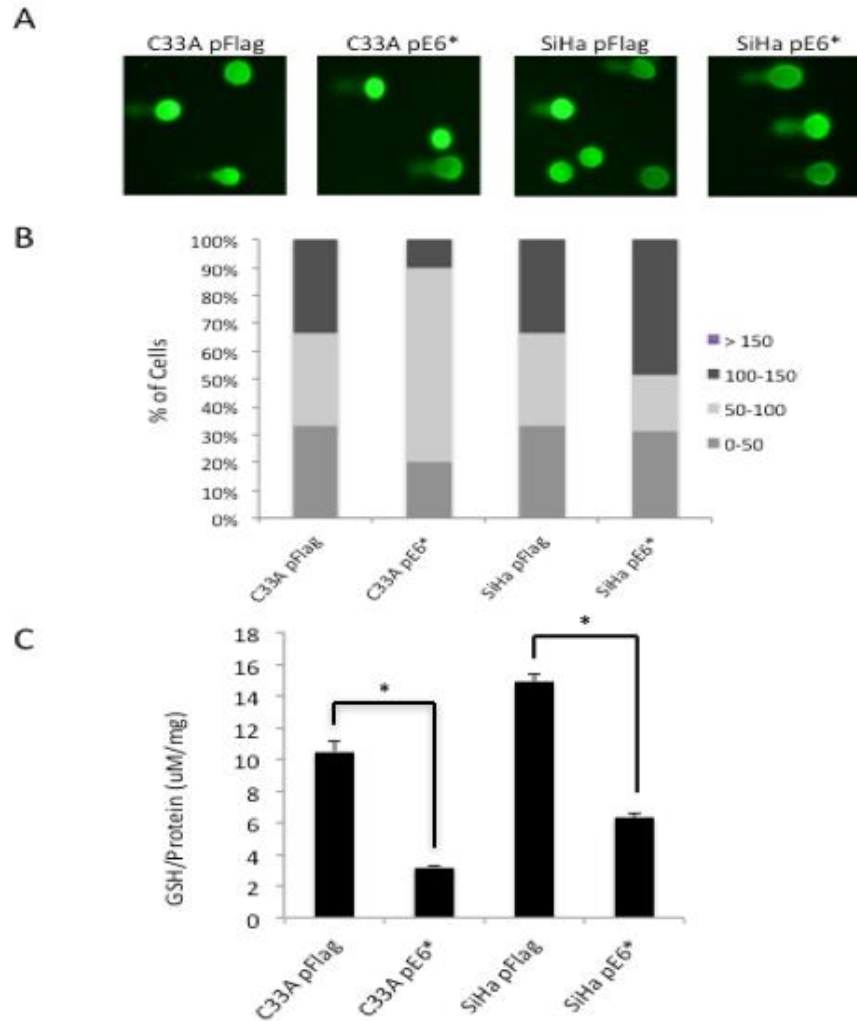
Figure 8. E6*-mediated changes in DNA damage and glutathione (GSH) levels. A: Measurement of DNA damage in SiHa and C33A cells by the comet assay. Representative images from comet assay showing variations in tail length between E6*-expressing cells and control cells. SiHa pE6* cells displayed the most severe DNA damage of all the groups. B: Percentage of cells with different degrees of DNA damage. SiHa pE6* and C33A pE6* cells exhibited comparable levels of DNA damage overall. However, a greater percentage of SiHa pE6* cells had more severe DNA damage than did SiHa pFlag, C33A pFlag, and C33A pE6* cells. C33A pE6* cells suffered more DNA injury compared to C33A pFlag cells, although the distribution of the extent of DNA damage was different. C: Measurement of GSH level in SiHa and C33A cells by GSH-Glo assay. Although SiHa pFlag cells displayed more glutathione than C33A pFlag cells, E6* appeared to reduce the amount of GSH in both SiHa and C33A cells proportional to their initial levels of GSH. Triplicate measurements of GSH concentration were performed to generate the graph, and error bars represent the standard deviations. *Significantly different at $p<0.05$.

Interestingly, SiHa and C33A pE6* cells, with more DNA damage compared to their controls, displayed significantly lower GSH levels (Figure 8C; $p<0.05$). Therefore, the findings presented herein further endorse the inverse relationship between cellular DNA damage and antioxidant capacity. Of note, GSH levels in C33A pE6* cells were the lowest of all four groups of cells. This observation is congruent with the fact that C33A pE6* cells are the most likely to display DNA damage (8B), although the extent of this DNA damage is less severe in these cells compared to the other three cell lines.

Discussion

Over the years, major discoveries in virology and oncology have allowed us to grasp the transformative impact of the E6 oncoprotein. Although a wealth of information exists regarding the roles of full-length HPV16 E6 in pathways involving apoptosis (136, 137, 177-179) and the mechanisms used by this virus to evade the immune system (180), much less is known of the activities of its splice variants that are present only in HR-HPVs, collectively known as E6*.

In this report, we analyzed the proteomes and cellular pathways of HPV[+] and HPV[−] cervical carcinoma cells expressing HPV16 E6* to gain a better understanding of the anti-oncogenic mechanisms by which E6* reduces tumor formation, as previously reported (160). SiHa and C33A cells were selected as models to determine how E6* interacts with its cellular host in the presence and absence of other HPV proteins. Because these two cell lines are derived from very different patients with cervical carcinoma and differ in both HPV status and p53 level (C33A has mutant p53 and other structural abnormalities) (164), we expected to see variations in the changes to the

cellular proteome observed following expression of E6*. Indeed, proteomic analysis

revealed that E6* produces unique effects in different cellular environments. For

example, the top canonical pathways affected by E6* in SiHa cells included the ILK

pathway, whereas mitochondrial dysfunction and OXPHOS pathways were most affected

in C33A cells (Tables I and II).

Proteomic analysis demonstrated that the β-Integrin pathway via ILK was

activated in SiHa cells (Table I, Figure 3A), but not in C33A cells that expressed E6*

(Table II), and immunoblotting analysis suggested that the level of β1-Integrin in SiHa

cells was increased (Figure 3B). The integrin family, in general, mediates interactions

between the extracellular matrix (ECM) and cells, as well as cell-to-cell communications.

Kindlin-1, a co-stimulatory molecule of β1-Integrin inside-out signaling (as well as a

mediator for outside-in communication) (181), was also up-regulated (Figure 3C), and

the increase in its expression is consistent with the amplification of β1-Integrin

expression. Kindlin-1 is known to regulate actin cytoskeleton remodeling during cell

translocation, circumferential actin assembly and cell spreading via Rho GTPase

signaling (166). Therefore, we probed further downstream of the β-Integrin pathway and

found that E6* expression in SiHa cells reduced RhoA GTPase expression, although this

change was not as prominent in C33A pE6* cells (Figure 3D). Importantly, RhoA

operates under the regulation of numerous molecules to execute cellular changes.

Changes in RhoA expression mediated by kindlin-1 are reported to assist in actin

cytoskeleton remodeling and the formation of stress fibers (166). Of note, RhoA is

capable of integrating and transducing cell-shape and soluble growth-factor cues into

regulatory signals that influence cell lineage (169), which may induce the expression of

early differentiation markers (166). Interestingly, our data suggested that E6* may also slightly increase RhoA levels in C33A pE6* cells, although direct stimulation of RhoA by Kindlin-1 in these cells was lacking (Figure 3C). This may reflect subtle, yet significant, differences in the upstream molecules controlling RhoA activity and subsequent cellular behavior. For example, it has been shown that changes in Rho activity mediated by kindlin are distinct from Rho activity mediated by G protein-coupled receptor or tumor necrosis factor (182-184). Such complexity may be necessary for ubiquitous, downstream molecules. Clearly, an E6*-mediated increase, via ILK, in ECM interactions and in cell–cell communication would have the potential to reduce tumor growth in SiHa cells.

The involvement of these particular proteins from the β-Integrin signaling pathway in our system inferred that cell shape could be affected by the expression of E6*. Indeed, morphological analysis allowed the detection of a visible difference between SiHa pE6* cells, with reduced RhoA and increased β1-Integrin expression, and SiHa pFlag cells (Figure 4A). These morphological observations are harmonious with previous research linking cell spreading and outward membrane protrusion to reduced RhoA activity and cell migration (174), and these observed differences might be attributed to changes in expression of β-Integrin pathway components mediated by E6*.

The expression of E6* in SiHa cells may, indeed, affect cell differentiation factors by modifying the expression pattern of β-integrin signaling molecules. According to our proteomic data and supporting experiments, ALPP levels and activity were significantly reduced in SiHa pE6* cells due to the increased expression of E6* (Figure 5). ALPP is a ubiquitous membrane-bound enzyme and is categorized into a family of four isoenzymes,

each with different functions and biochemical properties. Some ALPPs can be found in normal, as well as cancerous tissues (170). High ALPP is correlated with pluripotency and undifferentiated cell phenotypes, whereas low ALPP activity implies differentiation (170). Moreover, ALPP is currently most recognized and valued as a prognostic factor in cancer (such as ovarian and colorectal carcinomas) (171, 172), with a decrease in ALPP being defined as a positive indicator of patient survival. A reduction in ALPP activity is reported to accompany overexpression of the tumor suppressor protein phosphatase 2 (PP2A) (185). Although our investigation did not include validation of an E6*-mediated increase in PP2A, a previous study reported the co-localization of β1-Integrin and PP2A (186). Furthermore, one investigation reported that the up-regulation of colonic ALPP in response to inflammation might serve as a protective mechanism against oxidative stress (187), implying that the down-regulation of ALPP might render cells more susceptible to insult. Together, these observations, as well as those studies classifying certain forms of ALPP as stem cell markers and a target of developmental and differentiation processes (170, 185), make it a fascinating subject of study in the context of cancer research. Therefore, the investigation of their expression in diverse conditions could prove important, and this study may assist in such efforts.

The mitochondrial dysfunction and OXPHOS pathways are closely related and are profoundly affected by the overexpression of E6*, particularly in C33A cells (Figure 6A and B). The study of both pathways led to the conclusion that electron transport chain complex molecules are highly activated in E6*-expressing C33A cells compared to control C33A cells. Our data showed that mitochondria in C33A pE6* cells experienced more depolarization, and were more energized compared to those in C33A pFlag cells

108

(Figure 7A). It is possible that the up-regulation of electron transport chain molecules, as seen in C33A pE6* cells, could reflect the mitochondria's attempt to adapt to the stresses imposed by E6*-mediated increases in ROS production (163). Some researchers speculate that certain conditions in the mitochondria (such as alkalization) can cause transient depolarization, which is repetitive and reversible (188), leading to suppression of ROS generation (189). In fact, protective mechanisms engaging the mitochondria have been described in other types of epithelial-derived cancer (190).

We were somewhat surprised to find that mitochondrial injury was greatest in SiHa pE6* cells, as determined by Mito ID analysis (Figure 7B), since significant changes in the associated protein levels were not detected by our proteomic data when SiHa pE6* cells were compared to SiHa controls. It is possible that the expression of E6* might stress SiHa cells enough, through increased ROS (163), to cause harm to mitochondria that is beyond repair. Therefore, it is reasonable to suppose that such cells, experiencing oxidative stress and continued ROS production, could undergo sustained MMP (188), rather than less-damaging transient depolarization. Therefore, these two mitochondrial mechanisms might contribute to the different effects E6* has on MMP in SiHa and C33A cells.

The mechanisms regulating MMP fluctuations in mitochondria have not been fully elucidated because the dynamics controlling the depolarized and energized states are highly complex. According to the mitochondrial life-cycle model summarized in Figure 9 [see (191, 192)], our data may suggest that mitochondria in C33A pE6* experience transient, reversible depolarization, resulting in a larger population of re-energized mitochondria, whereas those in SiHa pE6* cells may suffer more harm by

109

sustained depolarization. The differences detected in mitochondrial depolarization between the SiHa and C33A cell lines may help explain cell type-specific vulnerabilities to E6*-mediated increases in oxidative stress. Our studies suggest that understanding the role of mitochondrial dysfunction in cancer is essential to the study of cancer cell behavior and possibly overcoming therapy resistance (193).

Boland et al. describe several types of mitochondrial dysfunction that can occur in response to cell stress: i) loss of MMP leading to membrane depolarization, ii) opening of mitochondrial membrane pores causing mitochondrial membrane permeability; iii) altered expression of molecules in the electron transport chain (174), resulting in defective respiration and oxygen consumption; iv) an imbalance in the expression of mitochondrial versus nuclear proteins, leading to initiation of the unfolded mitochondrial protein response; v) oxidative damage of the mitochondrial genome; and vi) inappropriate release of cytochrome c, causing pre-mature apoptosis (193). Our proteomic studies, and the subsequent experiments performed to validate those results, detected the first three out of these six mechanisms of mitochondrial dysfunction, although many of them overlap. For example, defective respiration might be associated with mitochondrial membrane depolarization, since the proton gradient is coupled to the redox reactions occurring along the electron transport chain and is dependent on the MMP. This premise is further illustrated by our own data, that show involvement of both the OXPHOS and mitochondrial dysfunction pathways in C33A cells under the stresses of E6* expression.
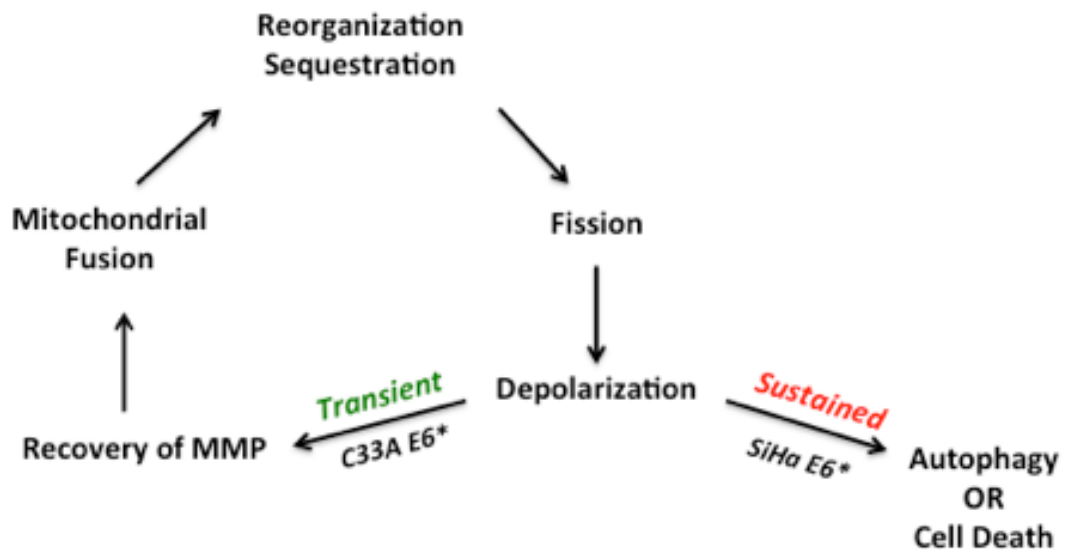
Figure 9. The mitochondrial life cycle. This schematic of the mitochondrial life cycle was adapted from Hyde and Twig et al. (191). E6*-mediated changes in mitochondrial function may be cell-specific and may activate different mechanisms affecting cell survival and cell death in SiHa and C33A cells. Mitochondrial dynamics are highly complex and determine the condition and fate of mitochondria within a cell. Mitochondria in the same cell can be at different stages of the mitochondrial life cycle. Among the multiple states mitochondria can assume, mitochondrial membrane depolarization is key and may be reversible. MMP: Mitohondrial membrane permeabilization.

While our study did not test the possibility that oxidative stress caused by E6*

induces mitochondrial DNA damage (see mechanism v above), our data do show that

E6* overexpression increases nuclear DNA damage in both SiHa and C33A cells, with

the damage more severe in SiHa E6* cells (Figure 9A and B). Intriguingly, nuclear DNA

damage has been linked to mitochondrial dysfunction in chronic disease (194). Thus, we

could speculate that the mitochondrial dysfunction detected by Mito ID in SiHa pE6*

cells (Figure 7B) may correspond to the increased severity of DNA damage. Because the

cell is dependent on antioxidants for protection from oxidative stress, GSH is essential for

cell survival. Not surprisingly, GSH levels were affected by E6* expression in both SiHa

and C33A cells (Figure 9C), as cellular oxidative stress is well known to deplete the GSH

level. However, researchers are now realizing that a reduced GSH level may also be an

early marker of cell death and essential to apoptosis (195). The same reports also state

that GSH is accompanied by cytochrome c release, suggesting the presence of a more

permeable mitochondrial membrane. Furthermore, studies reveal that GSH interacts with

the cytoskeleton through glutathionylation, causing changes in organization and function

(196, 197). However, more research is required to investigate whether E6* facilitates

interactions between antioxidant and cytoskeleton components. In any case, the reduction

in GSH seen following E6* overexpression in both SiHa and C33A cells has the potential

to predispose the expressing cells to DNA damage and to apoptosis, thereby potentially

contributing to reduced tumor growth.

Additionally, it might be the fact that the increased level of DNA damage in

C33A pE6* cells, in particular, reaches a degree of chronic oxidative stress that depletes

GSH stores to a greater extent (198). Because the GSH level in C33A cells is lower than

that in SiHa cells this observation may highlight the influence and efficacy of additional intact compensatory antioxidative stress mechanisms in C33A cells other than those involving GSH (199). These mechanisms may be more intrinsically linked to mitochondria, as discussed earlier, evoking mitohormetic responses (200).

Overall, our pathway analysis suggests that the mechanisms by which E6* reduces tumor growth in SiHa cells may include an increase in the activation of β1-Integrin-mediated pathways, thereby increasing ECM and cell–cell communication; reduction of ALPP expression, thus enhancing differentiation and sensitivity of expressing cells to insults; changes in mitochondrial function and an increase in more severe DNA damage, thereby compromising cell viability; and a decrease in the protective molecule, GSH. E6* may reduce tumor growth in C33A cells by increasing the amount of moderate DNA damage, consequently forfeiting cell viability (but to a lesser extent than the impact of DNA damage to SiHa cells). Overexpression of E6* in C33A cells also reduces the level of GSH, which might activate other protective responses not triggered in SiHa cells, and involve mitochondrial dysfunction pathways. Differences in the cellular response to E6*, as exemplified here, may also help explain why SiHa pE6* tumors exhibited a greater growth reduction than did C33A pE6* tumors, as previously reported (160). This investigation has, therefore, added to our knowledge of the cellular pathways through which HPV16 E6* influences cell behavior, while suggesting possible avenues for explanation into novel and effective therapeutic options.

CHAPTER FOUR

DISCUSSION

Summary of Findings

High-risk papillomavirus infections remain a significant cause of morbidity and mortality, both within the U.S. and worldwide. Although three HPV vaccines are now available (Cervarix, Gardasil, and Gardasil 9), their projected impact will not become fully apparent for 20-30 years, since most women become infected in their late teens/early twenties, while cancer appears in their late forties/early fifties. Furthermore, with the introduction of the 9-valent vaccine, ~30% of HR-HPVs with the potential to cause cancer are not covered. For these reasons and others, the development of novel and effective therapeutic interventions for established cases of cervical cancer remains an urgent and unmet need. Importantly, this need remains profoundly disproportionate worldwide amongst individuals of diverse populations. The data presented here, as well as other novel breakthroughs in virology pertaining to virus-associated cancers (e.g. EBV, KSHV, HBV, CMV, and MCPyV), continue to underscore the importance of persistent research in clarifying how viruses interact with and usurp host molecules and pathways to enhance completion of the infectious cycle and carcinogenesis.

In the experiments described in chapter two, we presented data demonstrating that, of the multiple E6* splice variants from HPV16, E6*I (E6*) is produced at greater levels compared to the E6 and E6*II splice products in our HPV$^+$ CaSki and SiHa cell systems. But E6* was significantly lower in SiHa cells compared to CaSki cells, which could be related to the aggressiveness of the cell lines. We also found that expression of E6* increases the levels of caspase 8, p53, and E-cadherin. Furthermore, E6* sensitized

SiHa cells to TNF-induced apoptosis, which corroborates previous experiments using U2OS cells. These findings are also consistent with earlier findings that E6* may act antagonistically to its parent molecule, the full-length E6 oncoprotein (20). The involvement of such molecules suggests that E6* is capable of impacting apoptotic, cell cycle, and extracellular matrix signaling mechanisms, which are essential for normal cellular function, and implies a link to cell transformation processes.

Based on our cellular results, we predicted that E6* would reduce tumor growth *in vivo*. As anticipated, we found that SiHa cells overexpressing E6* produced smaller tumors in mice than did SiHa pFlag cells. Consistent with these results, increased levels of caspase, p53, and E-cadherin levels) were also observed. Surprisingly, the overexpression of E6* in HPV$^-$ C33A cells also produced smaller tumors than did the C33A pFlag cells. This particular result was unanticipated yet intriguing, because E6* was unable to increase the levels of caspase 8, p53, or E-cadherin in HPV$^-$ C33A cervical cancer cells. In comparing the sizes of the tumors generated by SiHa and C33A E6* cells and their controls, we found that there was less of a difference in size between the C33A control tumors and the corresponding E6* tumors than between the SiHa E6* and SiHa pFlag tumors; that is, we found that E6* reduced tumor size in SiHa cells to a greater degree.

Confirmatory RT-PCR was performed on tissue harvested from the mice, which showed that E6* expression had been maintained within the cells during *in vivo* passage, and that this E6* expression could be linked to reduced tumor formation. Further histologic examination of the xenograft tissue by haematoxylin-eosin staining revealed that SiHa control cells exhibited larger necrotic regions than did tissue derived from SiHa

E6*-expressing cells, though this difference was not detected between the C33A tumors. In addition to the difference in histologic organization, SiHa E6* tumors demonstrated a decrease in VEGFR-1 expression, indicating that E6* has a permeating influence on the SiHa tumor phenotype, since no difference in VEGFR-1 expression in C33A tumors was detected.

Co-immunoprecipitation experiments confirmed that E6* was able to bind the full-length E6 molecule, thus disrupting its cancer-promoting functions. This is consistent with the SiHa E6* cells exhibiting a significantly decreased growth rate compared to SiHa pFlag cells, C33A E6*, and C33A pFlag cells (C33A cells naturally lack viral proteins including full-length E6). This data is significant, because it is the first report that HPV16 E6* can impact tumor growth using an *in vivo* model, and suggests that HR-HPV have mechanisms available that can control tumor formation by impeding cellular growth rates and interacting to oppose actions of the E6 oncoprotein. Importantly and surprisingly, some of these E6* activities are independent of the presence of the E6 oncoprotein in their reduction of tumor growth, thereby demonstrating the versatility of E6* in influencing cellular anti-oncogenic mechanisms in various milieus, a desired quality for cancer therapeutics.

In chapter three, we utilized proteomic analysis by mass spectrometry to detect differences in cellular protein expression resulting from E6* overexpression in SiHa and C33A cells. We observed that of the many pathways affected by E6* in SiHa cells, the β-Integrin signaling pathway was the most prominent. Up-regulation of β-Integrin activation in SiHa E6* cells was confirmed by immunoblot, which demonstrated increased expression of β-Integrin in SiHa E6* cells as compared to SiHa control. This

increased expression was not seen in the C33A system. SiHa cells were also probed for

Kindlin-1 expression, since Kindlin-1 is a co-stimulatory molecule of β-Integrin. These

findings verified integrin pathway activation. The expression of RhoA, a downstream

signaling molecule of the β-Integrin pathway, was decreased in SiHa E6* cells as

compared to controls. These findings were harmonious with cell morphology

experiments showing SiHa E6* cells to exhibit more cell spreading and membrane

protrusion, and are characteristic of an inhibited capacity to proliferate mediated by

RhoA (201). Once again, no difference in the morphology or expression of β-Integrin

signaling components were observed despite low basal levels of RhoA between the C33A

pFlag and C33A E6* cells. ALPP levels in SiHa E6* cells were noted to be significantly

reduced, which is also consistent with the potential role of E6* in cell transformation.

Although components of the β-Integrin signaling pathway were not significantly

altered in E6*-expressing C33A cells, the oxidative phosphorylation and mitochondrial

dysfunction pathways were profoundly affected. In fact, mitochondrial membrane

depolarization was increased in C33A E6* cells as compared to C33A control cells. In

addition to this disturbance of mitochondrial electrophysiology, IPA analysis detected

increased expression of protein complexes of the electron transport chain, which might

reflect the organelle's attempt to compensate for the dysfunction of other critical cellular

mechanisms. Our data describing increased DNA damage in C33A E6* and SiHa E6*

cells, accompanied by a reduction in GSH levels (202), supports this hypothesis.

Interestingly, proteomic analysis did not detect significant changes in the mitochondrial

or oxidative phosphorylation proteins in SiHa cells. However, *in vitro* experiments

showed mitochondrial membrane depolarization to be more pronounced in SiHa E6*

cells as compared to the control group, with the SiHa E6* cells experiencing more DNA damage along with reduced GSH levels. This data agrees with previous findings from our laboratory that linked E6* expression with ROS generation and oxidative stress (163). Importantly, these findings elucidate potential mechanisms that may be targeted by small molecular inhibitors mimicking the anti-tumor properties of E6*.

Conclusions

In the studies preceding the data presented here, HPV16 E6* was known to bind to and stabilize procaspase 8, thus opposing the action of the parent molecule to accelerate the degradation of the apoptotic protein (18). The importance of the ratio of expression between the full-length E6 and E6* on extrinsic apoptotic pathways was also determined, and led to the discovery that E6* sensitizes U2OS, NOK, and CaSki cells to TNF-mediated apoptosis through the formation of a pseudo-death-inducing signaling complex (135). Williams et al. demonstrated that this E6*-induced cell death is, in part, mediated by increased ROS generation and a decrease in cellular antioxidants such as superoxide dismutase 2 and glutathione peroxidase (163). This investigation stressed the important link between oxidative stress and virus-induced mutagenesis, which ultimately contributes to damaged cellular DNA and favorable conditions for HPV DNA integration into the host genome (163). Previous studies also reported HPV18 E6* as capable of inhibiting E6-mediated p53 degradation by binding to E6, a similar interaction between HPV16 E6 and E6* as described in chapter two (25, 26). More recently, the same group reported direct degradation of cellular proteins by E6* in the absence of other viral proteins, agreeing with our observation of E6* activity in the C33A model (17). Other

118

studies also contributed to our current knowledge of E6*. Examples include its strict association with cancer-causing types of HPVs (203, 204) and its acceleration of cell differentiation in normal oral keratinocytes (unpublished data from our lab). However, this body of work describing the activities of E6* is much smaller than that available for the full-length E6 oncoprotein.

To expand our understanding of this important splice variant, therefore, we sought to determine: 1) Whether the previously reported anti-oncogenic qualities of E6* could be detected in an *in vivo* context? This question was addressed affirmatively in chapter two. 2) What cellular mechanisms are engaged by E6* to produce the anti-tumor effect, and do the effects of E6* on tumor growth match the molecular patterns? This question was answered in chapters two and three.

In summary, the results from the experiments supporting this dissertation show for the first time that E6* reduces the *in vivo* formation of tumors by HPV16^{+} SiHa cells and HPV^{-} C33A cells. Furthermore, we found that the mechanism principally driving the E6*-mediated reduction in SiHa E6* tumor size involves the β-Integrin signaling pathway. Conversely, the E6*-mediated growth reduction in C33A E6* tumors is primarily due to E6* engaging with mitochondrial dysfunction and oxidative phosphorylation mechanisms. Thus, the overall findings of these studies state that HPV16 E6* overexpression reduces SiHa and C33A tumor growth by engaging the β-Integrin signaling pathway and the mitochondrial dysfunction and oxidative phosphorylation pathways, respectively.

Future Directions

In this dissertation, we established that the overexpression of E6* in cervical cancer cells influences distinct cellular mechanisms, such as the β-integrin signaling and mitochondrial dysfunction and oxidative phosphorylation pathways, to slow the formation of SiHa and C33A tumors *in vivo,* respectively. To date, we are the first to describe these phenomena linking E6* directly to HR-HPV carcinogenesis.

Intriguingly, Tseliou et al. newly reported that silencing RhoA reduced the growth of human CMV (HCMV)-infected and uninfected glioblastoma cells. Glioblastoma cells are taken from gliomas, and glioblastoma multiforme is the most aggressive and most common of all the glial tumor types and arises from astrocytes in the central nervous system (CNS). These researchers observed that Rho GTPases are important in determining glioblastoma cell migration, proliferation, and morphology, as demonstrated here with SiHa and C33A cervical carcinoma cells (201). This finding corresponds to the RhoA and cell morphology data presented here (see chapter three) and suggests a vital connection between the virus' ability to hijack cellular processes throughout carcinogenesis and the host cell's response to its environment *via* extracellular and intracellular cues. Additionally, researchers are now detecting HR-HPVs in glioblastoma samples (205) though this relationship is controversial. Therefore, it may be beneficial to use specific approaches, such as a Rho knockdown model, to determine how this might affect HPV16 E6/E6* levels within cervical cancer cells. In observing these complementary findings in two very different virus-host systems we obtain only a preview of the great utility of continued, rigorous research on all virus-associated cancers. However, among these malignancies, HPV-mediated cervical cancer represents

one of the best-defined models of virus-mediated carcinogenesis, and any improvements in our understanding of how to treat it will be far more meaningful and relevant than redundant, as illustrated here.

The Neurofibromatosis type 2 tumor suppressor protein (NF2) is also implicated in the growth of CNS tumors. In fact, inactivation of the NF2 gene results in the autosomal dominant neurofibromatosis syndrome, which is characterized by the development of Schwannomas. Loss of NF2 leads to decreased contact inhibition and a gain of anchorage independence, which is crucial to promote the invasion of malignant cells (206). NF2, also called Merlin, belongs to a large family of proteins containing the FERM domain, resembling the kindlin protein family (207). The FERM domain localizes proteins to the plasma membrane and can be found in cytoskeletal-associated proteins linking the cell membrane to the cytoskeleton. Though Merlin has been documented to regulate cell proliferation and differentiation, it can also control antiangiogenic factors (208) and, if participating in the mechanisms here, may be able to partly explain E6*-mediated changes in tumor VEGFR-1 expression. Merlin has also been linked to the Hippo signaling cascade, which was another pathway that appeared in our proteomic analysis (although the fold changes in the expression of its constituents were not consistently significant). While known for regulating organ size in animals, the Hippo pathway promotes cell death and differentiation and inhibits cell proliferation, as well (207).

As the field of prevention continues to advance, one might ask why additional resources should be directed towards the discovery of small molecule HPV inhibitors. The short answer is that due to the timeline of disease progression, it will be a few

decades before these preventative measures will make a significant impact on the disease burden. In the meantime, infected women and others who do not benefit from these approaches have access to only a limited, and frequently inadequate, set of options such as lesion removal. In addition to the obvious drawbacks of surgical treatment, such as invasiveness and cytodestruction, it is well established that viral persistence is mainly responsible for disease, especially among the elderly and the immunodeficient (209). Hence, lesions do frequently recur. Therefore, it is essential that we maintain a sense of urgency with regards to developing more comprehensive and long-lasting approaches.

References

1   Markowitz LE, Hariri S, Lin C, Dunne EF, Steinau M, McQuillan G and Unger ER: Reduction in human papillomavirus (hpv) prevalence among young women following hpv vaccine introduction in the united states, national health and nutrition examination surveys, 2003-2010. J Infect Dis *208(3)*: 385-393, 2013.

2   Damin DC, Ziegelmann PK and Damin AP: Human papillomavirus infection and colorectal cancer risk: A meta-analysis. Colorectal Dis *15(8)*: e420-428, 2013.

3   Doorbar J, Egawa N, Griffin H, Kranjec C and Murakami I: Human papillomavirus molecular biology and disease association. Rev Med Virol *25 Suppl 1(*2-23, 2015.

4   Doorbar J: The papillomavirus life cycle. J Clin Virol *32 Suppl 1(*S7-15, 2005.

5   Flores ER, Allen-Hoffmann BL, Lee D and Lambert PF: The human papillomavirus type 16 e7 oncogene is required for the productive stage of the viral life cycle. J Virol *74(14)*: 6622-6631, 2000.

6   Scott B. Vande Pol AJK: Papillomavirus e6 oncoproteins. Virology *445(*115-137, 2013.

7   Feller L, Wood NH, Khammissa RA and Lemmer J: Human papillomavirus-mediated carcinogenesis and hpv-associated oral and oropharyngeal squamous cell carcinoma. Part 2: Human papillomavirus associated oral and oropharyngeal squamous cell carcinoma. Head Face Med *6(*15, 2010.

8   Williams VM, Filippova M, Soto U and Duerksen-Hughes PJ: Hpv-DNA integration and carcinogenesis: Putative roles for inflammation and oxidative stress. Future Virol *6(1)*: 45-57, 2011.

9   Pett M and Coleman N: Integration of high-risk human papillomavirus: A key event in cervical carcinogenesis? J Pathol *212(4)*: 356-367, 2007.

10   Steben M and Duarte-Franco E: Human papillomavirus infection: Epidemiology and pathophysiology. Gynecol Oncol *107(2 Suppl 1)*: S2-5, 2007.

11   Rosenberger S, De-Castro Arce J, Langbein L, Steenbergen RD and Rosl F: Alternative splicing of human papillomavirus type-16 e6/e6* early mrna is coupled to egf signaling via erk1/2 activation. Proc Natl Acad Sci U S A *107(15)*: 7006-7011, 2010.

12   Whitney Evans MF, Ron Swenson, and Penelope Duerksen-Hughes: Modern molecular and clinical approaches to eradicate hpv-mediated cervical cancer. InTech: 288-325, 2013.

13   Tungteakkhun SS and Duerksen-Hughes PJ: Cellular binding partners of the human papillomavirus e6 protein. Arch Virol *153(3)*: 397-408, 2008.

14   Niccoli S, Abraham S, Richard C and Zehbe I: The asian-american e6 variant protein of human papillomavirus 16 alone is sufficient to promote immortalization, transformation, and migration of primary human foreskin keratinocytes. J Virol *86(22)*: 12384-12396, 2012.

15   Chakrabarti O, Veeraraghavalu K, Tergaonkar V, Liu Y, Androphy EJ, Stanley MA and Krishna S: Human papillomavirus type 16 e6 amino acid 83 variants enhance e6-mediated mapk signaling and differentially regulate tumorigenesis by notch signaling and oncogenic ras. J Virol *78(11)*: 5934-5945, 2004.

16   Hernandez-Lopez HR and Graham SV: Alternative splicing in human tumour viruses: A therapeutic target? Biochem J *445(2)*: 145-156, 2012.

17   Pim D, Tomaic V and Banks L: The human papillomavirus (hpv) e6* proteins from high-risk, mucosal hpvs can direct degradation of cellular proteins in the absence of full-length e6 protein. J Virol *83(19)*: 9863-9874, 2009.

18   Filippova M, Johnson MM, Bautista M, Filippov V, Fodor N, Tungteakkhun SS, Williams K and Duerksen-Hughes PJ: The large and small isoforms of human papillomavirus type 16 e6 bind to and differentially affect procaspase 8 stability and activity. J Virol *81(8)*: 4116-4129, 2007.

19   Filippova M, Evans W., Aragon R., Filippov V., Williams V. M., Hong L., Reeves M.E., and Duerksen-Hughes P.: The small splice variant of hpv16 e6, e6*, reduces tumor formation in cervical carcinoma xenografts. Virology *450-451(*153-164, 2014.

20   Tungteakkhun SS, Filippova M, Fodor N and Duerksen-Hughes PJ: The full-length isoform of human papillomavirus 16 e6 and its splice variant e6* bind to different sites on the procaspase 8 death effector domain. J Virol *84(3)*: 1453-1463, 2010.

21   David CJ and Manley JL: Alternative pre-mrna splicing regulation in cancer: Pathways and programs unhinged. Genes Dev *24(21)*: 2343-2364, 2010.

22   Douglas AG and Wood MJ: Rna splicing: Disease and therapy. Brief Funct Genomics *10(3)*: 151-164, 2011.

23   Stoppler MC, Ching K, Stoppler H, Clancy K, Schlegel R and Icenogle J: Natural variants of the human papillomavirus type 16 e6 protein differ in their abilities to alter keratinocyte differentiation and to induce p53 degradation. J Virol *70(10)*: 6987-6993, 1996.

24   Blaustein M, Pelisch F and Srebrow A: Signals, pathways and splicing regulation. Int J Biochem Cell Biol *39(11)*: 2031-2048, 2007.

25   Pim D, Massimi P and Banks L: Alternatively spliced hpv-18 e6* protein inhibits e6 mediated degradation of p53 and suppresses transformed cell growth. Oncogene *15(3)*: 257-264, 1997.

26   Pim D and Banks L: Hpv-18 e6*i protein modulates the e6-directed degradation of p53 by binding to full-length hpv-18 e6. Oncogene *18(52)*: 7403-7408, 1999.

27   Garcia-Blanco MA, Baraniak AP and Lasda EL: Alternative splicing in disease and therapy. Nat Biotechnol *22(5)*: 535-546, 2004.

28   Rambout L, Hopkins L, Hutton B and Fergusson D: Prophylactic vaccination against human papillomavirus infection and disease in women: A systematic review of randomized controlled trials. CMAJ *177(5)*: 469-479, 2007.

29   Lowy DR and Schiller JT: Prophylactic human papillomavirus vaccines. J Clin Invest *116(5)*: 1167-1173, 2006.

30   Debbie Saslow KSA, Deana Manassaram-Baptiste, Lacey Loomer, Kristina E. Lam, Marcie Fisher-Bome, Robert A. Smith, Elizabeth T. H. Fontham: Human papillomavirus vaccination guideline update: American cancer society guideline endorsement. Cancer Journal for Clnicians *00(0)*: 00-00, 2016.

31   Saslow D and Castle PE: American cancer society guideline for human papillomavirus (hpv) vaccine use to prevent cervical cancer and its precursors. 2006.

32   Quadrivalent vaccine against human papillomavirus to prevent high-grade cervical lesions. N Engl J Med *356(19)*: 1915-1927, 2007.

33   Prophylactic efficacy of a quadrivalent human papillomavirus (hpv) vaccine in women with virological evidence of hpv infection. J Infect Dis *196(10)*: 1438-1446, 2007.

34   Tjalma WA: There are two prophylactic human papillomavirus vaccines against cancer, and they are different. J Clin Oncol *33(8)*: 964-965, 2015.

35   Garland SM: Can cervical cancer be eradicated by prophylactic hpv vaccination? Challenges to vaccine implementation. Indian J Med Res *130(3)*: 311-321, 2009.

36   Kahn JA, Brown DR, Ding L, Widdice LE, Shew ML, Glynn S and Bernstein DI: Vaccine-type human papillomavirus and evidence of herd protection after vaccine introduction. Pediatrics, 2012.

37   Villa LL: Hpv prophylactic vaccination: The first years and what to expect from now. Cancer Lett *305(2)*: 106-112, 2011.

38   Kane MA, Serrano B, de Sanjose S and Wittet S: Implementation of human papillomavirus immunization in the developing world. Vaccine *30 Suppl 5(*F192-200, 2012.

39   Agoston I, Sandor J, Karpati K and Pentek M: Economic considerations of hpv vaccination. Prev Med *50(1-2)*: 93, 2010.

40   Katz IT, Ware NC, Gray G, Haberer JE, Mellins CA and Bangsberg DR: Scaling up human papillomavirus vaccination: A conceptual framework of vaccine adherence. Sex Health *7(3)*: 279-286, 2010.

41   Adams M, Jasani B and Fiander A: Human papilloma virus (hpv) prophylactic vaccination: Challenges for public health and implications for screening. Vaccine *25(16)*: 3007-3013, 2007.

42   Massad LS, Evans CT, Weber KM, Goderre JL, Hessol NA, Henry D, Colie C, Strickler HD, Watts DH and Wilson TE: Changes in knowledge of cervical cancer prevention and human papillomavirus among women with human immunodeficiency virus. Obstet Gynecol *116(4)*: 941-947, 2010.

43   Massad LS, Evans CT, Wilson TE, Goderre JL, Hessol NA, Henry D, Colie C, Strickler HD, Levine AM, Watts DH and Weber KM: Knowledge of cervical cancer prevention and human papillomavirus among women with hiv. Gynecol Oncol *117(1)*: 70-76, 2010.

44   Bergot AS, Kassianos A, Frazer IH and Mittal D: New approaches to immunotherapy for hpv associated cancers. Cancers (Basel) *3(3)*: 3461-3495, 2011.

45   Palefsky JM, Gillison ML and Strickler HD: Chapter 16: Hpv vaccines in immunocompromised women and men. Vaccine *24 Suppl 3(*S3/140-146, 2006.

46   Auvert B, Marais D, Lissouba P, Zarca K, Ramjee G and Williamson AL: High-risk human papillomavirus is associated with hiv acquisition among south african female sex workers. Infect Dis Obstet Gynecol *2011(*692012, 2011.

47   Fitzgerald DW, Bezak K, Ocheretina O, Riviere C, Wright TC, Milne GL, Zhou XK, Du B, Subbaramaiah K, Byrt E, Goodwin ML, Rafii A and Dannenberg AJ: The effect of hiv and hpv coinfection on cervical cox-2 expression and systemic prostaglandin e2 levels. Cancer Prev Res (Phila) *5(1)*: 34-40, 2012.

48   Stanley M: Immune responses to human papillomavirus. Vaccine *24 Suppl 1(*S16-22, 2006.

49   Gormley RH and Kovarik CL: Human papillomavirus-related genital disease in the immunocompromised host: Part ii. J Am Acad Dermatol *66(6)*: 883 e881-817; quiz 899-900, 2012.

50   Ghazizadeh S, Lessan-Pezeshki M and Nahayati MA: Human papilloma virus infection in female kidney transplant recipients. Saudi J Kidney Dis Transpl *22(3)*: 433-436, 2011.

51   Massad LS, Evans CT, Minkoff H, Watts DH, Strickler HD, Darragh T, Levine A, Anastos K, Moxley M and Passaro DJ: Natural history of grade 1 cervical intraepithelial neoplasia in women with human immunodeficiency virus. Obstet Gynecol *104(5 Pt 1)*: 1077-1085, 2004.

52   Melmed GY: Vaccinations and the utilization of immunosuppressive ibd therapy. Gastroenterology & Hepatology *4(12)*: 859-861, 2008.

53   Nimako M, Fiander AN, Wilkinson GW, Borysiewicz LK and Man S: Human papillomavirus-specific cytotoxic t lymphocytes in patients with cervical intraepithelial neoplasia grade iii. Cancer Res *57(21)*: 4855-4861, 1997.

54   Kenter GG, Welters MJ, Valentijn AR, Lowik MJ, Berends-van der Meer DM, Vloon AP, Essahsah F, Fathers LM, Offringa R, Drijfhout JW, Wafelman AR, Oostendorp J, Fleuren GJ, van der Burg SH and Melief CJ: Vaccination against hpv-16 oncoproteins for vulvar intraepithelial neoplasia. N Engl J Med *361(19)*: 1838-1847, 2009.

55   Anderson J: Cervical cancer screening & prevention for hiv-infected women in the developingworld. 2010.

56   Duraisamy K: Methods of detecting cervical cancer. Advances in Biological Research *5(4)*: 226-232, 2011.

57   Saslow D, Solomon D, Lawson HW, Killackey M, Kulasingam SL, Cain JM, Garcia FA, Moriarty AT, Waxman AG, Wilbur DC, Wentzensen N, Downs LS, Jr., Spitzer M, Moscicki AB, Franco EL, Stoler MH, Schiffman M, Castle PE and Myers ER: American cancer society, american society for colposcopy and cervical pathology, and american society for clinical pathology screening guidelines for the prevention and early detection of cervical cancer. J Low Genit Tract Dis *16(3)*: 175-204, 2012.

58   Winer RL, Hughes JP, Feng Q, O'Reilly S, Kiviat NB, Holmes KK and Koutsky LA: Condom use and the risk of genital human papillomavirus infection in young women. N Engl J Med *354(25)*: 2645-2654, 2006.

59   Chen C, Yang Z, Li Z and Li L: Accuracy of several cervical screening strategies for early detection of cervical cancer: A meta-analysis. Int J Gynecol Cancer *22(6)*: 908-921, 2012.

60   Clavel C, Masure M, Bory JP, Putaud I, Mangeonjean C, Lorenzato M, Nazeyrollas P, Gabriel R, Quereux C and Birembaut P: Human papillomavirus testing in primary screening for the detection of high-grade cervical lesions: A study of 7932 women. Br J Cancer *84(12)*: 1616-1623, 2001.

61   Flores YN, Bishai DM, Lorincz A, Shah KV, Lazcano-Ponce E, Hernandez M, Granados-Garcia V, Perez R and Salmeron J: Hpv testing for cervical cancer screening appears more cost-effective than papanicolau cytology in mexico. Cancer Causes Control *22(2)*: 261-272, 2011.

62   Ronco G, Cuzick J, Pierotti P, Cariaggi MP, Dalla Palma P, Naldoni C, Ghiringhello B, Giorgi-Rossi P, Minucci D, Parisio F, Pojer A, Schiboni ML, Sintoni C, Zorzi M, Segnan N and Confortini M: Accuracy of liquid based versus conventional cytology: Overall results of new technologies for cervical cancer screening: Randomised controlled trial. BMJ *335(7609)*: 28, 2007.

63   Origoni M, Cristoforoni P, Costa S, Mariani L, Scirpa P, Lorincz A and Sideri M: Hpv-DNA testing for cervical cancer precursors: From evidence to clinical practice. Ecancermedicalscience *6(*258, 2012.

64   Gravitt PE, Coutlee F, Iftner T, Sellors JW, Quint WG and Wheeler CM: New technologies in cervical cancer screening. Vaccine *26 Suppl 10(*K42-52, 2008.

65   Brown AJ and Trimble CL: New technologies for cervical cancer screening. Best Pract Res Clin Obstet Gynaecol *26(2)*: 233-242, 2012.

66   Hogewoning CJ, Bleeker MC, van den Brule AJ, Voorhorst FJ, Snijders PJ, Berkhof J, Westenend PJ and Meijer CJ: Condom use promotes regression of cervical intraepithelial neoplasia and clearance of human papillomavirus: A randomized clinical trial. Int J Cancer *107(5)*: 811-816, 2003.

67   Fradet-Turcotte A and Archambault J: Recent advances in the search for antiviral agents against human papillomaviruses. Antivir Ther *12(4)*: 431-451, 2007.

68   Buck CB, Thompson CD, Roberts JN, Muller M, Lowy DR and Schiller JT: Carrageenan is a potent inhibitor of papillomavirus infection. PLoS Pathog *2(7)*: e69, 2006.

69   Roberts JN, Buck CB, Thompson CD, Kines R, Bernardo M, Choyke PL, Lowy DR and Schiller JT: Genital transmission of hpv in a mouse model is potentiated by nonoxynol-9 and inhibited by carrageenan. Nat Med *13(7)*: 857-861, 2007.

70   Castle PE and Giuliano AR: Chapter 4: Genital tract infections, cervical inflammation, and antioxidant nutrients--assessing their roles as human papillomavirus cofactors. J Natl Cancer Inst Monogr *31)*: 29-34, 2003.

71   Morrison MA, Morreale RJ, Akunuru S, Kofron M, Zheng Y and Wells SI: Targeting the human papillomavirus e6 and e7 oncogenes through expression of the bovine papillomavirus type 1 e2 protein stimulates cellular motility. J Virol *85(20)*: 10487-10498, 2011.

72   Sanchez-Perez AM, Soriano S, Clarke AR and Gaston K: Disruption of the human papillomavirus type 16 e2 gene protects cervical carcinoma cells from e2f-induced apoptosis. J Gen Virol *78 (Pt 11)(*3009-3018, 1997.

73   Srivastava S, Natu SM, Gupta A, Pal KA, Singh U, Agarwal GG, Singh U, Goel MM and Srivastava AN: Lipid peroxidation and antioxidants in different stages of cervical cancer: Prognostic significance. Indian J Cancer *46(4)*: 297-302, 2009.

74   Di Domenico F, Foppoli C, Coccia R and Perluigi M: Antioxidants in cervical cancer: Chemopreventive and chemotherapeutic effects of polyphenols. Biochim Biophys Acta *1822(5)*: 737-747, 2012.

75   Crespo-Ortiz MP and Wei MQ: Antitumor activity of artemisinin and its derivatives: From a well-known antimalarial agent to a potential anticancer drug. J Biomed Biotechnol *2012(*247597, 2012.

76   James RM, Cruickshank ME and Siddiqui N: Management of cervical cancer: Summary of sign guidelines. BMJ *336(7634)*: 41-43, 2008.

77   Blomfield P: Management of cervical cancer. Aust Fam Physician *36(3)*: 122-125, 2007.

78   I. AJ: The current management of cervical cancer. 6: 196-202, 2004.

79   Trimble EL: Cervical cancer state-of-the-clinical-science meeting on pretreatment evaluation and prognostic factors, september 27-28, 2007: Proceedings and recommendations. Gynecol Oncol *114(2)*: 145-150, 2009.

80   Greggi S and Scaffa C: Surgical management of early cervical cancer: The shape of future studies. Curr Oncol Rep, 2012.

81   Bansal N, Herzog TJ, Shaw RE, Burke WM, Deutsch I and Wright JD: Primary therapy for early-stage cervical cancer: Radical hysterectomy vs radiation. Am J Obstet Gynecol *201(5)*: 485 e481-489, 2009.

82   Movva S, Rodriguez L, Arias-Pulido H and Verschraegen C: Novel chemotherapy approaches for cervical cancer. Cancer *115(14)*: 3166-3180, 2009.

83   Adnane J, Bizouarn FA, Qian Y, Hamilton AD and Sebti SM: P21(waf1/cip1) is upregulated by the geranylgeranyltransferase i inhibitor ggti-298 through a transforming growth factor beta- and sp1-responsive element: Involvement of the small gtpase rhoa. Mol Cell Biol *18(12)*: 6962-6970, 1998.

84   Sivanesaratnam V: The role of chemotherapy in cervical cancer--a review. Singapore Med J *29(4)*: 397-401, 1988.

85   Tao X, Hu W, Ramirez PT and Kavanagh JJ: Chemotherapy for recurrent and metastatic cervical cancer. Gynecol Oncol *110(3 Suppl 2)*: S67-71, 2008.

86   Friedlander M and Grogan M: Guidelines for the treatment of recurrent and metastatic cervical cancer. Oncologist *7(4)*: 342-347, 2002.

87   Tewari KS and Monk BJ: The rationale for the use of non-platinum chemotherapy doublets for metastatic and recurrent cervical carcinoma. Clin Adv Hematol Oncol *8(2)*: 108-115, 2010.

88   Waggoner SE: Cervical cancer. Lancet *361(9376)*: 2217-2225, 2003.

89   Rose PG: Combined-modality therapy of locally advanced cervical cancer. J Clin Oncol *21(10 Suppl)*: 211s-217s, 2003.

90   Rose PG, Ali S, Watkins E, Thigpen JT, Deppe G, Clarke-Pearson DL and Insalaco S: Long-term follow-up of a randomized trial comparing concurrent single agent cisplatin, cisplatin-based combination chemotherapy, or hydroxyurea during pelvic irradiation for locally advanced cervical cancer: A gynecologic oncology group study. J Clin Oncol *25(19)*: 2804-2810, 2007.

91   Moore DH: Cervical cancer. Obstet Gynecol *107(5)*: 1152-1161, 2006.

92   Lin K, Roosinovich E, Ma B, Hung CF and Wu TC: Therapeutic hpv DNA vaccines. Immunol Res *47(1-3)*: 86-112, 2010.

93   Mustafa W, Maciag PC, Pan ZK, Weaver JR, Xiao Y, Isaacs SN and Paterson Y: Listeria monocytogenes delivery of hpv-16 major capsid protein l1 induces systemic and mucosal cell-mediated cd4+ and cd8+ t-cell responses after oral immunization. Viral Immunol *22(3)*: 195-204, 2009.

94   Hussain SF and Paterson Y: What is needed for effective antitumor immunotherapy? Lessons learned using listeria monocytogenes as a live vector for hpv-associated tumors. Cancer Immunol Immunother *54(6)*: 577-586, 2005.

95   Sewell DA, Douven D, Pan ZK, Rodriguez A and Paterson Y: Regression of hpv-positive tumors treated with a new listeria monocytogenes vaccine. Arch Otolaryngol Head Neck Surg *130(1)*: 92-97, 2004.

96   Lin CW, Lee JY, Tsao YP, Shen CP, Lai HC and Chen SL: Oral vaccination with recombinant listeria monocytogenes expressing human papillomavirus type 16 e7 can cause tumor growth in mice to regress. Int J Cancer *102(6)*: 629-637, 2002.

97   Wu CY, Monie A, Pang X, Hung CF and Wu TC: Improving therapeutic hpv peptide-based vaccine potency by enhancing cd4+ t help and dendritic cell activation. J Biomed Sci *17(*88, 2010.

98   Huang CF, Monie A, Weng WH and Wu T: DNA vaccines for cervical cancer. Am J Transl Res *2(1)*: 75-87, 2010.

99   Hung CF, Monie A, Alvarez RD and Wu TC: DNA vaccines for cervical cancer: From bench to bedside. Exp Mol Med *39(6)*: 679-689, 2007.

100   Hsu KF, Hung CF, Cheng WF, He L, Slater LA, Ling M and Wu TC: Enhancement of suicidal DNA vaccine potency by linking mycobacterium tuberculosis heat shock protein 70 to an antigen. Gene Ther *8(5)*: 376-383, 2001.

101   Kim TW, Hung CF, Juang J, He L, Hardwick JM and Wu TC: Enhancement of suicidal DNA vaccine potency by delaying suicidal DNA-induced cell death. Gene Ther *11(3)*: 336-342, 2004.

102   Weiss JM, Subleski JJ, Wigginton JM and Wiltrout RH: Immunotherapy of cancer by il-12-based cytokine combinations. Expert Opin Biol Ther *7(11)*: 1705-1721, 2007.

103   Bellati F, Napoletano C, Gasparri ML, Visconti V, Zizzari IG, Ruscito I, Caccetta J, Rughetti A, Benedetti-Panici P and Nuti M: Monoclonal antibodies in gynecological cancer: A critical point of view. Clin Dev Immunol *2011(*890758, 2011.

104   White PW, Titolo S, Brault K, Thauvette L, Pelletier A, Welchner E, Bourgon L, Doyon L, Ogilvie WW, Yoakim C, Cordingley MG and Archambault J: Inhibition of human papillomavirus DNA replication by small molecule antagonists of the e1-e2 protein interaction. J Biol Chem *278(29)*: 26765-26772, 2003.

105   White PW, Faucher AM and Goudreau N: Small molecule inhibitors of the human papillomavirus e1-e2 interaction. Curr Top Microbiol Immunol *348(*61-88, 2011.

106   Hafner N, Driesch C, Gajda M, Jansen L, Kirchmayr R, Runnebaum IB and Durst M: Integration of the hpv16 genome does not invariably result in high levels of viral oncogene transcripts. Oncogene *27(11)*: 1610-1617, 2008.

107   D'Abramo CM and Archambault J: Small molecule inhibitors of human papillomavirus protein - protein interactions. Open Virol J *5(*80-95, 2011.

108   Hudson JB, Bedell MA, McCance DJ and Laiminis LA: Immortalization and altered differentiation of human keratinocytes in vitro by the e6 and e7 open reading frames of human papillomavirus type 18. J Virol *64(2)*: 519-526, 1990.

109   Song S, Liem A, Miller JA and Lambert PF: Human papillomavirus types 16 e6 and e7 contribute differently to carcinogenesis. Virology *267(2)*: 141-150, 2000.

110   Song S, Pitot HC and Lambert PF: The human papillomavirus type 16 e6 gene alone is sufficient to induce carcinomas in transgenic animals. J Virol *73(7)*: 5887-5893, 1999.

111   Song S, Gulliver GA and Lambert PF: Human papillomavirus type 16 e6 and e7 oncogenes abrogate radiation-induced DNA damage responses in vivo through p53-dependent and p53-independent pathways. Proc Natl Acad Sci U S A *95(5)*: 2290-2295, 1998.

112   Tan S, de Vries EG, van der Zee AG and de Jong S: Anticancer drugs aimed at e6 and e7 activity in hpv-positive cervical cancer. Curr Cancer Drug Targets *12(2)*: 170-184, 2012.

113   Talis AL, Huibregtse JM and Howley PM: The role of e6ap in the regulation of p53 protein levels in human papillomavirus (hpv)-positive and hpv-negative cells. J Biol Chem *273(11)*: 6439-6445, 1998.

114   Magal SS, Jackman A, Ish-Shalom S, Botzer LE, Gonen P, Schlegel R and Sherman L: Downregulation of bax mrna expression and protein stability by the e6 protein of human papillomavirus 16. J Gen Virol *86(Pt 3)*: 611-621, 2005.

115   Vogt M, Butz K, Dymalla S, Semzow J and Hoppe-Seyler F: Inhibition of bax activity is crucial for the antiapoptotic function of the human papillomavirus e6 oncoprotein. Oncogene *25(29)*: 4009-4015, 2006.

116   Tungteakkhun SS, Filippova M, Neidigh JW, Fodor N and Duerksen-Hughes PJ: The interaction between human papillomavirus type 16 and fadd is mediated by a novel e6 binding domain. J Virol *82(19)*: 9600-9614, 2008.

117   Yuan CH, Filippova M, Tungteakkhun SS, Duerksen-Hughes PJ and Krstenansky JL: Small molecule inhibitors of the hpv16-e6 interaction with caspase 8. Bioorg Med Chem Lett *22(5)*: 2125-2129, 2012.

118   Yuan CH, Filippova M, Krstenansky JL and Duerksen-Hughes PJ: Flavonol and imidazole derivatives block hpv16 e6 activities and reactivate apoptotic pathways in hpv(+) cells. Cell Death Dis *7(*2060, 2016.

119   Bodily J and Laimins LA: Persistence of human papillomavirus infection: Keys to malignant progression. Trends Microbiol *19(1)*: 33-39, 2011.

120   Ghittoni R, Accardi R, Hasan U, Gheit T, Sylla B and Tommasino M: The biological properties of e6 and e7 oncoproteins from human papillomaviruses. Virus Genes *40(1)*: 1-13, 2010.

121   Graham SV: Human papillomavirus: Gene expression, regulation and prospects for novel diagnostic methods and antiviral therapies. Future Microbiol *5(10)*: 1493-1506, 2010.

122   McLaughlin-Drubin ME and Munger K: Oncogenic activities of human papillomaviruses. Virus Res *143(2)*: 195-208, 2009.

123   Moody CA and Laimins LA: Human papillomavirus oncoproteins: Pathways to transformation. Nat Rev Cancer *10(8)*: 550-560, 2010.

124   Munger K and Howley PM: Human papillomavirus immortalization and transformation functions. Virus Res *89(2)*: 213-228, 2002.

125   Pim D and Banks L: Interaction of viral oncoproteins with cellular target molecules: Infection with high-risk vs low-risk human papillomaviruses. APMIS *118(6-7)*: 471-493, 2010.

126   Doorbar J, Ely S, Sterling J, McLean C and Crawford L: Specific interaction between hpv-16 e1-e4 and cytokeratins results in collapse of the epithelial cell intermediate filament network. Nature *352(6338)*: 824-827, 1991.

127   Davy CE, Jackson DJ, Wang Q, Raj K, Masterson PJ, Fenner NF, Southern S, Cuthill S, Millar JB and Doorbar J: Identification of a g(2) arrest domain in the e1 wedge e4 protein of human papillomavirus type 16. J Virol *76(19)*: 9806-9818, 2002.

128   Stubenrauch F, Hummel M, Iftner T and Laimins LA: The e8e2c protein, a negative regulator of viral transcription and replication, is required for extrachromosomal maintenance of human papillomavirus type 31 in keratinocytes. J Virol *74(3)*: 1178-1186, 2000.

129   Stubenrauch F, Zobel T and Iftner T: The e8 domain confers a novel long-distance transcriptional repression activity on the e8e2c protein of high-risk human papillomavirus type 31. J Virol *75(9)*: 4139-4149, 2001.

130   Zheng ZM and Baker CC: Papillomavirus genome structure, expression, and post-transcriptional regulation. Front Biosci *11(*2286-2302, 2006.

131   Sotlar K, Diemer D, Dethleffs A, Hack Y, Stubner A, Vollmer N, Menton S, Menton M, Dietz K, Wallwiener D, Kandolf R and Bultmann B: Detection and typing of human papillomavirus by e6 nested multiplex pcr. J Clin Microbiol *42(7)*: 3176-3184, 2004.

132   Zheng ZM: Viral oncogenes, noncoding rnas, and rna splicing in human tumor viruses. Int J Biol Sci *6(7)*: 730-755, 2010.

133   Tang S, Tao M, McCoy JP, Jr. and Zheng ZM: The e7 oncoprotein is translated from spliced e6*i transcripts in high-risk human papillomavirus type 16- or type 18-positive cervical cancer cell lines via translation reinitiation. J Virol *80(9)*: 4249-4263, 2006.

134   Zheng ZM, Tao M, Yamanegi K, Bodaghi S and Xiao W: Splicing of a cap-proximal human papillomavirus 16 e6e7 intron promotes e7 expression, but can be restrained by distance of the intron from its rna 5' cap. J Mol Biol *337(5)*: 1091-1108, 2004.

135   Filippova M, Filippov VA, Kagoda M, Garnett T, Fodor N and Duerksen-Hughes PJ: Complexes of human papillomavirus type 16 e6 proteins form pseudo-death-inducing signaling complex structures during tumor necrosis factor-mediated apoptosis. J Virol *83(1)*: 210-227, 2009.

136   Filippova M, Brown-Bryan TA, Casiano CA and Duerksen-Hughes PJ: The human papillomavirus 16 e6 protein can either protect or further sensitize cells to tnf: Effect of dose. Cell Death Differ *12(12)*: 1622-1635, 2005.

137   Filippova M, Parkhurst L and Duerksen-Hughes PJ: The human papillomavirus 16 e6 protein binds to fas-associated death domain and protects cells from fas-triggered apoptosis. J Biol Chem *279(24)*: 25729-25744, 2004.

138   Filippova M, Song H, Connolly JL, Dermody TS and Duerksen-Hughes PJ: The human papillomavirus 16 e6 protein binds to tumor necrosis factor (tnf) r1 and protects cells from tnf-induced apoptosis. J Biol Chem *277(24)*: 21730-21739, 2002.

139   Filippova M and Duerksen-Hughes PJ: Inorganic and dimethylated arsenic species induce cellular p53. Chem Res Toxicol *16(3)*: 423-431, 2003.

140   Crook T, Wrede D and Vousden KH: P53 point mutation in hpv negative human cervical carcinoma cell lines. Oncogene *6(5)*: 873-875, 1991.

141   Hazan RB, Qiao R, Keren R, Badano I and Suyama K: Cadherin switch in tumor progression. Ann N Y Acad Sci *1014(*155-163, 2004.

142   Harris AL: Hypoxia--a key regulatory factor in tumour growth. Nat Rev Cancer *2(1)*: 38-47, 2002.

143   Mercatante D and Kole R: Modification of alternative splicing pathways as a potential approach to chemotherapy. Pharmacol Ther *85(3)*: 237-243, 2000.

144   Guccione E, Pim D and Banks L: Hpv-18 e6*i modulates hpv-18 full-length e6 functions in a cell cycle dependent manner. Int J Cancer *110(6)*: 928-933, 2004.

145   Pang E, Delic NC, Hong A, Zhang M, Rose BR and Lyons JG: Radiosensitization of oropharyngeal squamous cell carcinoma cells by human papillomavirus 16 oncoprotein e6 *i. Int J Radiat Oncol Biol Phys *79(3)*: 860-865, 2011.

146   Takeichi M: Cadherins in cancer: Implications for invasion and metastasis. Curr Opin Cell Biol *5(5)*: 806-811, 1993.

147   Hazan RB, Phillips GR, Qiao RF, Norton L and Aaronson SA: Exogenous expression of n-cadherin in breast cancer cells induces cell migration, invasion, and metastasis. J Cell Biol *148(4)*: 779-790, 2000.

148   Bai L, Wei L, Wang J, Li X and He P: Extended effects of human papillomavirus 16 e6-specific short hairpin rna on cervical carcinoma cells. Int J Gynecol Cancer *16(2)*: 718-729, 2006.

149   Chang JT, Kuo TF, Chen YJ, Chiu CC, Lu YC, Li HF, Shen CR and Cheng AJ: Highly potent and specific sirnas against e6 or e7 genes of hpv16- or hpv18-infected cervical cancers. Cancer Gene Ther *17(12)*: 827-836, 2010.

150   Chan DW, Yu SY, Chiu PM, Yao KM, Liu VW, Cheung AN and Ngan HY: Over-expression of foxm1 transcription factor is associated with cervical cancer progression and pathogenesis. J Pathol *215(3)*: 245-252, 2008.

151   Delmas AL, Riggs BM, Pardo CE, Dyer LM, Darst RP, Izumchenko EG, Monroe M, Hakam A, Kladde MP, Siegel EM and Brown KD: Wif1 is a frequent target for epigenetic silencing in squamous cell carcinoma of the cervix. Carcinogenesis *32(11)*: 1625-1633, 2011.

152   Kwan HT, Chan DW, Cai PC, Mak CS, Yung MM, Leung TH, Wong OG, Cheung AN and Ngan HY: Ampk activators suppress cervical cancer cell growth through inhibition of dvl3 mediated wnt/beta-catenin signaling activity. PLoS One *8(1)*: e53597, 2013.

153   Berumen J, Ordonez RM, Lazcano E, Salmeron J, Galvan SC, Estrada RA, Yunes E, Garcia-Carranca A, Gonzalez-Lira G and Madrigal-de la Campa A: Asian-american variants of human papillomavirus 16 and risk for cervical cancer: A case-control study. J Natl Cancer Inst *93(17)*: 1325-1330, 2001.

154   De la Cruz-Hernandez E, Garcia-Carranca A, Mohar-Betancourt A, Duenas-Gonzalez A, Contreras-Paredes A, Perez-Cardenas E, Herrera-Goepfert R and Lizano-Soberon M: Differential splicing of e6 within human papillomavirus type 18 variants and functional consequences. J Gen Virol *86(Pt 9)*: 2459-2468, 2005.

155   WHO 2013 Sexual and Reproductive Health: http://www.who.int/reproductivehealth/topics/cancers/en/

156   Hoste G, Vossaert K and Poppe WA: The clinical role of hpv testing in primary and secondary cervical cancer screening. Obstet Gynecol Int *2013(*610373, 2013.

157   Jung YS, Kato I and Kim HR: A novel function of hpv16-e6/e7 in epithelial-mesenchymal transition. Biochem Biophys Res Commun *435(3)*: 339-344, 2013.

158   Parkin DM and Bray F: Chapter 2: The burden of hpv-related cancers. Vaccine *24 Suppl 3(*S3/11-25, 2006.

159   Vande Pol SB and Klingelhutz AJ: Papillomavirus e6 oncoproteins. Virology *445(1-2)*: 115-137, 2013.

160   Filippova M, Evans W, Aragon R, Filippov V, Williams VM, Hong L, Reeves ME and Duerksen-Hughes P: The small splice variant of hpv16 e6, e6, reduces tumor formation in cervical carcinoma xenografts. Virology *450-451(*153-164, 2014.

161   Schneider CA, Rasband WS and Eliceiri KW: Nih image to imagej: 25 years of image analysis. Nat Methods *9(7)*: 671-675, 2012.

162   Filippova M, Filippov V, Williams VM, Zhang K, Kokoza A, Bashkirova S and Duerksen-Hughes P: Cellular levels of oxidative stress affect the response of cervical cancer cells to chemotherapeutic agents. Biomed Res Int *2014(*574659, 2014.

163   Williams VM, Filippova M, Filippov V, Payne KJ and Duerksen-Hughes P: Human papillomavirus type 16 e6* induces oxidative stress and DNA damage. J Virol *88(12)*: 6751-6761, 2014.

164   Zimonjic DB, Simpson S, Popescu NC and DiPaolo JA: Molecular cytogenetics of human papillomavirus-negative cervical carcinoma cell lines. Cancer Genet Cytogenet *82(1)*: 1-8, 1995.

165   Wu C and Dedhar S: Integrin-linked kinase (ilk) and its interactors: A new paradigm for the coupling of extracellular matrix to actin cytoskeleton and signaling complexes. J Cell Biol *155(4)*: 505-510, 2001.

166   Has C, Herz C, Zimina E, Qu HY, He Y, Zhang ZG, Wen TT, Gache Y, Aumailley M and Bruckner-Tuderman L: Kindlin-1 is required for rhogtpase-mediated lamellipodia formation in keratinocytes. Am J Pathol *175(4)*: 1442-1452, 2009.

167   Tkach V, Bock E and Berezin V: The role of rhoa in the regulation of cell morphology and motility. Cell Motil Cytoskeleton *61(1)*: 21-33, 2005.

168   Leung T, Chen XQ, Manser E and Lim L: The p160 rhoa-binding kinase rok alpha is a member of a kinase family and is involved in the reorganization of the cytoskeleton. Mol Cell Biol *16(10)*: 5313-5327, 1996.

169   McBeath R, Pirone DM, Nelson CM, Bhadriraju K and Chen CS: Cell shape, cytoskeletal tension, and rhoa regulate stem cell lineage commitment. Dev Cell *6(4)*: 483-495, 2004.

170   Stefkova K, Prochazkova J and Pachernik J: Alkaline phosphatase in stem cells. Stem Cells Int *2015(*628368, 2015.

171   Ben-Arie A, Hagay Z, Ben-Hur H, Open M and Dgani R: Elevated serum alkaline phosphatase may enable early diagnosis of ovarian cancer. Eur J Obstet Gynecol Reprod Biol *86(1)*: 69-71, 1999.

172   Saif MW, Alexander D and Wicox CM: Serum alkaline phosphatase level as a prognostic tool in colorectal cancer: A study of 105 patients. J Appl Res *5(1)*: 88-95, 2005.

173   Ren HY, Sun LL, Li HY and Ye ZM: Prognostic significance of serum alkaline phosphatase level in osteosarcoma: A meta-analysis of published data. Biomed Res Int *2015(*160835, 2015.

174   Arthur WT, Petch LA and Burridge K: Integrin engagement suppresses rhoa activity via a c-src-dependent mechanism. Curr Biol *10(12)*: 719-722, 2000.

175   Joshi DC and Bakowska JC: Determination of mitochondrial membrane potential and reactive oxygen species in live rat cortical neurons. J Vis Exp *51)*, 2011.

176   Cui H, Kong Y and Zhang H: Oxidative stress, mitochondrial dysfunction, and aging. J Signal Transduct *2012(*646354, 2012.

177   Garnett TO and Duerksen-Hughes PJ: Modulation of apoptosis by human papillomavirus (hpv) oncoproteins. Arch Virol *151(12)*: 2321-2335, 2006.

178   Garnett TO, Filippova M and Duerksen-Hughes PJ: Accelerated degradation of fadd and procaspase 8 in cells expressing human papilloma virus 16 e6 impairs trail-mediated apoptosis. Cell Death Differ *13(11)*: 1915-1926, 2006.

179   Yuan CH, Filippova M and Duerksen-Hughes P: Modulation of apoptotic pathways by human papillomaviruses (hpv): Mechanisms and implications for therapy. Viruses *4(12)*: 3831-3850, 2012.

180   Ganguly N and Parihar SP: Human papillomavirus e6 and e7 oncoproteins as risk factors for tumorigenesis. J Biosci *34(1)*: 113-123, 2009.

181   Meves A, Stremmel C, Gottschalk K and Fassler R: The kindlin protein family: New members to the club of focal adhesion proteins. Trends Cell Biol *19(10)*: 504-513, 2009.

182   Kant S, Swat W, Zhang S, Zhang ZY, Neel BG, Flavell RA and Davis RJ: Tnf-stimulated map kinase activation mediated by a rho family gtpase signaling pathway. Genes Dev *25(19)*: 2069-2078, 2011.

183   Meiri D, Marshall CB, Mokady D, LaRose J, Mullin M, Gingras AC, Ikura M and Rottapel R: Mechanistic insight into gpcr-mediated activation of the microtubule-associated rhoa exchange factor gef-h1. Nat Commun *5(*4857, 2014.

184   Shen B, Delaney MK and Du X: Inside-out, outside-in, and inside-outside-in: G protein signaling in integrin-mediated cell adhesion, spreading, and retraction. Curr Opin Cell Biol *24(5)*: 600-606, 2012.

185   Okamura H, Yoshida K, Yang D and Haneji T: Protein phosphatase 2a calpha regulates osteoblast differentiation and the expressions of bone sialoprotein and osteocalcin via osterix transcription factor. J Cell Physiol *228(5)*: 1031-1037, 2013.

186   Ivaska J, Nissinen L, Immonen N, Eriksson JE, Kahari VM and Heino J: Integrin alpha 2 beta 1 promotes activation of protein phosphatase 2a and dephosphorylation of akt and glycogen synthase kinase 3 beta. Mol Cell Biol *22(5)*: 1352-1359, 2002.

187   Lalles JP: Intestinal alkaline phosphatase: Novel functions and protective effects. Nutr Rev *72(2)*: 82-94, 2014.

188   Massa SM, Swanson RA and Sharp FR: The stress gene response in brain. Cerebrovasc Brain Metab Rev *8(2)*: 95-158, 1996.

189   Hattori T, Watanabe K, Uechi Y, Yoshioka H and Ohta Y: Repetitive transient depolarizations of the inner mitochondrial membrane induced by proton pumping. Biophys J *88(3)*: 2340-2349, 2005.

190   Whitaker-Menezes D, Martinez-Outschoorn UE, Flomenberg N, Birbe RC, Witkiewicz AK, Howell A, Pavlides S, Tsirigos A, Ertel A, Pestell RG, Broda P, Minetti C, Lisanti MP and Sotgia F: Hyperactivation of oxidative mitochondrial metabolism in epithelial cancer cells in situ: Visualizing the therapeutic effects of metformin in tumor tissue. Cell Cycle *10(23)*: 4047-4064, 2011.

191   Hyde BB, Twig G and Shirihai OS: Organellar vs cellular control of mitochondrial dynamics. Semin Cell Dev Biol *21(6)*: 575-581, 2010.

192   Twig G and Shirihai OS: The interplay between mitochondrial dynamics and mitophagy. Antioxid Redox Signal *14(10)*: 1939-1951, 2011.

193   Boland ML, Chourasia AH and Macleod KF: Mitochondrial dysfunction in cancer. Front Oncol *3(*292, 2013.

194   Mercer JR, Cheng KK, Figg N, Gorenne I, Mahmoudi M, Griffin J, Vidal-Puig A, Logan A, Murphy MP and Bennett M: DNA damage links mitochondrial dysfunction to atherosclerosis and the metabolic syndrome. Circ Res *107(8)*: 1021-1031, 2010.

195   Franco R and Cidlowski JA: Apoptosis and glutathione: Beyond an antioxidant. Cell Death Differ *16(10)*: 1303-1314, 2009.

196   Carletti B, Passarelli C, Sparaco M, Tozzi G, Pastore A, Bertini E and Piemonte F: Effect of protein glutathionylation on neuronal cytoskeleton: A potential link to neurodegeneration. Neuroscience *192(*285-294, 2011.

197   John Gardiner RO, and Jan Marc: The nervous system cytoskeleton under oxidative stress. diseases *1(*36-50, 2013.

198   Hashimoto K, Takasaki W, Yamoto T, Manabe S, Sato I and Tsuda S: Effect of glutathione (gsh) depletion on DNA damage and blood chemistry in aged and young rats. J Toxicol Sci *33(4)*: 421-429, 2008.

199   Birben E, Sahiner UM, Sackesen C, Erzurum S and Kalayci O: Oxidative stress and antioxidant defense. World Allergy Organ J *5(1)*: 9-19, 2012.

200   Yun J and Finkel T: Mitohormesis. Cell Metab *19(5)*: 757-766, 2014.

201   Tseliou M, Al-Qahtani A, Alarifi S, Alkahtani SH, Stournaras C and Sourvinos G: The role of rhoa, rhob and rhoc gtpases in cell morphology, proliferation and migration in human cytomegalovirus (hcmv) infected glioblastoma cells. Cell Physiol Biochem *38(1)*: 94-109, 2016.

202   Evans W, Filippova M, Filippov V, Bashkirova S, Zhang G, Reeves ME and Duerksen-Hughes P: Overexpression of hpv16 e6* alters beta-integrin and mitochondrial dysfunction pathways in cervical cancer cells. Cancer Genomics Proteomics *13(4)*: 259-273, 2016.

203   Vaeteewoottacharn K, Chamutpong S, Ponglikitmongkol M and Angeletti PC: Differential localization of hpv16 e6 splice products with e6-associated protein. Virol J *2(*50, 2005.

204   Smotkin D, Prokoph H and Wettstein FO: Oncogenic and nononcogenic human genital papillomaviruses generate the e7 mrna by different mechanisms. J Virol *63(3)*: 1441-1447, 1989.

205   Hashida Y, Taniguchi A, Yawata T, Hosokawa S, Murakami M, Hiroi M, Ueba T and Daibata M: Prevalence of human cytomegalovirus, polyomaviruses, and oncogenic viruses in glioblastoma among japanese subjects. Infect Agent Cancer *10(*3, 2015.

206   Beltrami S, Kim R and Gordon J: Neurofibromatosis type 2 protein, nf2: An uncoventional cell cycle regulator. Anticancer Res *33(1)*: 1-11, 2013.

207   Yu FX and Guan KL: The hippo pathway: Regulators and regulations. Genes Dev *27(4)*: 355-371, 2013.

208   Wong HK, Shimizu A, Kirkpatrick ND, Garkavtsev I, Chan AW, di Tomaso E, Klagsbrun M and Jain RK: Merlin/nf2 regulates angiogenesis in schwannomas through a rac1/semaphorin 3f-dependent mechanism. Neoplasia *14(2)*: 84-94, 2012.

209   Costa S, De Simone P, Venturoli S, Cricca M, Zerbini ML, Musiani M, Terzano P, Santini D, Cristiani P, Syrjanen S and Syrjanen K: Factors predicting human

papillomavirus clearance in cervical intraepithelial neoplasia lesions treated by conization. Gynecol Oncol *90(2)*: 358-365, 2003.